

Beyond Lindblad Dynamics: Rigorous Guarantees for Thermal and Ground State Preservation under System–Bath Interactions

Ke Wang^{1,*} and Zhiyan Ding^{1,†}

¹*Department of Mathematics, University of Michigan, Ann Arbor, MI 48109, USA*

We establish new theoretical results demonstrating the efficiency and robustness of system–bath interaction models for quantum thermal and ground state preparation. Unlike prior analyses, which typically relies on the Lindblad limit and require vanishing coupling strengths $o(1)$, we rigorously show that efficient state preparation remains possible far beyond this regime, even when the coupling strength is $\Theta(1)$. We first prove that even with constant coupling strength, the induced quantum channel still approximately fixes the target state. For thermal state preparation, we then develop a general perturbative framework that yields end-to-end complexity bounds outside weak coupling, and in particular proves that the mixing time scales as the inverse square of the coupling strength. This framework extends to broad Hamiltonian for which KMS detailed balance Lindbladians are known to mix. These bounds substantially improve upon prior results, and numerical simulations further confirm the robustness of the system–bath interaction framework across both weak and strong coupling regimes.

I. INTRODUCTION

Quantum thermal state and ground state preparation are fundamental primitives with broad applications in quantum many body physics, quantum chemistry, and materials science. Inspired by natural thermalization and cooling processes in open quantum systems, quantum algorithms based on dissipative dynamics have recently emerged as a powerful and efficient framework for state preparation [1–23]. These algorithms employ carefully engineered dissipative processes, often modeled as quantum Markov chains, to drive the system toward a desired thermal or ground state.

Within this dissipative framework, a particularly prominent approach is to employ Lindblad dynamics [24, 25]. Originally formulated as a Markovian approximation to the continuous time evolution of open quantum systems, the Lindblad equation has recently become a versatile algorithmic tool for quantum state preparation, owing to its clean and manageable mathematical structure that facilitates algorithm design. Numerous Lindblad-based works have been developed for both thermal state preparation [11–14] and ground state preparation [21, 23], with rigorous performance guarantees established for a wide range of physically relevant models [21, 26–35].

One drawback of Lindblad-based algorithms is that their practical implementation often requires complex quantum operations and intricate simulation procedures. In particular, these dynamics typically involve engineering jump operators that appear as linear combinations of Heisenberg evolutions. Simulating such Lindbladians on quantum devices therefore requires a nontrivial block-encoding of these jump operators [12, 36–38], a process that frequently demands multiple ancilla qubits and

highly structured controlled operations. These requirements pose substantial challenges for early fault-tolerant quantum devices. More recently, a different class of dissipative dynamics, the system–bath interaction framework, has been explored as a way to overcome these difficulties. In contrast to Lindbladian dynamics, this framework models the system as evolving unitarily while weakly coupled to a small ancillary bath, with dissipation arising from tracing out and resetting the bath after a prescribed duration of joint evolution. The system–bath interaction models have long been used for state preparation [10, 39–44]. However, these works often lack rigorous performance guarantees and it can be challenging to engineer with the precision needed to reliably reach the desired target state. These difficulties have motivated a surge of recent efforts to develop system–bath interaction models that are both theoretically grounded and experimentally feasible [17–19, 22, 45].

Although there are many ways to engineer system–bath interaction models for state preparation, theoretical analyses in the literature typically follow a common routine [17, 19, 22]: The discrete system–bath quantum channel is first approximated by an effective Lindblad evolution in the weak-coupling limit, and one then shows that the fixed point of this Lindbladian is close to the desired target state. Because this analysis relies on the validity of the weak-coupling approximation, the coupling strength must vanish with the target precision, often chosen to be $\text{poly}(\epsilon)$ in the accuracy parameter ϵ [17, 19, 22]. Such weak coupling typically leads to slow mixing of the underlying discrete quantum channel, resulting in a large number of iterations to reach the target state.

To overcome this limitation, a natural question arises:

Can a system–bath interaction model prepare thermal or ground states beyond the weak coupling (Lindblad) limit?

In this work, we provide the first affirmative theoretical answer to this question. Our first theoretical contribu-

* kwmath@umich.edu

† zyding@umich.edu

tion is a rigorous proof that the discrete quantum channel induced by the system–bath interaction can still approximately fix the target thermal or ground state even when the coupling strength is not weak but remains $\Theta(1)$, i.e., *beyond the traditional Lindblad limit*. This regime permits a stronger contraction toward the target state in each iteration, which in turn reduces the number of iterations required for convergence. In the case of ground state preparation, our analysis removes the $\text{poly}(\epsilon)$ dependence in the iteration complexity with respect to the target precision ϵ , improving upon the prior rigorous bounds established in [22].

A second component of our theoretical contribution is a rigorous mixing-time analysis for system–bath interaction models for thermal state preparation *beyond the Lindblad limit*. Building on the recent monotonic spectral-gap result proved in [46], we develop a perturbative framework to analyze the contraction rate of the discrete quantum channel in our algorithm. By combining this general framework with existing spectral-gap bounds for Lindbladian dynamics satisfying the KMS detailed balance condition, we rigorously prove that the mixing time scales inversely with the square of the coupling strength. This yields *end-to-end complexity* guarantees for the algorithm and establishes improved efficiency in the case of $\Theta(1)$ coupling strength.

Finally, guided by these theoretical insights, we perform numerical experiments that validate our analysis and the predicted speedups in the $\Theta(1)$ coupling regime. Moreover, we observe robust convergence even in the strong coupling regime, which goes beyond the scope of our current theoretical analysis, suggesting that system–bath interaction models may perform even better in practice than suggested by our theoretical bounds.

The rest of the paper is organized as follows. In Section II, we review the system–bath interaction algorithm proposed in [22], which is the main algorithm studied in this work. In Section III, we present our main theoretical results on the fixed point and mixing time property beyond the Lindblad limit. In Section IV, we outline the main analytical techniques underlying the proof. In Section V, we provide numerical evidence that supports our theory and demonstrates improved practical efficiency. We conclude in Section VI with a discussion of future research directions. A review of related literature (Appendix B) and the detailed proofs of our theoretical results are provided in Appendix.

II. SYSTEM-BATH INTERACTION ALGORITHM

We review the system–bath interaction algorithm introduced in [22]. Given a n -qubit system Hamiltonian H and inverse temperature $0 < \beta \leq \infty$, the thermal state is defined as $\sigma_\beta = e^{-\beta H} / \text{Tr}(e^{-\beta H})$, with the ground state corresponding to the limit $\beta \rightarrow \infty$. The system–bath interaction algorithm aims to prepare the target state

by iteratively applying a quantum channel Φ_Γ generated from a system–bath interaction evolution:

$$\rho_{n+1} = \Phi_\Gamma(\rho_n) := \mathbb{E} [\text{Tr}_E (U^\Gamma(T) (\rho_n \otimes \rho_E) U^\Gamma(T)^\dagger)]. \quad (1)$$

Here $U^\Gamma(t) := \mathcal{T} \exp \left(-i \int_{-T}^t H_\Gamma(s) ds \right)$ denotes the time-evolution operator of the joint system–bath dynamics up to time t . The total Hamiltonian is given by

$$H_\Gamma(t) = H + H_E + \Gamma f(t) \left(A_S \otimes B_E + A_S^\dagger \otimes B_E^\dagger \right). \quad (2)$$

where H is the system Hamiltonian, H_E, B_E are the bath Hamiltonian and operator. Here, Γ is a parameter that controls the coupling strength between the system and the bath, and $f(t)$ is a filter function that satisfies the normalization condition $\|f(t)\|_{L^1(\mathbb{R})} = \Theta(1)$. We refer to the *weak coupling regime* as $\Gamma = o(1)$, i.e., vanishing coupling strength. For example, analysis in [17, 19, 22, 46] mainly conducted on a regime where Γ scales polynomially with the accuracy, i.e., $\Gamma = \mathcal{O}(\text{poly}(\epsilon))$. Here we instead focus on the physically more relevant *constant coupling* regime $\Gamma = \Theta(1)$ to characterize performance beyond the Lindblad limit.

Following [22], we take a single ancilla bath with $H_E = -\omega Z/2$ and $B_E = (X_E - iY_E)/2 = |1\rangle\langle 0|$, where ω is randomly sampled from a probability density $g(\omega)$. The choice of $g(\omega)$ will be specified later. A_S is a system coupling operator which generates transitions between different energy levels of the system. In this work, A_S is uniformly sampled from a set of coupling operators $\mathcal{A} = \{A^i, -A^i\}_i$ with $\{(A^i)^\dagger\}_i = \{A^i\}_i$ and $\|A^i\| \leq 1$. Specifically, for spin systems, we set $\mathcal{A} = \{\pm X_j, \pm Y_j, \pm Z_j\}_{j=1}^n$; for fermionic systems, we set $\mathcal{A} = \{\pm c_j, \pm c_j^\dagger\}_{j=1}^n$. Finally, we choose the filter function $f(t)$ as $f_\sigma(t) = \frac{1}{(2\pi)^{1/4}\sigma} \exp \left(-\frac{t^2}{4\sigma^2} \right)$. Both Γ and σ are user-specified parameters that control the accuracy of the algorithm.

End to end complexity characterization. The algorithm approximates the target state by iteratively applying the quantum channel Φ_Γ . Each iteration requires simulating the time-dependent Hamiltonian $H_\Gamma(t)$ over the interval $t \in [-T, T]$. Since the auxiliary terms H_E and $A_S \otimes B_E$ are strictly local, their computational overhead relative to simulating H is negligible. Consequently, we define the main cost metric as the total simulation time, $T_{\text{total}} := 2TN_{\text{iter}}$, where N_{iter} denotes the number of iterations required for convergence. Similar characterization has been widely adopted in the literature of dissipative dynamics based algorithm [12–14, 22, 23, 46].

III. MAIN RESULTS

a. Main Result I: Approximate Fixed Point: Let $\rho_{\text{fix}}(\Phi_\Gamma)$ denote the fixed point of the quantum channel Φ_Γ and τ_{mix} be the mixing time of the quantum channel Φ_Γ (defined in Appendix C Definition C.1). We summarize first main theoretical results below.

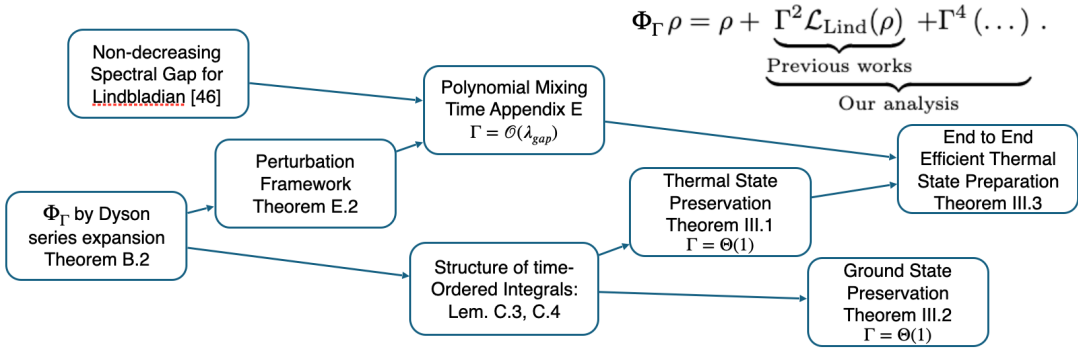


Figure 1: Analysis Flowchart

Theorem III.1 (Informal: thermal state). *For any inverse temperature $\beta > 0$, we can choose the coupling strength $\Gamma = \Theta(1)$ and $T = \tilde{\Omega}(\sigma)$ such that $\|\rho_{\text{fix}}(\Phi_\Gamma) - \sigma_\beta\|_1 = \mathcal{O}\left(\frac{\Gamma^2 \beta}{\sigma^2} \tau_{\text{mix}}\right)$.*

Theorem III.2 (Informal: ground state). *Assume H has a spectral gap Δ . Given precision $\epsilon > 0$, we can choose $\Gamma = \Theta(1)$, $T = \tilde{\Omega}(\sigma)$, and $\sigma = \tilde{\Omega}(\Delta^{-1} \text{polylog}(\tau_{\text{mix}}/\epsilon))$ such that $\|\rho_{\text{fix}}(\Phi_\Gamma) - \sigma_\beta\|_1 \leq \epsilon$.*

Here, we omit the ϵ dependence in τ_{mix} and logarithmic factors in $\|H\|$, β , and $1/\epsilon$ for simplicity. The detailed statements and proofs appear in Appendix D and Appendix E, respectively. The mixing time τ_{mix} (defined in Appendix C Definition C.1) of Φ_Γ characterizes the number of iterations required to reach the fixed point from an arbitrary initial state.

According to Theorem III.1 and Theorem III.2, by choosing $\Gamma = \Theta(1)$ with sufficiently large σ , the fixed point of Φ_Γ can be made arbitrarily close to the target thermal or ground state. Notably, this choice of Γ lies beyond the traditional weak-coupling (Lindblad) regime. In contrast, previous works require $\Gamma = \mathcal{O}(\text{poly}(\epsilon))$, as in [17, 19, 22, 46]. In particular, [22] imposes $\Gamma = \mathcal{O}(\epsilon^{1/2})$ for both cases.

According to the mixing time analysis in Appendix F and [22], the mixing dynamics of Φ_Γ are characterized by the rescaled mixing time $t_{\text{mix}} := \Gamma^2 \tau_{\text{mix}}/\sigma$, which remains constant as σ increases. Consequently, provided t_{mix} is upper bounded, our analysis demonstrates that $\tau_{\text{mix}} = \mathcal{O}(\sigma t_{\text{mix}})$ iterations are sufficient to reach the target state with high accuracy. This constitutes a substantial improvement over the previous bound of $\tau_{\text{mix}} = \mathcal{O}(\sigma^2 \epsilon^{-1} t_{\text{mix}})$ established in [22, 46]. In practice, setting $N_{\text{iter}} = \Theta(t_{\text{mix}})$ suffices, meaning the iteration complexity is reduced by a factor of $\sigma \epsilon^{-1}$. This improvement is rigorously achieved in Theorem III.3 for thermal state preparation. Furthermore, for ground state preparation, where $\sigma = \Theta(\Delta^{-1} \text{polylog}(1/\epsilon))$, this result eliminates the polynomial dependence on the target precision ϵ present in prior work [22].

b. Main result II: End-to-end complexity beyond Lindblad limit Existing literature has studied spectral

gaps of Lindblad dynamics [13] for a broad class of physical models [29, 32–35, 47], including high-temperature local spin Hamiltonians [29, 32], weakly interacting fermionic/spin systems at all temperatures [47], and 1D local Hamiltonians at all temperatures [35]. Our second main theoretical contribution is a general framework that can be combined directly with **all of** these results to analyze the mixing time of the system–bath interaction algorithm *beyond the Lindblad limit*. This yields explicit end-to-end complexity bounds for thermal state preparation via system–bath interaction across a wide range of physical models, as summarized in the following informal theorem.

Theorem III.3 (Informal: Total simulation time bound). *For all the above models with proper choice of parameter. The system-bath interaction algorithm can prepare an ϵ -approximation of the thermal state σ_β with total Hamiltonian simulation time $T_{\text{total}} = \tilde{\mathcal{O}}\left(\frac{n^7}{\epsilon^2}\right)$.*

We put the detailed version of Theorem III.3 (Corollary F.3) and its proof in Appendix F. The above theorem is a direct generalization of the end-to-end complexity results in [46] beyond the Lindblad limit. Because Γ is not required to be small, the above result saves a factor of n^3/ϵ^2 in total runtime compared to [46, Theorem 7].

IV. ANALYSIS OVERVIEW

Our analysis has two components: (i) Rigorous guarantees that the target thermal/ground state is approximately preserved by the discrete quantum channel Φ_Γ ; (ii) a polynomial bound on the total Hamiltonian simulation time for thermal state preparation. Both results are build beyond the Lindblad dynamics, i.e., when $\Gamma = \Theta(1)$. The analysis flow is summarized in Fig. 1.

First, the discrete quantum channel Φ_Γ induced by the system-bath interaction can be written as shown in Fig. 1. Due to the intricate structure of higher-order terms, previous analyses typically truncate the expansion to the leading Lindblad term. The system-bath coupling is then calibrated to ensure that the fixed point

of the Lindbladian approximates the target state. However, this approach is limited by the requirement that the coupling strength is sufficiently small to control the approximation error, thereby necessitating the weak coupling assumption $\Gamma = o(1)$. In this work, as we aim to investigate performance beyond the Lindblad limit, a key technical challenge is characterizing the higher-order terms of the Dyson series expansion when $\Gamma = \Theta(1)$. Since these higher-order terms are non-negligible in this regime, they cannot be treated simply as bounded error terms. Instead, we must demonstrate that the higher-order terms also preserve the target state. This requires analyzing the full series expansion and exploiting cancellations among higher-order contributions—most notably between even and odd terms—to prove state preservation directly, thereby extending the validity of our analysis to $\Gamma = \Theta(1)$. A key technical ingredient of our work is a time-domain framework for the detailed-balance transformation (see Lemma D.3 and Lemma D.4), designed to handle the multidimensional operator Fourier transform structure. Compared to previous Bohr-frequency domain approximation techniques [12, 17], this framework significantly simplifies the expansion of the Dyson series and offers superior compatibility with the time-ordered integral structure of higher-order terms. We expect this time-domain framework to be of independent interest and broadly useful for analyzing discrete channels generated by system-bath interaction models.

Second, Theorem III.1 establishes that the end-to-end complexity is governed by the mixing time of the channel Φ_Γ . To the best of our knowledge, existing literature focuses exclusively on the mixing time of Lindbladian or near-Lindbladian dynamics; consequently, these techniques are not directly applicable to our setting where $\Gamma = \Theta(1)$. To bridge this gap, we decompose Φ_Γ into a second-order term and a higher-order remainder. The second-order term corresponds to a KMS detailed-balance Lindbladian with a nonvanishing spectral gap. Leveraging a recent monotonic spectral gap result from [46], we lower bound this gap by a constant independent of σ . While the second-order term possesses the desired spectral gap and fixed point, our regime of interest includes $\Theta(1)$ higher-order terms that could potentially close the gap and slow down mixing. To address this, we develop a general perturbation framework for quantum channels, inspired by [12, 22, 46], that bounds the spectral gap stability under perturbations. By utilizing the time-domain framework developed for our fixed-point analysis, we directly control the higher-order terms within the KMS inner-product structure. Specifically, we demonstrate that if the second-order truncation has a spectral gap λ_{gap} , choosing $\Gamma^2 = \mathcal{O}(\lambda_{\text{gap}})$ suffices to preserve the gap up to a constant factor. This analysis establishes the mixing-time bound in Theorem III.3. Our result generalizes [46] by incorporating higher-order terms via perturbation theory. Furthermore, this general framework is compatible with the KMS inner-product structure and can be seamlessly combined with all exist-

ing mixing-time results for KMS detailed-balance Lindbladians.

V. NUMERICAL RESULTS

We numerically implement the system bath interaction algorithm to validate our analysis results in the constant coupling regime $\Gamma = \Theta(1)$ and to probe its behavior in the strong coupling regime $\Gamma = \Theta(\sigma)$. As we discussed before, we expect the rescaled mixing time $t_{\text{mix}} := \Gamma^2 \tau_{\text{mix}} / \sigma$ to remain constant as σ increases. We define $\alpha = \Gamma / \sqrt{\sigma}$ and characterize the mixing time τ_{mix} as a function of α to verify the predicted $\mathcal{O}(\alpha^{-2})$ scaling.

We first consider the transverse field Ising model (TFIM) with up to $L = 8$ sites:

$$H = -J \sum_{i=1}^{L-1} Z_i Z_{i+1} - g \sum_{i=1}^L X_i, \quad (3)$$

with $J = 1, g = 1.2$. We sample A_S uniformly chosen from the single qubit Pauli set, with positive and negative signs assigned with equal probability. Starting from the initial state, we simulate the dynamics by iteratively applying the discrete quantum channel Φ_Γ and track the evolution via the fidelity $F(\rho, \sigma_\beta) = \left(\text{Tr} \sqrt{\sqrt{\sigma_\beta} \rho \sqrt{\sigma_\beta}} \right)^2$ recorded as a function of the number of channel applications along a single trajectory. Fig. 2a shows that, upon fixing the filter width $\sigma = 1$ and varying the coupling strength $\Gamma = \Theta(1)$, the iterates converge to σ_β , with a faster convergence for larger α . This observation is in quantitative agreement with the scaling predicted in Theorem III.1.

Next we consider the 1-D Hubbard model defined with up to $L = 4$ spinful sites with open boundary conditions,

$$H = -t \sum_{j=1}^{L-1} \sum_{\sigma \in \{\uparrow, \downarrow\}} c_{j,\sigma}^\dagger c_{j+1,\sigma} + U \sum_{j=1}^L (n_{j,\uparrow} - \frac{1}{2})(n_{j,\downarrow} - \frac{1}{2}). \quad (4)$$

where the number operator $n_{j,\sigma} = c_{j,\sigma}^\dagger c_{j,\sigma}$ and the dimension is 2^{2L} . We choose $t = 1, U = -4$, and sample A_S uniformly from $\mathcal{A} = \left\{ \pm c_{j,\sigma}, \pm c_{j,\sigma}^\dagger \right\}_{j=1, \dots, L, \sigma=\uparrow, \downarrow}$. We numerically calculate the quantum channel Φ_Γ as a superoperator and compute its fixed point and spectral gap. This enables us to quantify the accuracy of the fixed point in approximating the target state and to assess the spectral gap of the channel under various parameter settings, which directly characterize the accuracy of the fixed point and the mixing time. Fig. 2b shows that the spectral gap remains independent of σ and scales quadratically as α^2 . The mixing time follows $\mathcal{O}(\alpha^{-2})$ scaling over the tested range, with no sensitive dependence on σ .

Finally, we consider the ground state preparation for the one-dimensional axial next-nearest-neighbor Ising (ANNI) model [48] in the *strong coupling* regime $\Gamma = \Theta(\sigma)$. In [21], it was shown that preparing the ground

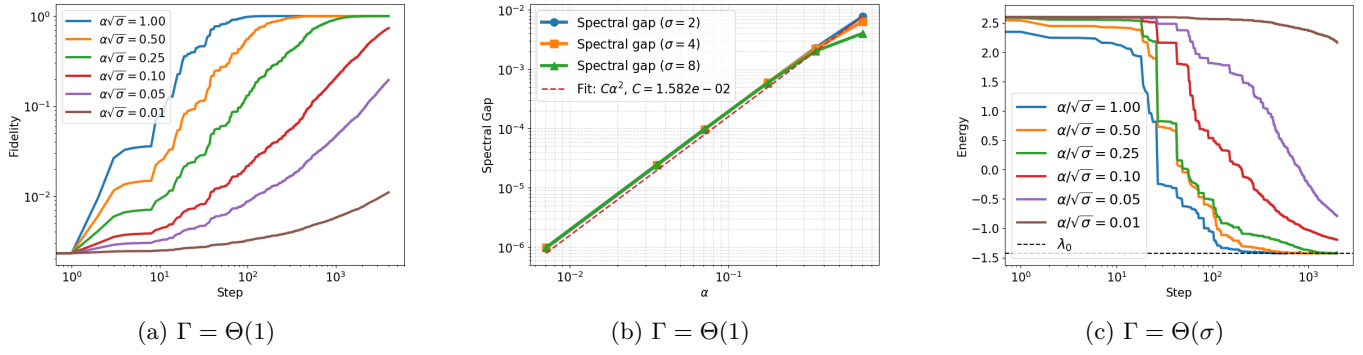


Figure 2: (a) Fidelity of thermal state preparation for TFIM with $L = 4$ sites in the $\Gamma = \Theta(1)$ regime. Parameters are $\beta = 1$, $\sigma = 2$, and $T = 5\sigma$. The frequency ω is sampled uniformly from the interval $[0, 5]$. (b) Spectral gap of Φ_Γ of thermal state preparation for the Hubbard model with $L = 2$ sites in the $\Gamma = \Theta(1)$ regime. The spectral gap scales as α^2 and is independent of σ . (c) Evolution of energy for ground state preparation of the ANNNI model in the $\Gamma = \Theta(\sigma)$ regime, λ_0 is the ground state energy.

state of H_{ANNNI} via adiabatic evolution is challenging, as the effective spectral gap closes multiple times along the adiabatic path if the initial Hamiltonian is set to be $H_0 = -Z$. In our work, we evaluate the performance of our ground state preparation algorithm on this model with the same choice of parameters as that in the case of TFIM or Hubbard models. We continue to observe clear convergence of the energy toward the ground state energy versus the number of iterative steps, which is consistent with the state preservation result in Theorem III.2. Moreover, the flexibility to choose $\Gamma = \Theta(\sigma)$ in Fig. 2c enables the use of larger couplings, leading to a larger spectral gap and faster mixing. Developing a corresponding theoretical understanding in this strong-coupling regime remains an interesting direction for future work.

We note that the strong coupling regime $\Gamma = \Theta(\sigma)$ is not a special case of ANNNI model. In Appendix G, we conduct more detailed numerical experiments for all three models in both constant coupling regime $\Gamma = \Theta(1)$ and the strong coupling regime $\Gamma = \Theta(\sigma)$.

VI. CONCLUSION AND OUTLOOK

In this work, we theoretically demonstrated that system-bath interaction models can prepare thermal and ground states beyond the traditional weak-coupling (Lindblad) limit. We prove that, when the interaction strength per iteration is $\Theta(1)$, the fixed point of the induced quantum channel can still closely approximate the target state. Furthermore, for the thermal state preparation problem, we establish a rigorous mixing-time analysis beyond the Lindblad limit, leading to improved end-to-end complexity. This result substantially broadens the theoretical understanding of system-bath interaction

frameworks and significantly improves the previous rigorous performance guarantees for dissipative state preparation algorithms. Conceptually, it suggests that thermalization and cooling processes may be far more robust than previously anticipated, opening new avenues for designing more efficient quantum state preparation algorithms suitable for near-term devices.

Beyond our theoretical results, several promising directions for future research remain. First, our numerical experiments suggest that system-bath interaction models may perform even better in practice than our current bounds indicate, particularly in the strong-coupling regime where $\Gamma = \Theta(\sigma)$. Developing a theoretical understanding of this regime would further clarify the robustness and efficiency of these algorithms. Second, while we provide a rigorous end-to-end complexity for thermal state preparation, extending the analysis to ground state preparation remains open. The complexity bound in Theorem III.3 is also likely not tight, and sharpening it is an interesting direction for future work (see the detailed discussion in Appendix F 3). Third, our work varies the coupling parameter Γ while keeping σ large to ensure an accurate fixed point approximation. Although large σ improves accuracy, it also increases the required interaction time T and thus the implementation cost per-iteration. An interesting question is whether one can further reduce the dependence on σ while maintaining good performance, analogous to the improvement achieved in [13] over [12] in the context of Lindbladian dynamics.

Acknowledgments— This work was supported in part by the University of Michigan through a startup grant of Z.D. (Z.D., K.W.) and the Van Loo Postdoctoral Fellowship (K.W.). The authors thank Yongtao Zhan, Lin Lin, Daniel Stilck França, Chi-Fang Chen, Andréas Gilyén for helpful discussions.

[1] Frank Verstraete, Michael M. Wolf, and I. Cirac. Quantum computation and quantum-state engineering driven by dissipation. *Nat. Phys.*, 5(9):633–636, 2009.

[2] Frederik Nathan and Mark S. Rudner. Universal lindblad equation for open quantum systems. *Phys. Rev. B*, 102:115109, Sep 2020.

[3] Sthitadhi Roy, JT Chalker, IV Gornyi, and Yuval Gefen. Measurement induced steering of quantum systems. *Phys. Rev. Research*, 2(3):033347, 2020.

[4] Leo Zhou, Soonwon Choi, and Mikhail D Lukin. Symmetry-protected dissipative preparation of matrix product states. *Phys. Rev. A*, 104(3):032418, 2021.

[5] Toby S. Cubitt. Dissipative ground state preparation and the dissipative quantum eigensolver. *arXiv:2303.11962*, 2023.

[6] Yunzhao Wang, Kyrylo Snizhko, Alessandro Romito, Yuval Gefen, and Kater Murch. Dissipative preparation and stabilization of many-body quantum states in a superconducting qutrit array. *Phys. Rev. A*, 108:013712, 2023.

[7] Tsung-Cheng Lu, Leonardo A Lessa, Isaac H Kim, and Timothy H Hsieh. Measurement as a shortcut to long-range entangled quantum matter. *PRX Quantum*, 3(4):040337, 2022.

[8] K. Temme, T. J. Osborne, K. G. Vollbrecht, D. Poulin, and F. Verstraete. Quantum Metropolis sampling. *Nature*, 471(7336):87–90, March 2011.

[9] Evgeny Mozgunov and Daniel Lidar. Completely positive master equation for arbitrary driving and small level spacing. *Quantum*, 4:227, February 2020.

[10] Oles Shtanko and Ramis Movassagh. Preparing thermal states on noiseless and noisy programmable quantum processors. *arXiv:2112.14688*, 2021.

[11] Patrick Rall, Chunhao Wang, and Paweł Wocjan. Thermal state preparation via rounding promises. *Quantum*, 7:1132, 2023.

[12] Chi-Fang Chen, Michael J Kastoryano, Fernando GSL Brandão, and András Gilyén. Quantum thermal state preparation. *arXiv:2303.18224*, 2023.

[13] Chi-Fang Chen, Michael J Kastoryano, and András Gilyén. An efficient and exact noncommutative quantum Gibbs sampler. *arXiv:2311.09207*, 2023.

[14] Zhiyan Ding, Bowen Li, and Lin Lin. Efficient quantum Gibbs samplers with Kubo–Martin–Schwinger detailed balance condition. *Commun. Math. Phys.*, 406(3):67, 2025.

[15] András Gilyén, Chi-Fang Chen, Joao F. Doriguello, and Michael J. Kastoryano. Quantum generalizations of Glauber and Metropolis dynamics. *arXiv:2405.20322*, 2024.

[16] Hao-En Li, Yongtao Zhan, and Lin Lin. Dissipative ground state preparation in ab initio electronic structure theory. *arXiv:2411.01470*, 2024.

[17] Dominik Hahn, S. A. Parameswaran, and Benedikt Placke. Provably efficient quantum thermal state preparation via local driving. *arXiv:2505.22816*, 2025.

[18] Josias Langbehn, George Mouloudakis, Emma King, Raphaël Menu, Igor Gornyi, Giovanna Morigi, Yuval Gefen, and Christiane P. Koch. Universal cooling of quantum systems via randomized measurements. *arXiv:2506.11964*, 2025.

[19] Jerome Lloyd and Dmitry A. Abanin. Quantum thermal state preparation for near-term quantum processors. *arXiv:2506.21318*, 2025.

[20] Matteo Scandi and Álvaro M. Alhambra. Thermalization in open many-body systems and KMS detailed balance. *arXiv:2505.20064*, 2025.

[21] Yongtao Zhan, Zhiyan Ding, Jakob Huhn, Johnnie Gray, John Preskill, Garnet Kin-Lic Chan, and Lin Lin. Rapid quantum ground state preparation via dissipative dynamics. *arXiv:2503.15827*, 2025.

[22] Zhiyan Ding, Yongtao Zhan, John Preskill, and Lin Lin. End-to-end efficient quantum thermal and ground state preparation made simple. *arXiv:2508.05703*, 2025.

[23] Zhiyan Ding, Chi-Fang Chen, and Lin Lin. Single-ancilla ground state preparation via Lindbladians. *Phys. Rev. Research*, 6:033147, 2024.

[24] Goran Lindblad. On the generators of quantum dynamical semigroups. *Commun. Math. Phys.*, 48:119–130, 1976.

[25] Vittorio Gorini, Andrzej Kossakowski, and Ennackal Chandy George Sudarshan. Completely positive dynamical semigroups of n -level systems. *J. Math. Phys.*, 17:821–825, 1976.

[26] Kristan Temme, Michael James Kastoryano, Mary Beth Ruskai, Michael Marc Wolf, and Frank Verstraete. The χ^2 -divergence and mixing times of quantum Markov processes. *J. Math. Phys.*, 51(12), 2010.

[27] Michael J Kastoryano and Kristan Temme. Quantum logarithmic Sobolev inequalities and rapid mixing. *J. Math. Phys.*, 54(5):1–34, 2013.

[28] Ivan Bardet, Ángela Capel, Li Gao, Angelo Lucia, David Pérez-García, and Cambyse Rouzé. Rapid thermalization of spin chain commuting Hamiltonians. *Phys. Rev. Lett.*, 130(6):060401, 2023.

[29] Cambyse Rouzé, Daniel Stilck França, and Álvaro M. Alhambra. Efficient thermalization and universal quantum computing with quantum gibbs samplers. In *STOC 25*, page 1488–1495, 2025.

[30] Zhiyan Ding, Bowen Li, Lin Lin, and Ruizhe Zhang. Polynomial-time preparation of low-temperature Gibbs states for 2D Toric Code. *arXiv:2410.01206*, 2024.

[31] Jan Kochanowski, Alvaro M Alhambra, Angela Capel, and Cambyse Rouzé. Rapid thermalization of dissipative many-body dynamics of commuting Hamiltonians. *Commun. Math. Phys.*, 2024.

[32] Cambyse Rouzé, Daniel Stilck França, and Álvaro M Alhambra. Optimal quantum algorithm for Gibbs state preparation. *arXiv:2411.04885*, 2024.

[33] Yu Tong and Yongtao Zhan. Fast mixing of weakly interacting fermionic systems at any temperature. *PRX Quantum*, 6:030301, Jul 2025.

[34] Štěpán Šmid, Richard Meister, Mario Berta, and Roberto Bondesan. Polynomial time quantum Gibbs sampling for Fermi–Hubbard model at any temperature. *arXiv:2501.01412*, 2025.

[35] Thiago Bergamaschi and Chi-Fang Chen. Fast mixing of quantum spin chains at all temperatures. *arXiv:2510.08533*, 2026.

[36] Richard Cleve and Chunhao Wang. Efficient quantum algorithms for simulating Lindblad evolution. In *ICALP 2017*, volume 80, pages 17:1–17:14, 2017.

[37] Xiantao Li and Chunhao Wang. Simulating Markovian open quantum systems using higher-order series expansion. In *ICALP 2023*, volume 261, pages 87:1–87:20, 2023.

[38] Zhiyan Ding, Xiantao Li, and Lin Lin. Simulating open quantum systems using Hamiltonian simulations. *PRX Quantum*, 5:020332, 2024.

[39] Trond I Andersen, Nikita Astrakhantsev, Amir H Karamlou, Julia Berndtsson, Johannes Motruk, Aaron Szasz, Jonathan A Gross, Alexander Schuckert, Tom Westerhout, Yaxing Zhang, et al. Thermalization and criticality on an analogue–digital quantum simulator. *Nature*, 638(8049):79–85, 2025.

[40] Matthew Hagan and Nathan Wiebe. The thermodynamic cost of ignorance: Thermal state preparation with one ancilla qubit. *arXiv:2502.03410*, 2025.

[41] Stefano Polla, Yaroslav Herasymenko, and Thomas E. O’Brien. Quantum digital cooling. *Phys. Rev. A*, 104:012414, Jul 2021.

[42] Hong-Yi Su and Ying Li. Quantum algorithm for the simulation of open-system dynamics and thermalization. *Phys. Rev. A*, 101:012328, Jan 2020.

[43] X. Mi, A. A. Michailidis, S. Shabani, K. C. Miao, P. V. Klimov, J. Lloyd, E. Rosenberg, R. Acharya, I. Aleiner, T. I. Andersen, M. Ansmann, F. Arute, K. Arya, A. Asfaw, J. Atalaya, J. C. Bardin, A. Bengtsson, G. Bortoli, A. Bourassa, J. Bovaard, L. Brill, M. Broughton, B. B. Buckley, D. A. Buell, T. Burger, B. Burkett, N. Bushnell, Z. Chen, B. Chiaro, D. Chik, C. Chou, J. Cogan, R. Collins, P. Conner, W. Courtney, A. L. Crook, B. Curtin, A. G. Dau, D. M. Debroy, A. Del Toro Barba, S. Demura, A. Di Paolo, I. K. Drozdov, A. Dunsworth, C. Erickson, L. Faoro, E. Farhi, R. Fatemi, V. S. Ferreira, L. F. Burgos, E. Forati, A. G. Fowler, B. Foxen, É. Genois, W. Giang, C. Gidney, D. Gilboa, M. Giustina, R. Gosula, J. A. Gross, S. Habegger, M. C. Hamilton, M. Hansen, M. P. Harrigan, S. D. Harrington, P. Heu, M. R. Hoffmann, S. Hong, T. Huang, A. Huff, W. J. Huggins, L. B. Ioffe, S. V. Isakov, J. Iveland, E. Jeffrey, Z. Jiang, C. Jones, P. Juhas, D. Kafri, K. Kechedzhi, T. Khattar, M. Khezri, M. Kieferová, S. Kim, A. Kitaev, A. R. Klots, A. N. Korotkov, F. Kostritsa, J. M. Kreikebaum, D. Landhuis, P. Laptev, K.-M. Lau, L. Laws, J. Lee, K. W. Lee, Y. D. Lensky, B. J. Lester, A. T. Lill, W. Liu, A. Locharla, F. D. Malone, O. Martin, J. R. McClean, M. McEwen, A. Mieszala, S. Montazeri, A. Morvan, R. Movassagh, W. Mruczkiewicz, M. Neeley, C. Neill, A. Nersisyan, M. Newman, J. H. Ng, A. Nguyen, M. Nguyen, M. Y. Niu, T. E. O’Brien, A. Opremcak, A. Petukhov, R. Potter, L. P. Pryadko, C. Quintana, C. Rocque, N. C. Rubin, N. Saei, D. Sank, K. Sankaragomathi, K. J. Satzinger, H. F. Schurkus, C. Schuster, M. J. Shearn, A. Shorter, N. Shutty, V. Shvarts, J. Skrzyni, W. C. Smith, R. Somma, G. Sterling, D. Strain, M. Szalay, A. Torres, G. Vidal, B. Villalonga, C. V. Heidweiller, T. White, B. W. K. Woo, C. Xing, Z. J. Yao, P. Yeh, J. Yoo, G. Young, A. Zalcman, Y. Zhang, N. Zhu, N. Zobrist, H. Neven, R. Babbush, D. Bacon, S. Boixo, J. Hilton, E. Lucero, A. Megrant, J. Kelly, Y. Chen, P. Roushan, V. Smelyanskiy, and D. A. Abanin. Stable quantum-correlated many-body states through engineered dissipation. *Science*, 383(6689):1332–1337, 2024.

[44] Jerome Lloyd, Alexios A. Michailidis, Xiao Mi, Vadim Smelyanskiy, and Dmitry A. Abanin. Quasiparticle cooling algorithms for quantum many-body state preparation. *PRX Quantum*, 6:010361, March 2025.

[45] Carlos Ramon-Escandell, Alessandro Prostutto, and Dvira Segal. Thermal state preparation by repeated interactions at and beyond the Lindblad limit. *arXiv:2506.12166*, 2025.

[46] Samuel Slezak, Matteo Scandi, Álvaro M. Alhambra, Daniel Stilck França, and Cambyse Rouzé. Polynomial-time thermalization and gibbs sampling from system–bath couplings. *arXiv/2601.16154*, 2026.

[47] Štěpán Šmíd, Richard Meister, Mario Berta, and Roberto Bondesan. Rapid mixing of quantum gibbs samplers for weakly-interacting quantum systems. *arXiv/2510.04954*, 2025.

[48] Walter Selke. The anni model-theoretical analysis and experimental application. *Physics Reports*, 170(4):213–264, 1988.

[49] Daniel Molpeceres, Sirui Lu, J. Ignacio Cirac, and Barbara Kraus. Quantum algorithms for cooling: a simple case study. *arXiv:2503.24330*, 2025.

[50] Chi-Fang Chen and Fernando G. S. L. Brandão. Fast thermalization from the eigenstate thermalization hypothesis. *arXiv:2112.07646*, 2023.

[51] Dominik Hahn, Ryan Sweke, Abhinav Deshpande, and Oles Shtanko. Efficient quantum Gibbs sampling with local circuits. *arXiv:2506.04321*, 2025.

[52] Some of the result here prove the rapid mixing property for KMS generators using oscillator norm technique instead of spectral gap. However, rapid mixing directly implies a lower bound for the spectral gap. Thus, we can directly apply their result in our case.

[53] Although it has not been explicitly proved in the literature, we expect similar results should also hold for local fermionic Hamiltonians using similar techniques as in [29, 32–34].

[54] Michael J Kastoryano and Fernando GSL Brandao. Quantum Gibbs samplers: The commuting case. *Commun. Math. Phys.*, 344(3):915–957, 2016.

[55] Franco Fagnola and Veronica Umanità. Generators of detailed balance quantum Markov semigroups. *Infin. Dimens. Anal. Quantum Probab. Relat. Top.*, 10(03):335–363, 2007.

Appendix A: Organization of the appendix

The appendix is organized as follows.

- Appendix B: A review of related works on dissipative state preparation algorithms, with a focus on system–bath interaction models.
- Appendix C: Notations and preliminaries.

- Appendix D: Detailed analysis for thermal state preparation, including the fixed point approximation and mixing time analysis.
- Appendix E: Detailed analysis for ground state preparation, including the fixed point approximation.
- Appendix F: Detailed mixing time analysis for thermal state preparation and proof of Theorem III.3.
- Appendix G: Additional numerical results.

For simplicity, we follow [22] to define $\alpha := \Gamma/\sqrt{\sigma}$ and will use α, Γ interchangeably in the analysis.

Appendix B: Related works

In the literature, there is a vast of work on dissipation quantum algorithms for thermal and ground state preparation [1, 3–23]. Because our paper mainly focuses on the system-bath interaction model, we will mainly review the works that are closely related to ours in this section.

Recently, several system-bath-interaction-based algorithms have been proposed for thermal state preparation [17–20, 22, 40, 49, 50]. While these works share a broadly similar algorithmic structure, they differ in the choice of bath model and in the design of the system-bath interaction. Their theoretical analyses also follow a common pattern, as discussed in Section I: one first approximates the discrete system-bath quantum channel by an effective Lindblad evolution in the weak-coupling limit, and then shows that the fixed point of this Lindbladian is close to the desired target state.

However, because this approach relies critically on the weak-coupling approximation, these methods typically require the coupling strength to vanish with the target precision, often chosen to be polynomially small in the accuracy parameter ϵ [17, 19, 22]. This, in turn, leads to slow mixing of the underlying discrete quantum channel and consequently demands a large number of iterations to reach the target state. Our work departs from this paradigm by directly analyzing the fixed point properties of the discrete quantum channel beyond the weak-coupling limit. This allows us to choose larger coupling strengths, thereby accelerating convergence to the target state and improving overall algorithmic efficiency. It is worth noting that the non-vanishing coupling-strength regime has also been explored in [45], where the authors theoretically study a special three-level system-bath interaction model and numerically investigate a repeated interaction model for thermal and ground-state preparation under moderate coupling strength. However, for general Hamiltonians H , a rigorous theoretical characterization of the fixed-point property in this regime remains open.

Finally, for the mixing time analysis, a large body of work studies mixing times in the Lindbladian framework [21, 26–35], while extensions to discrete quantum channels induced by system-bath interactions have appeared only recently [22, 46]. In particular, [46] provides the first polynomial mixing-time guarantees for the system-bath model [20, 22] in the Lindblad limit for a broad class of physically relevant systems. Its key insight is that the approximating Lindblad dynamics in the weak-coupling regime exhibits a monotonic spectral-gap improvement as the filter width decreases. This monotonicity allows one to choose a sharper filter to ensure correctness of the fixed point while maintaining a nonvanishing spectral gap, which was previously difficult because the quasi-locality of the jump operators deteriorates as the filter sharpens. Building on [46], we extend the mixing-time analysis beyond the Lindblad limit and provide an universal improved end-to-end complexity characterization.

Appendix C: Notations and preliminaries

Notations for norms: For a matrix $A \in \mathbb{C}^{N \times N}$, we denote the complex conjugate, transpose, and Hermitian adjoint by A^* , A^T , and A^\dagger , respectively. The Schatten p -norm is defined as $\|A\|_p := (\sum_i \sigma_i(A)^p)^{1/p}$, where $\sigma_i(A)$ are the singular values of A . This encompasses the trace norm ($\|A\|_1$), the Hilbert–Schmidt/Frobenius norm ($\|A\|_2$), and the operator norm ($\|A\|_\infty \equiv \|A\|$). The trace distance between states ρ and σ is $D(\rho, \sigma) := \frac{1}{2}\|\rho - \sigma\|_1$. Given a superoperator $\Phi : \mathbb{C}^{N \times N} \rightarrow \mathbb{C}^{N \times N}$, the induced trace norm is

$$\|\Phi\|_{1 \rightarrow 1} := \sup_{\|A\|_1=1} \|\Phi(A)\|_1.$$

Bohr frequency: We denote eigenstates of the Hamiltonian H by $\{|\psi_i\rangle\}$ and the corresponding eigenvalues by $\{\lambda_i\}$. Each difference of eigenvalues $\lambda_i - \lambda_j$ is called a Bohr frequency, and $B(H)$ denotes the set of all Bohr frequencies.

Also, given $\nu \in B(H)$ and a matrix A , we define

$$A(\nu) = \sum_{\lambda_j - \lambda_i = \nu} |\psi_j\rangle \langle \psi_j| A |\psi_i\rangle \langle \psi_i|, \quad (\text{C1})$$

where $|\psi_i\rangle$ is an eigenvector of H with eigenvalue λ_i .

Detailed balance condition and mixing time: Let $\sigma_\beta \propto \exp(-\beta H)$ denote the thermal state at inverse temperature β . For $s \in (0, 1)$, we define the s -inner product on the space of operators as

$$\langle A, B \rangle_{s, \sigma_\beta} = \langle A, \sigma_\beta^{1-s} B \sigma_\beta^s \rangle = \text{Tr} \left(A^\dagger \sigma_\beta^{1-s} B \sigma_\beta^s \right).$$

A Lindbladian \mathcal{L} satisfies the KMS detailed balance condition (KMS DBC) if its adjoint \mathcal{L}^\dagger is self-adjoint with respect to the inner product $\langle \cdot, \cdot \rangle_{1/2, \sigma_\beta}$. Similarly, \mathcal{L} satisfies the GNS detailed balance condition (GNS DBC) if \mathcal{L}^\dagger is self-adjoint with respect to $\langle \cdot, \cdot \rangle_{s, \sigma_\beta}$ for all $s \in (0, 1)$. We note that GNS DBC is a strictly stronger condition: if \mathcal{L} satisfies GNS DBC, it naturally satisfies KMS DBC and typically takes the generic form of a Davies generator. Assuming \mathcal{L} satisfies either condition, we define the spectral gap as

$$\text{Gap}(\mathcal{L}) = \inf_{\substack{A \neq 0 \\ \text{Tr}(A \sigma_\beta) = 0}} \frac{-\langle A, \mathcal{L}^\dagger(A) \rangle_{1/2, \sigma_\beta}}{\langle A, A \rangle_{1/2, \sigma_\beta}}.$$

Since we focus on discrete channel Φ_Γ in this work, we define the integer mixing time of Φ_Γ . It quantifies the worst-case convergence speed, i.e. the minimum number of iterations required for an arbitrary initial state to become ϵ -close to the target fixed point.

Definition C.1. Let Φ be a CPTP map with a unique fixed point $\rho_{\text{fix}}(\Phi)$. For any $\epsilon > 0$, the integer mixing time $\tau_{\text{mix}, \Phi}(\epsilon)$ is defined as

$$\tau_{\text{mix}, \Phi}(\epsilon) = \min \left\{ t \in \mathbb{N} \mid \sup_{\rho} \|\Phi^t(\rho) - \rho_{\text{fix}}(\Phi)\|_1 \leq \epsilon \right\}. \quad (\text{C2})$$

According to [22], we define the (rescaled) mixing time as

$$t_{\text{mix}, \Phi}(\epsilon) = \alpha^2 \tau_{\text{mix}, \Phi}(\epsilon). \quad (\text{C3})$$

In the literature, alternative definitions of mixing time are often employed. For instance, the contraction mixing time is defined as

$$t_{\text{mix};c} = \min \left\{ t \in \mathbb{N} \mid \sup_{\rho_1 \neq \rho_2} \frac{\|\Phi^t(\rho_1) - \Phi^t(\rho_2)\|_1}{\|\rho_1 - \rho_2\|_1} \leq \frac{1}{2} \right\}.$$

A well-known result relates these quantities by $t_{\text{mix}}(\epsilon) \leq t_{\text{mix};c} (\log_2(1/\epsilon) + 1)$, implying that $t_{\text{mix}}(\epsilon)$ scales logarithmically with $1/\epsilon$ provided $t_{\text{mix};c}$ is finite [27].

Asymptotic notations: We adopt the following asymptotic notations beside the usual big \mathcal{O} one. We write $f = \Omega(g)$ if $g = \mathcal{O}(f)$; $f = \Theta(g)$ if $f = \mathcal{O}(g)$ and $g = \mathcal{O}(f)$. The notations $\tilde{\mathcal{O}}$, $\tilde{\Omega}$, $\tilde{\Theta}$ are used to suppress subdominant polylogarithmic factors. If not specified, $f = \tilde{\mathcal{O}}(g)$ if $f = \mathcal{O}(g \text{ polylog}(g))$; $f = \tilde{\Omega}(g)$ if $f = \Omega(g \text{ polylog}(g))$; $f = \tilde{\Theta}(g)$ if $f = \Theta(g \text{ polylog}(g))$. Note that these tilde notations do not remove or suppress dominant polylogarithmic factors. For instance, if $f = \mathcal{O}(\log g \log \log g)$, then we write $f = \tilde{\mathcal{O}}(\log g)$ instead of $f = \tilde{\mathcal{O}}(1)$.

1. Dyson series expansion of Φ_Γ

In this section, we introduce the Dyson series expansion of Φ_Γ in Eq. (1). We use the subindex $\{-1, 1\}$ to relabel the system and bath operator as

$$S_1 = A_S, \quad S_{-1} = A_S^\dagger, \quad B_1 = B_E, \quad B_{-1} = B_E^\dagger.$$

Define the system evolution operator $U_S(t) = \exp(-itH)$. The Dyson series expansion of Φ_Γ is summarized in the following theorem:

Theorem C.2. Let $\rho_{n+1} = \Phi_\Gamma(\rho_n)$, then ρ_{n+1} can be generated by the following three steps:

- $\rho_{n+1/3} = U_S(T)\rho_n U_S^\dagger(T)$
- $$\begin{aligned} \rho_{n+2/3} &= \rho_{n+1/3} + \mathbb{E}_{A_S} \left(\sum_n \Gamma^{2n} (-1)^n \sum_{k=0}^{2n} (-1)^k \int \frac{g(\omega)}{1+e^{\beta\omega}} G_{2n-k, A_S}^\dagger(\omega) \rho_{n+1/3} G_{k, A_S}(\omega) d\omega \right. \\ &\quad \left. + \sum_n \Gamma^{2n} (-1)^n \sum_{k=0}^{2n} (-1)^k \int \frac{g(\omega)e^{\beta\omega}}{1+e^{\beta\omega}} F_{2n-k, A_S}^\dagger(\omega) \rho_{n+1/3} F_{k, A_S}(\omega) d\omega \right) = \Phi_{\text{part}, \Gamma} \rho_{n+1/3}; \end{aligned} \quad (\text{C4})$$
- $\rho_{n+1} = U_S(T)\rho_{n+2/3} U_S^\dagger(T).$

Here

$$\begin{aligned} G_{k, A_S}(\omega) &= \int_{-T < t_1 \leq \dots \leq t_k < T} A_S(t_1) A_S^\dagger(t_2) \cdots S_{(-1)^{k-1}}(t_k) e^{-i\omega \sum_{p=1}^k (-1)^p t_p} f(t_1) \cdots f(t_k) dt_1 \cdots dt_k \\ F_{k, A_S}(\omega) &= \int_{-T < t_1 \leq \dots \leq t_k < T} A_S^\dagger(t_1) A_S(t_2) \cdots S_{(-1)^k}(t_k) e^{i\omega \sum_{p=1}^k (-1)^p t_p} f(t_1) \cdots f(t_k) dt_1 \cdots dt_k. \end{aligned} \quad (\text{C5})$$

Define $\gamma(\omega) = \frac{g(\omega) + g(-\omega)}{1 + \exp(\beta\omega)}$. In the case when A_S is uniformly sampled from a set of coupling operators $\mathcal{A} = \{A^i, -A^i\}_i$ with $\{(A^i)^\dagger\}_i = \{A^i\}_i$, we can rewrite (C4) as

$$\rho_{n+2/3} = \rho_{n+1/3} + \mathbb{E}_{A_S} \left(\sum_n \Gamma^{2n} (-1)^n \sum_{k=0}^{2n} (-1)^k \int \gamma(\omega) G_{2n-k, A_S}^\dagger(\omega) \rho_{n+1/3} G_{k, A_S}(\omega) d\omega \right). \quad (\text{C6})$$

Proof. For simplicity, we fixed A_S . We use the subindex $\{-1, 1\}$ to relabel the system and bath operator as

$$S_1 = A_S, S_{-1} = A_S^\dagger, B_1 = B_E, B_{-1} = B_E^\dagger.$$

Recall Eq. (2):

$$H_\Gamma(t) = H + H_E + \Gamma f(t) \left(A_S \otimes B_E + A_S^\dagger \otimes B_E^\dagger \right), \quad H_E = -\omega Z/2, \quad B_E = |1\rangle \langle 0|.$$

For the dynamics described by

$$\begin{cases} \partial_t \rho(t) = -i[H_\Gamma(t), \rho(t)], \\ \rho(-T) = \rho_n \otimes \rho_E, \\ \rho_{n+1} = \mathbb{E}_{H_E, A_S}(\text{Tr}_E \rho(T)), \end{cases} \quad (\text{C7})$$

the evolution operator of the time-dependent Hamiltonian can be expressed using the time-ordered exponential as $U^\Gamma(t) := U^\Gamma(t; -T) = \mathcal{T} \left(\exp \left(-i \int_{-T}^t H_\Gamma(s) ds \right) \right)$, and it satisfies

$$\partial_t U^\Gamma(t; -T) = -i H_\Gamma(t) U^\Gamma(t; -T). \quad (\text{C8})$$

By Duhamel's expression, the Dyson series expansion can be written as $U^\Gamma(t; -T) = \sum_{n \geq 0} (-i\Gamma)^n U_n(t; -T)$, where

$$U_n(t; -T) = \int_{-T}^t \int_{-T}^{s_1} \cdots \int_{-T}^{s_{n-1}} f(s_1) f(s_2) \cdots f(s_n) U_0(t; s_1) H_{S, B} U_0(s_1; s_2) \cdots H_{S, B} U_0(s_n; -T) ds_n \cdots ds_1. \quad (\text{C9})$$

Here $H_{S, B} = S_1 \otimes B_1 + S_{-1} \otimes B_{-1}$ and $U_0(t; -T) = \exp(-i(t+T)(H + H_E))$. The Heisenberg picture evolution of the bath operator follows $B_{(-1)^p}(t) = e^{(-1)^p i t \omega} B_{(-1)^p}$.

After taking expectation in ω and tracing out the degree of freedom in the environment,

$$\begin{aligned}
\Phi_\Gamma \rho &= \int g(\omega) \text{Tr}_E[U^\Gamma(T)(\rho \otimes \rho_E)U^{\Gamma\dagger}(T)](\omega) d\omega \\
&= \sum_{n,m \geq 0} (-i\Gamma)^n (i\Gamma)^m \int g(\omega) \text{Tr}_E[U_n(T; -T)(\rho \otimes \rho_E)U_m^\dagger(T; -T)](\omega) d\omega \\
&= \sum_{n,m \geq 0} (-1)^n (i\Gamma)^{n+m} \int d\omega \int_{-T \leq s_n \leq \dots \leq s_1 \leq T, -T \leq \tau_m \leq \dots \leq \tau_1 \leq T} ds_1 \dots ds_n d\tau_1 \dots d\tau_m g(\omega) \\
&\quad \sum_{\alpha_i, \beta_j \in \{-1, 1\}} U_S(T) S_{\alpha_1}(s_1) \dots S_{\alpha_n}(s_n) f(s_1) \dots f(s_n) U_S(T) \rho U_S^\dagger(T) S_{\beta_m}^\dagger(\tau_m) \dots S_{\beta_1}^\dagger(\tau_1) U_S^\dagger(T) \\
&\quad f(\tau_1) \dots f(\tau_m) \text{Tr}_E(B_{\alpha_1}(s_1) \dots B_{\alpha_n}(s_n) \rho_E B_{\beta_m}^\dagger(\tau_m) \dots B_{\beta_1}^\dagger(\tau_1)),
\end{aligned} \tag{C10}$$

where $U_S(T) = \exp(-iT\mathcal{H})$ and $S_\alpha(t) = \exp(iHt)S_\alpha \exp(-iHt)$. Notice that $B_\alpha^\dagger(t) = B_{-\alpha}(t)$, the multi-point bath correlation function follows

$$\begin{aligned}
&\text{Tr}[B_{\alpha_1}(s_1) \dots B_{\alpha_n}(s_n) \rho_E B_{\beta_m}^\dagger(\tau_m) \dots B_{\beta_1}^\dagger(\tau_1)] \\
&= \text{Tr}[B_{-\beta_m}(\tau_m) \dots B_{-\beta_1}(\tau_1) B_{\alpha_1}(s_1) \dots B_{\alpha_n}(s_n) \rho_E] \\
&= e^{i\phi} \text{Tr}[B_{-\beta_m} \dots B_{-\beta_1} B_{\alpha_1} \dots B_{\alpha_n} \rho_E],
\end{aligned}$$

where $\phi = \omega \left(\sum_{j=1}^n \alpha_j s_j - \sum_{k=1}^m \beta_k \tau_k \right)$. It can be rewritten as

$$(\dots) = e^{i\phi} \times \begin{cases} \text{Tr}(|1\rangle\langle 1| \rho_E) = \frac{1}{e^{\beta\omega} + 1}, & \text{if } m+n \text{ even and } (-\beta_m, \dots, -\beta_1, \alpha_1, \dots, \alpha_n) = (1, -1)^{\otimes \frac{m+n}{2}}, \\ \text{Tr}(|0\rangle\langle 0| \rho_E) = \frac{e^{\beta\omega}}{e^{\beta\omega} + 1}, & \text{if } m+n \text{ even and } (-\beta_m, \dots, -\beta_1, \alpha_1, \dots, \alpha_n) = (-1, 1)^{\otimes \frac{m+n}{2}}, \\ 0, & \text{otherwise.} \end{cases} \tag{C11}$$

Substituting the expression of the bath correlation functions back to Eq. (C10), we have

$$\begin{aligned}
\Phi_\Gamma \rho_n &= U_S(2T) \rho_n U_S(2T)^\dagger \\
&+ \sum_{n \geq 1} \Gamma^{2n} (-1)^n \sum_{k=0}^{2n} (-1)^k \int \frac{g(\omega)}{1 + e^{\beta\omega}} U_S(T) G_{2n-k, A_S}^\dagger(\omega) U_S(T) \rho_n U_S^\dagger(T) G_{k, A_S}(\omega) U_S^\dagger(T) d\omega \\
&+ \sum_{n \geq 1} \Gamma^{2n} (-1)^n \sum_{k=0}^{2n} (-1)^k \int \frac{g(\omega) e^{\beta\omega}}{1 + e^{\beta\omega}} U_S(T) F_{2n-k, A_S}^\dagger(\omega) U_S(T) \rho_n U_S^\dagger(T) F_{k, A_S}(\omega) U_S^\dagger(T) d\omega,
\end{aligned} \tag{C12}$$

where

$$\begin{aligned}
G_{k, A_S}(\omega) &= \int_{-T < t_1 \leq \dots \leq t_k < T} A_S(t_1) A_S^\dagger(t_2) \dots S_{(-1)^{k-1}}(t_k) e^{-i\omega \sum_{p=1}^k (-1)^p t_p} f(t_1) \dots f(t_k) dt_1 \dots dt_k \\
F_{k, A_S}(\omega) &= \int_{-T < t_1 \leq \dots \leq t_k < T} A_S^\dagger(t_1) A_S(t_2) \dots S_{(-1)^k}(t_k) e^{i\omega \sum_{p=1}^k (-1)^p t_p} f(t_1) \dots f(t_k) dt_1 \dots dt_k.
\end{aligned}$$

Additionally, using the relation $F_{k, A_S^\dagger}(-\omega) = G_{k, A_S}(\omega)$, we can further simplify the expression to Eq. (C6) in the case $\mathcal{A}^\dagger = \mathcal{A}$. This concludes the proof. \square

Appendix D: Thermal state preparation beyond Lindblad limit

In this section, we introduce the rigorous version of Theorem III.1 and provide the proof. First, recall Theorem C.2 (C6),

- $\rho_{n+1/3} = U_S(T)\rho_n U_S^\dagger(T)$;
- $\rho_{n+2/3} = \rho_{n+1/3} + \mathbb{E}_{A_S} \left(\sum_n \Gamma^{2n} (-1)^n \sum_{k=0}^{2n} (-1)^k \int \gamma(\omega) G_{2n-k, A_S}^\dagger(\omega) \rho_{n+1/3} G_{k, A_S}(\omega) d\omega \right)$;
- $\rho_{n+1} = U_S(T)\rho_{n+2/3} U_S^\dagger(T)$.

We present the rigorous version of Theorem III.1 in the following.

Theorem D.1 (Thermal state, rigorous version). *Assume $0 \leq \beta < \infty$ and $\gamma(\omega)$ satisfies the property:*

- *decay fast at infinity, i.e. $\lim_{|\omega| \rightarrow \infty} \gamma(\omega) = 0$.*
- $\gamma'(\omega), (\tilde{\gamma}(\omega))' \in L^1$.

where $\tilde{\gamma}(\omega) = \gamma(\omega)e^{\beta\omega}$. Assume $\Gamma = \mathcal{O}(1)$, $\sigma = \Omega(\beta)$, and $T = \Omega(\sigma)$. Then,

$$\|\Phi_\Gamma \sigma_\beta - \sigma_\beta\|_1 < \mathcal{O} \left(\frac{\beta \Gamma^2}{\sigma^2} ((\|\gamma'\|_{L^1} + \|\tilde{\gamma}'\|_{L^1}) \log(\sigma)) + \frac{\Gamma^2 \sigma}{T} e^{-T^2/(4\sigma^2)} \right). \quad (\text{D1})$$

Furthermore, given any $\epsilon > 0$ and $\|\gamma'\|_{L^1} + \|\tilde{\gamma}'\|_{L^1} = \mathcal{O}(1)$, if $\Gamma = \mathcal{O}(1)$, $\sigma = \tilde{\Theta}(\beta t_{\text{mix}, \Phi}(\epsilon/4)/\epsilon)$, $T = \tilde{\Theta}(\sigma)$, then $\|\rho_{\text{fix}}(\Phi_\Gamma) - \sigma_\beta\|_1 \leq \epsilon/2$. In addition, for any initial state ρ_0 ,

$$\left\| \Phi_\Gamma^{\tau_{\text{mix}, \Phi}(\epsilon/4)}(\rho_0) - \sigma_\beta \right\|_1 < \epsilon. \quad (\text{D2})$$

Here, the rescaled mixing time $t_{\text{mix}, \Phi}(\epsilon) := \Gamma^2 \tau_{\text{mix}, \Phi}(\epsilon)/\sigma$ defined in Definition C.1.

We note that the second part of the result (D2) follows from combining the first part with [22, Theorem 8]. Now, we provide the proof of the first part of Theorem D.1. Letting $T \rightarrow \infty$, we define

$$\tilde{G}_{k, A_S}(\omega) := \int_{-\infty < t_1 \leq \dots \leq t_k < \infty} A_S(t_1) A_S^\dagger(t_2) \cdots e^{-i\omega \sum_{p=1}^k (-1)^p t_p} f(t_1) \cdots f(t_k) dt_1 \cdots dt_k, \quad (\text{D3})$$

and the limiting CPTP map

$$\tilde{\Phi}_\Gamma := U_S(2T)\rho_n U_S^\dagger(2T) + \mathbb{E}_{A_S} \left(\sum_{n \geq 1} \Gamma^{2n} (-1)^n \sum_{k=0}^{2n} (-1)^k \int \gamma(\omega) U_S(T) \tilde{G}_{2n-k, A_S}^\dagger(\omega) U_S(T) \rho_n U_S^\dagger(T) \tilde{G}_{k, A_S}(\omega) U_S^\dagger(T) d\omega \right). \quad (\text{D4})$$

The distance between Φ_Γ and $\tilde{\Phi}_\Gamma$ can be controlled in the following lemma:

Lemma D.2. *When $\Gamma = \mathcal{O}(1)$, we have*

$$\|\Phi_\Gamma - \tilde{\Phi}_\Gamma\|_{1 \rightarrow 1} = \mathcal{O} \left(\frac{\Gamma^2 \sigma}{T} e^{-T^2/(4\sigma^2)} \right). \quad (\text{D5})$$

Proof of Lemma D.2. For simplicity, we only consider the case when $\mathcal{A} = \{A_S, -A_S\}$ is fixed. The general case is almost the same. By the general expression of the dynamic map, we have

$$\begin{aligned} & \|\Phi_\Gamma - \tilde{\Phi}_\Gamma\|_{1 \rightarrow 1} \\ & \leq \max_{\rho_n: \|\rho_n\|=1} \sum_{n \geq 1} \Gamma^{2n} \sum_{k=0}^{2n} \int |\gamma(\omega)| \left\| \tilde{G}_{2n-k, A_S}^\dagger(\omega) U_S(T) \rho_n U_S^\dagger(T) \tilde{G}_{k, A_S}(\omega) - G_{2n-k, A_S}^\dagger(\omega) U_S(T) \rho_n U_S^\dagger(T) G_{k, A_S}(\omega) \right\|_1 d\omega \\ & \leq \sum_{n \geq 1} \Gamma^{2n} \sum_{k=0}^{2n} \int |\gamma(\omega)| \left\| \tilde{G}_{2n-k, A_S}^\dagger(\omega) - G_{2n-k, A_S}^\dagger(\omega) \right\| \left\| \tilde{G}_{k, A_S}(\omega) \right\| d\omega \\ & \quad + \sum_{n \geq 1} \Gamma^{2n} \sum_{k=0}^{2n} \int |\gamma(\omega)| \left\| G_{2n-k, A_S}^\dagger(\omega) \right\| \left\| G_{k, A_S}(\omega) - \tilde{G}_{k, A_S}(\omega) \right\| d\omega \end{aligned} \quad (\text{D6})$$

It is sufficient to bound $\|G_{k,A_S}(\omega) - \tilde{G}_{k,A_S}(\omega)\|$ and $\|G_{k,A_S}(\omega)\|$, $\|\tilde{G}_{k,A_S}(\omega)\|$. For the first term, we have

$$\begin{aligned}
& \|G_{k,A_S}(\omega) - \tilde{G}_{k,A_S}(\omega)\| \\
& \leq \left\| \left(\int_{-\infty < t_1 \leq \dots \leq t_k < \infty} - \int_{-T < t_1 \leq \dots \leq t_k < T} \right) A_S(t_1) A_S^\dagger(t_2) \dots e^{-i\omega \sum_{p=1}^k (-1)^p t_p} f(t_1) \dots f(t_k) dt_1 \dots dt_k \right\| \\
& \leq \left\| \int_{t_1 \leq \dots \leq t_k, \max_i |t_i| \geq T} A_S(t_1) A_S^\dagger(t_2) \dots e^{-i\omega \sum_{p=1}^k (-1)^p t_p} f(t_1) \dots f(t_k) dt_1 \dots dt_k \right\| \\
& \leq \|A_S\|^k \int_{t_1 \leq \dots \leq t_k} \chi_{\max_i |t_i| \geq T} f(t_1) \dots f(t_k) dt_1 \dots dt_k = \frac{\|A_S\|^k}{(k-1)!} \left(\int_{\mathbb{R}} f(t) dt \right)^{k-1} \int_{|t| \geq T} f(t) dt \\
& = \frac{\mathcal{O}(\sigma)}{(k-1)!} \frac{1}{T} e^{-T^2/(4\sigma^2)}
\end{aligned} \tag{D7}$$

where we use $\|A_S\| \leq 1$ in the last inequality.

For the second term, we have

$$\|G_{k,A_S}(\omega)\| \leq \|\tilde{G}_{k,A_S}(\omega)\| \leq \|A_S\|^k \int_{-\infty < t_1 \leq \dots \leq t_k < \infty} |f(t_1)| \dots |f(t_k)| dt_1 \dots dt_k = \frac{\mathcal{O}(1)}{k!} \tag{D8}$$

Combining these two bounds and $\|\gamma\|_{L^1} = 1$, we have

$$\begin{aligned}
\|\Phi_\Gamma - \tilde{\Phi}_\Gamma\|_{1 \rightarrow 1} & \leq \frac{\sigma}{T} e^{-T^2/(4\sigma^2)} \sum_{n \geq 1} \Gamma^{2n} \sum_{k=0}^{2n} \left(\frac{(\mathcal{O}(1))}{(2n-k-1)!k!} + \frac{(\mathcal{O}(1))}{(2n-k)!(k-1)!} \right) \\
& = \mathcal{O} \left(\frac{\Gamma^2 \sigma}{T} e^{-T^2/(4\sigma^2)} \sum_{n \geq 1} \frac{1}{(2n-2)!} (\mathcal{O}(\Gamma))^{2n-2} \right) = \mathcal{O} \left(\frac{\Gamma^2 \sigma}{T} e^{-T^2/(4\sigma^2)} \right).
\end{aligned} \tag{D9}$$

□

Using $\tilde{\Phi}_\Gamma$, we have

$$\|\Phi_\Gamma \sigma_\beta - \sigma_\beta\|_1 \leq \|\tilde{\Phi}_\Gamma \sigma_\beta - \Phi_\Gamma \sigma_\beta\|_1 + \|\tilde{\Phi}_\Gamma \sigma_\beta - \sigma_\beta\|_1 \leq \|\tilde{\Phi}_\Gamma - \Phi_\Gamma\|_{1 \rightarrow 1} + \|\tilde{\Phi}_\Gamma \sigma_\beta - \sigma_\beta\|_1. \tag{D10}$$

Thus, it suffices to show $\|\tilde{\Phi}_\Gamma \sigma_\beta - \sigma_\beta\|_1$ is small. Instead of relying directly on the detailed-balance condition of the Lindblad equation, we make use of an intrinsic property of the channel, namely $\tilde{\Phi}_\Gamma^\dagger I = I$. This condition is significantly easier to incorporate into the arbitrary-order expansion.

Lemma D.3. *(Intrinsic Detailed Balance Condition) We have*

$$\mathbb{E}_{A_S} \left(\sum_n \Gamma^{2n} (-1)^n \sum_{k=0}^{2n} (-1)^k \int \gamma((-1)^k \omega) \tilde{G}_{2n-k,A_S}^\dagger(\omega) \tilde{G}_{k,A_S}(\omega) d\omega \right) = 0. \tag{D11}$$

Proof. See Appendix D 1. □

In order to prove $\tilde{\Phi}_\Gamma$ preserves the thermal state, with Lemma D.3, it suffices to bound the following terms for each A_S :

$$\begin{aligned}
& \left\| \sum_{n \geq 1} \Gamma^{2n} (-1)^n \sum_{k=0}^{2n} (-1)^k \int \gamma(\omega) \tilde{G}_{2n-k, A_S}^\dagger(\omega) \sigma_\beta \tilde{G}_{k, A_S}(\omega) d\omega \right\|_1 \\
& \leq \underbrace{\left\| \sum_{n \geq 1} \Gamma^{2n} (-1)^n \left(\sum_{k=0, \text{even}}^{2n} (-1)^k \int \gamma(\omega) \tilde{G}_{2n-k, A_S}^\dagger(\omega) \sigma_\beta \tilde{G}_{k, A_S}(\omega) d\omega - \sigma_\beta \int \gamma(\omega) \tilde{G}_{2n-k, A_S}^\dagger(\omega) \tilde{G}_{k, A_S}(\omega) d\omega \right) \right\|_1}_{\text{Term 1}} \\
& + \underbrace{\left\| \sum_{n \geq 1} \Gamma^{2n} (-1)^n \left(\sum_{k=0, \text{odd}}^{2n} (-1)^k \int \gamma(\omega) \tilde{G}_{2n-k, A_S}^\dagger(\omega) \sigma_\beta \tilde{G}_{k, A_S}(\omega) d\omega - \sigma_\beta \int \underbrace{\gamma(\omega) \exp(\beta\omega)}_{=\gamma(-\omega)} \tilde{G}_{2n-k, A_S}^\dagger(\omega) \tilde{G}_{k, A_S}(\omega) d\omega \right) \right\|_1}_{\text{Term 2}} \tag{D12}
\end{aligned}$$

The analysis of both Term 1 and Term 2 can be simplified to the bound for $\sigma_\beta^{-1} \tilde{G}_{2n-k, A_S}^\dagger(\omega) \sigma_\beta - \tilde{G}_{2n-k, A_S}^\dagger$. For example, Term 1 can be rewritten as

$$\text{Term 1} = \left\| \sigma_\beta \sum_{n \geq 1} \Gamma^{2n} (-1)^n \left(\sum_{k=0, \text{even}}^{2n} (-1)^k \int \gamma(\omega) \left(\sigma_\beta^{-1} \tilde{G}_{2n-k, A_S}^\dagger(\omega) \sigma_\beta - \tilde{G}_{2n-k, A_S}^\dagger \right) \tilde{G}_{k, A_S}(\omega) d\omega \right) \right\|_1 \tag{D13}$$

In order to analyze this term, we introduce the following lemma to obtain an explicit expression for this difference.

Lemma D.4. *We have*

$$\begin{aligned}
\sigma_\beta^{-1} \tilde{G}_{k, A_S}^\dagger(\omega) \sigma_\beta &= \frac{1}{\pi^{k/4}} \int_{-\infty < \tau_1 \leq \dots \leq \tau_k < \infty} \dots A_S(2\sigma\tau_2) A_S^\dagger(2\sigma\tau_1) \\
&\quad \exp \left(i2\sigma\omega \sum_{p=1}^k (-1)^p \tau_p - \omega\beta\Lambda(k) - \sum_{p=1}^k \tau_p^2 + \frac{k\beta^2}{4\sigma^2} - i\frac{\beta}{\sigma} \sum_{p=1}^k \tau_p \right) d\tau_1 \dots d\tau_k. \tag{D14}
\end{aligned}$$

$$\text{where } \Lambda(k) = \begin{cases} 0 & \text{When } k \text{ is even} \\ -1 & \text{When } k \text{ is odd} \end{cases}.$$

Proof. See Appendix D 2. \square

In the following part of the proof, we assume that A_S is Hermitian to simplify the notation. The calculation for non-hermitian A_S is the same. By substituting Eq. (D14) to Term 1, we have

$$\begin{aligned}
\text{Term 1} &\leq \|\sigma_\beta\|_1 \sum_{n \geq 1} \frac{(2\Gamma)^{2n}}{((2\pi)^{1/4})^{2n}} \sum_{\substack{k=0 \\ \text{even}}}^{2n} \left\| \int_{-\infty < s_1 \leq s_2 \leq \dots \leq s_{2n-k} < \infty, -\infty < t_1 \leq t_2 \leq \dots \leq t_k < \infty} A_S(2\sigma s_{2n-k}) \dots A_S(2\sigma s_1) \right. \\
&\quad \left. A_S(2\sigma t_1) \dots A_S(2\sigma t_k) e^{-\sum_{p=1}^{2n-k} s_p^2 - \sum_{p=1}^k t_p^2} \right. \\
&\quad \left. \int \gamma(\omega) e^{i2\sigma\omega \sum_{p=1}^{2n-k} (-1)^p s_p - i2\sigma\omega \sum_{p=1}^k (-1)^p t_p} d\omega \left(\exp \left(\frac{(2n-k)\beta^2}{4\sigma^2} - i\frac{\beta}{\sigma} \sum_{p=1}^{2n-k} s_p \right) - 1 \right) ds_1 \dots ds_{2n-k} dt_1 \dots dt_k \right\| \\
&\leq \sum_{n \geq 1} \frac{(2\Gamma)^{2n}}{((2\pi)^{1/4})^{2n}} \|A_S\|^{2n} \sum_{\substack{k=0 \\ \text{even}}}^{2n} \int_{-\infty < s_1 \leq s_2 \leq \dots \leq s_{2n-k} < \infty, -\infty < t_1 \leq t_2 \leq \dots \leq t_k < \infty} e^{-\sum_{p=1}^{2n-k} s_p^2 - \sum_{p=1}^k t_p^2} \\
&\quad \left| \int \gamma(\omega) e^{i2\sigma\omega (\sum_{p=1}^{2n-k} (-1)^p s_p - \sum_{p=1}^k (-1)^p t_p)} d\omega \right| \left| \exp \left(\frac{(2n-k)\beta^2}{4\sigma^2} - i\frac{\beta}{\sigma} \sum_{p=1}^{2n-k} s_p \right) - 1 \right| ds_1 \dots ds_{2n-k} dt_1 \dots dt_k. \tag{D15}
\end{aligned}$$

It is sufficient to show the following term is upper bounded by $C_{n,k} \frac{\beta}{\sigma^2}$, with the preconstant $C_{n,k}$ depend on n and k ,

$$\begin{aligned}
& \int_{-\infty < s_1 \leq s_2 \leq \dots \leq s_{2n-k} < \infty, -\infty < t_1 \leq t_2 \leq \dots \leq t_k < \infty} e^{-\sum_{p=1}^{2n-k} s_p^2 - \sum_{p=1}^k t_p^2} \\
& \left| \int \gamma(\omega) e^{i2\sigma\omega(\sum_{p=1}^{2n-k} (-1)^p s_p - \sum_{p=1}^k (-1)^p t_p)} d\omega \right| \left| \exp \left(\frac{(2n-k)\beta^2}{4\sigma^2} - i\frac{\beta}{\sigma} \sum_{p=1}^{2n-k} s_p \right) - 1 \right| ds_1 \dots ds_{2n-k} dt_1 \dots dt_k \\
& \leq \int_{-\infty < s_1 \leq s_2 \leq \dots \leq s_{2n-k} < \infty, -\infty < t_1 \leq t_2 \leq \dots \leq t_k < \infty} e^{-\sum_{p=1}^{2n-k} s_p^2 - \sum_{p=1}^k t_p^2} \\
& \underbrace{\left| \int \gamma(\omega) e^{i2\sigma\omega(\sum_{p=1}^{2n-k} (-1)^p s_p - \sum_{p=1}^k (-1)^p t_p)} d\omega \right| \exp \left(\frac{(2n-k)\beta^2}{4\sigma^2} \right) \left| \exp \left(-i\frac{\beta}{\sigma} \sum_{p=1}^{2n-k} s_p \right) - 1 \right| ds_1 \dots ds_{2n-k} dt_1 \dots dt_k}_{\text{Term 1.1}} \\
& + \int_{-\infty < s_1 \leq s_2 \leq \dots \leq s_{2n-k} < \infty, -\infty < t_1 \leq t_2 \leq \dots \leq t_k < \infty} e^{-\sum_{p=1}^{2n-k} s_p^2 - \sum_{p=1}^k t_p^2} \\
& \underbrace{\left| \int \gamma(\omega) e^{i2\sigma\omega(\sum_{p=1}^{2n-k} (-1)^p s_p - \sum_{p=1}^k (-1)^p t_p)} d\omega \right| \left| \exp \left(\frac{(2n-k)\beta^2}{4\sigma^2} \right) - 1 \right| ds_1 \dots ds_{2n-k} dt_1 \dots dt_k}_{\text{Term 1.2}}. \tag{D16}
\end{aligned}$$

We bound Term 1.1 and Term 1.2 separately, with detailed calculation in Appendix D 3,

- For Term 1.1,

$$\text{Term 1.1} = \frac{\beta(2\pi)^n}{\sigma^2} \exp \left(\frac{(2n-k)\beta^2}{4\sigma^2} \right) \mathcal{O} \left(\|\gamma'\|_{L^1} \log(\sqrt{2n}\sigma) + \frac{1}{n} \right). \tag{D17}$$

- For Term 1.2,

$$\text{Term 1.2} = \frac{(2\pi)^n}{\sigma\sqrt{n}} \left| \exp \left(\frac{(2n-k)\beta^2}{4\sigma^2} \right) - 1 \right| \mathcal{O} \left(\|\gamma'\|_{L^1} \log(\sqrt{2n}\sigma) + \frac{\sqrt{n}}{\sigma} \right). \tag{D18}$$

Then

$$\begin{aligned}
\text{Term 1} & \leq \sum_{n \geq 1} \frac{\Gamma^{2n}}{\sqrt{2\pi}^n} \sum_{\substack{k=0 \\ \text{even}}}^{2n} \left(\frac{\beta(2\pi)^n}{\sigma^2} \exp \left(\frac{(2n-k)\beta^2}{4\sigma^2} \right) \mathcal{O} \left(\|\gamma'\|_{L^1} \log(\sqrt{2n}\sigma) + \frac{1}{n} \right) \right. \\
& \quad \left. + \frac{(2\pi)^n}{\sqrt{n}\sigma} \left| \exp \left(\frac{(2n-k)\beta^2}{4\sigma^2} \right) - 1 \right| \mathcal{O} \left(\log(\sqrt{2n}\sigma) \|\gamma'\|_{L^1} + \frac{\sqrt{n}}{\sigma} \right) \right). \tag{D19}
\end{aligned}$$

With $r = r(\sigma, \beta) := \exp(\beta^2/(2\sigma^2)) > 1$ and $R = R(\sigma, \Gamma) := \pi^{1/2}\Gamma^2r$, we have

$$\begin{aligned}
\text{Term 1} & \leq \mathcal{O} \left(\frac{\beta\|\gamma'\|_{L^1}}{\sigma^2} \sum_{n \geq 1} (n+1) \log(\sqrt{2n}\sigma) R^n + \frac{\beta}{\sigma^2} \sum_{n \geq 1} \frac{n+1}{n} R^n \right. \\
& \quad \left. + \frac{\|\gamma'\|_{L^1}}{\sigma} \sum_{n \geq 1} \frac{n+1}{\sqrt{n}} \log(\sqrt{2n}\sigma) \left(R^n - \frac{R^n}{r^n} \right) + \frac{1}{\sigma^2} \sum_{n \geq 1} (n+1) \left(R^n - \frac{R^n}{r^n} \right) \right). \tag{D20}
\end{aligned}$$

Let $\theta = \beta^2/\sigma^2$. With the bound of the polylogarithm function and $r-1 = \mathcal{O}(\theta)$, we have

$$\text{Term 1} \leq \frac{\beta R \|\gamma'\|_{L^1}}{\sigma^2} \mathcal{O}(1 + \log(\sigma)) + \frac{\beta R}{\sigma^2} \mathcal{O}(1) + \frac{\|\gamma'\|_{L^1} R \theta}{\sigma} \mathcal{O}(1 + \log(\sigma)) + \frac{R \theta}{\sigma^2} \mathcal{O}(1) \tag{D21}$$

when $R < 1$ and $\theta R < 1$ (i.e. $\Gamma = \mathcal{O}(1)$). Substitute the expression of R, r, θ back to the bound, we have

$$\text{Term 1} \leq \frac{\beta \Gamma^2}{\sigma^2} \exp(\beta^2/\sigma^2) \mathcal{O} \left(\|\gamma'\|_{L^1} \left(\log(\sigma) + 1 \right) \left(1 + \frac{\beta}{\sigma} \right) \right) = \mathcal{O} \left(\frac{\beta \Gamma^2 \log(\sigma)}{\sigma^2} \|\gamma'\|_{L^1} \right). \tag{D22}$$

when

$$\pi^{1/2}\Gamma^2 \exp(\beta^2/(2\sigma^2)) < 1, \quad \frac{\pi^{1/2}\beta^2\Gamma^2}{\sigma^2} \exp(\beta^2/(2\sigma^2)) < 1. \quad (\text{D23})$$

When k is odd, the bound for Term 2 is obtained in exactly the same way, with $\gamma(\omega)$ replaced by $\tilde{\gamma}(\omega) = \gamma(\omega)\exp(\beta\omega)$. In particular, the additional factor $e^{\beta\omega}$ in $\tilde{\gamma}(\omega)$ is precisely the one appearing in Eq. (D14) for odd indices. Similar to Eq. (D15) and Eq. (D22), we have

$$\begin{aligned} \text{Term 2} &\leq \sum_{n \geq 1} \frac{(2\Gamma)^{2n}}{((2\pi)^{1/4})^{2n}} \|A_S\|^{2n} \sum_{\substack{k=0 \\ \text{odd}}}^{2n} \int_{-\infty < s_1 \leq s_2 \leq \dots \leq s_{2n-k} < \infty, -\infty < t_1 \leq t_2 \leq \dots \leq t_k < \infty} e^{-\sum_{p=1}^{2n-k} s_p^2 - \sum_{p=1}^k t_p^2} \\ &\quad \left| \int \tilde{\gamma}(\omega) e^{i2\sigma\omega(\sum_{p=1}^{2n-k} (-1)^p s_p - \sum_{p=1}^k (-1)^p t_p)} d\omega \right| \left| \exp \left(\frac{(2n-k)\beta^2}{4\sigma^2} - i\frac{\beta}{\sigma} \sum_{p=1}^{2n-k} s_p \right) - 1 \right| ds_1 \dots ds_{2n-k} dt_1 \dots dt_k \quad (\text{D24}) \\ &= \mathcal{O} \left(\frac{\beta\Gamma^2 \log(\sigma)}{\sigma^2} \|\tilde{\gamma}'\|_{L_1} \right). \end{aligned}$$

Summing all terms, we conclude the proof of Theorem D.1.

1. Proof of Lemma D.3

Notice that the expression of $\tilde{G}_{k,A_S}(\omega)$ depends on the system Hamiltonian H and the coupling operator A_S . We define

$$\tilde{G}_{k,H,A_S}(\omega) = \tilde{G}_{k,A_S}(\omega) = \int_{-\infty < t_1 \leq \dots \leq t_k < \infty} A_S(t_1) A_S^\dagger(t_2) \dots e^{-i\omega \sum_{p=1}^k (-1)^p t_p} f(t_1) \dots f(t_k) dt_1 \dots dt_k.$$

Then,

$$\begin{aligned} \tilde{G}_{k,H,A_S}^\dagger(\omega) &= \int_{-\infty < t_1 \leq \dots \leq t_k < \infty} \dots A_S(t_2) A_S^\dagger(t_1) e^{i\omega \sum_{p=1}^k (-1)^p t_p} f(t_1) \dots f(t_k) dt_1 \dots dt_k \\ &= \int_{-\infty < s_1 \leq \dots \leq s_k < \infty} \dots A_S(-s_{k-1}) A_S^\dagger(-s_k) e^{-i\omega(-1)^{k-1} \sum_{p=1}^k (-1)^p s_p} f(s_1) \dots f(s_k) dt_1 \dots dt_k, \quad s_j = -t_{k-j+1} \\ &= \begin{cases} \tilde{G}_{k,-H,A_S^\dagger}(\omega), & k \text{ odd}, \\ \tilde{G}_{k,-H,A_S}(-\omega), & k \text{ even}. \end{cases} \end{aligned}$$

Similarly, we have

$$\tilde{G}_{k,H,A_S}(\omega) = \begin{cases} \tilde{G}_{k,-H,A_S^\dagger}^\dagger(\omega), & k \text{ odd} \\ \tilde{G}_{k,-H,A_S}^\dagger(-\omega), & k \text{ even} \end{cases}.$$

Now, we generate evolution operator $\tilde{\Psi}_\Gamma$, defined in analogy with $\tilde{\Phi}_\Gamma$, by replacing Hamiltonian in \tilde{G}_k with $-H$ and inverse temperature with $-\beta$,

$$\begin{aligned} \tilde{\Psi}_\Gamma \rho_0 &= \int g(\omega) \text{Tr}_E[U^\Gamma(T)(\rho_0 \otimes \rho_E)U^{\Gamma\dagger}(T)](\omega) d\omega \\ &= U_S(2T)\rho_0 U_S^\dagger(2T) \\ &\quad + \mathbb{E}_{A_S} \left(\sum_n \Gamma^{2n} (-1)^n \sum_{k=0}^{2n} (-1)^k \int \underbrace{\frac{g(\omega) + g(-\omega)}{1 + e^{-\beta\omega}}}_{=\gamma(-\omega)} U_S(T) \tilde{G}_{2n-k,-H,A_S}^\dagger(\omega) U_S(T) \rho_0 U_S^\dagger(T) \tilde{G}_{k,-H,A_S}(\omega) U_S^\dagger(T) d\omega \right) \end{aligned}$$

It is straightforward to see that $\tilde{\Psi}_\Gamma$ is a quantum channel. This implies

$$\tilde{\Psi}_\Gamma^\dagger[I] = I \Rightarrow \mathbb{E}_{A_S} \left(\sum_n \Gamma^{2n} (-1)^n \sum_{k=0}^{2n} (-1)^k \int \gamma(-\omega) \tilde{G}_{2n-k,-H,A_S}(\omega) \tilde{G}_{k,-H,A_S}^\dagger(\omega) d\omega \right) = 0.$$

Because $\{(A_i)^\dagger\} = \{A_i\}$, we have

$$\begin{aligned}
& \mathbb{E}_{A_S} \left(\sum_n \Gamma^{2n} (-1)^n \sum_{k=0}^{2n} (-1)^k \int \gamma((-1)^k \omega) \tilde{G}_{2n-k, H, A_S}^\dagger(\omega) \tilde{G}_{k, H, A_S}(\omega) d\omega \right) \\
&= \mathbb{E}_{A_S} \left(\sum_n \Gamma^{2n} (-1)^n \sum_{k=0, \text{even}}^{2n} (-1)^k \int \gamma(\omega) \tilde{G}_{2n-k, -H, A_S}(-\omega) \tilde{G}_{k, -H, A_S}^\dagger(-\omega) d\omega \right) \\
&+ \underbrace{\mathbb{E}_{A_S} \left(\sum_n \Gamma^{2n} (-1)^n \sum_{k=0, \text{odd}}^{2n} (-1)^k \int \gamma(-\omega) \tilde{G}_{2n-k, -H, A_S}^\dagger(\omega) \tilde{G}_{k, -H, A_S}^\dagger(\omega) d\omega \right)}_{= \mathbb{E}_{A_S} \left(\sum_n \Gamma^{2n} (-1)^n \sum_{k=0, \text{odd}}^{2n} (-1)^k \int \gamma(-\omega) \tilde{G}_{2n-k, -H, A_S}(\omega) \tilde{G}_{k, -H, A_S}^\dagger(\omega) d\omega \right)} \\
&= \mathbb{E}_{A_S} \left(\sum_n \Gamma^{2n} (-1)^n \sum_{k=0}^{2n} (-1)^k \int \gamma(-\omega) \tilde{G}_{2n-k, -H, A_S}(\omega) \tilde{G}_{k, -H, A_S}^\dagger(\omega) d\omega \right) = 0,
\end{aligned} \tag{D25}$$

The proof is complete.

2. Proof of Lemma D.4

The main goal of this section is to prove an explicit expression of $\sigma_\beta^{-1} \tilde{G}_{k, A_S}^\dagger \sigma_\beta$. We show that it admits the same structural form as $\tilde{G}_{k, A_S}^\dagger$ after a β -dependent shift of the integration variable. In addition, for notation simplicity, we assume A_S is hermitian. The extension to the non-hermitian A_S is straightforward.

We first calculate $\sigma_\beta^{-1} \tilde{G}_{k, A_S} \sigma_\beta$, the expression of $\sigma_\beta^{-1} \tilde{G}_{k, A_S}^\dagger \sigma_\beta$ can be obtained by applying the complex conjugate on it. We apply the change of variable,

$$t_p = \sum_{q=p}^k s_q, \forall p = 1, \dots, k \Leftrightarrow \begin{cases} s_p = t_p - t_{p+1}, & 1 \leq p < k \\ s_k = t_k & \end{cases}. \tag{D26}$$

to \tilde{G}_{k, A_S} in Eq. (D3), then

$$\tilde{G}_{k, A_S}(\omega) = \int_{-\infty < s_1, \dots, s_{k-1} \leq 0, -\infty < s_k < \infty} A_S \left(\sum_{p=1}^k s_p \right) \dots A_S(s_k) e^{-i\omega \sum_{p=1}^k (-1)^p \sum_{q=p}^k s_q} f \left(\sum_{p=1}^k s_p \right) \dots f(s_k) ds_1 \dots ds_k. \tag{D27}$$

Notice that applying the commutator once on the product of system operators is equivalent to differentiating with respect to s_k ,

$$\left[H, A_S \left(\sum_{p=1}^k s_p \right) \dots A_S(s_k) \right] = -i\partial_{s_k} \left(A_S \left(\sum_{p=1}^k s_p \right) \dots A_S(s_k) \right). \tag{D28}$$

By integration by parts, we have

$$\begin{aligned}
\left[H, \tilde{G}_{k, A_S} \right] &= \int_{-\infty < s_1, \dots, s_{k-1} \leq 0, -\infty < s_k < \infty} A_S \left(\sum_{p=1}^k s_p \right) \dots A_S(s_k) \\
&\quad i\partial_{s_k} \left(e^{-i\omega \sum_{p=1}^k (-1)^p \sum_{q=p}^k s_q} f \left(\sum_{p=1}^k s_p \right) \dots f(s_k) \right) ds_1 \dots ds_k.
\end{aligned} \tag{D29}$$

It reveals that when we apply the commutator operator m times,

$$\begin{aligned}
& \underbrace{\left[H, \left[H, \dots, \left[H, \tilde{G}_{k, A_S} \right] \right] \right]}_{m \text{ commutator}} = \int_{-\infty < s_1, \dots, s_{k-1} \leq 0, -\infty < s_k < \infty} A_S \left(\sum_{p=1}^k s_p \right) \dots A_S(s_k) \\
& i^m \partial_{s_k}^m \left(e^{-i\omega \sum_{p=1}^k (-1)^p \sum_{q=p}^k s_q} f \left(\sum_{p=1}^k s_p \right) \dots f(s_k) \right) ds_1 \dots ds_k.
\end{aligned} \tag{D30}$$

We use the Baker–Campbell–Hausdorff formula to expand $\sigma_\beta \tilde{G}_{k,A_S} \sigma_\beta^{-1}$ as a series of the commutators,

$$\begin{aligned}
\sigma_\beta \tilde{G}_{k,A_S} \sigma_\beta^{-1} &= \tilde{G}_{k,A_S} + (-\beta) \left[H, \tilde{G}_{k,A_S} \right] + \frac{1}{2!} (-\beta)^2 \left[H, \left[H, \tilde{G}_{k,A_S} \right] \right] + \cdots + \frac{1}{m!} (-\beta)^m \underbrace{\left[H, \left[H, \cdots, \left[H, \tilde{G}_{k,A_S} \right] \right] \right]}_{m \text{ commutator}} + \cdots \\
&= \int_{-\infty < s_1, \dots, s_{k-1} \leq 0, -\infty < s_k < \infty} A_S \left(\sum_{p=1}^k s_p \right) \cdots A_S(s_k) \\
&\quad \sum_{n \geq 0} \frac{1}{m!} (-\beta)^m i^m \partial_{s_k}^m \left(e^{-i\omega \sum_{p=1}^k (-1)^p \sum_{q=p}^k s_q} f \left(\sum_{p=1}^k s_p \right) \cdots f(s_k) \right) ds_1 \cdots ds_k \\
&= \int_{-\infty < s_1, \dots, s_{k-1} \leq 0, -\infty < s_k < \infty} A_S \left(\sum_{p=1}^k s_p \right) \cdots A_S(s_k) \\
&\quad \left(e^{-i\omega \sum_{p=1}^{k-1} (-1)^p \sum_{q=p}^{k-1} s_q - i\omega(s_k - i\beta) \sum_{p=1}^k (-1)^p} f(s_1 + \cdots + s_k - i\beta) \cdots f(s_k - i\beta) \right) ds_1 \cdots ds_k. \tag{D31}
\end{aligned}$$

where the last equality follows from Taylor expansion in s_k . Substituting the expression of $f(t)$ yields,

$$\begin{aligned}
\sigma_\beta \tilde{G}_{k,A_S} \sigma_\beta^{-1} &= \int_{-\infty < s_1, \dots, s_{k-1} \leq 0, -\infty < s_k < \infty} A_S \left(\sum_{p=1}^k s_p \right) \cdots A_S(s_k) e^{-i\omega \sum_{p=1}^k (-1)^p \sum_{q=p}^k s_q - \omega\beta \sum_{p=1}^k (-1)^p} \\
&\quad \exp \left(-\frac{1}{4\sigma^2} \sum_{p=1}^k \left(\sum_{q=p}^k s_q - i\beta \right)^2 \right) \left(\frac{1}{(2\pi)^{1/4}\sigma} \right)^k ds_1 \cdots ds_k \tag{D32}
\end{aligned}$$

By rescaling the variable $s_q \rightarrow 2\sigma s_q$ for $q = 1, \dots, k$, we have

$$\begin{aligned}
\sigma_\beta \tilde{G}_{k,A_S} \sigma_\beta^{-1} &= \frac{(2\sigma)^k}{((2\pi)^{1/4}\sigma)^k} \int_{-\infty < s_1, \dots, s_{k-1} \leq 0, -\infty < s_k < \infty} A_S \left(2\sigma \sum_{p=1}^k s_p \right) \cdots A_S(2\sigma s_k) \\
&\quad e^{-i2\sigma\omega \sum_{p=1}^k (-1)^p \sum_{q=p}^k s_q - \omega\beta \sum_{p=1}^k (-1)^p} \exp \left(-\sum_{p=1}^k \left(\sum_{q=p}^k s_q \right)^2 \right) \exp \left(\frac{k\beta^2}{4\sigma^2} + i\frac{\beta}{\sigma} (s_1 + 2s_2 + \cdots + ks_k) \right) ds_1 \cdots ds_k. \tag{D33}
\end{aligned}$$

Define the function

$$\Lambda(k) := \sum_{p=1}^k (-1)^p = \begin{cases} 0 & \text{When } k \text{ is even} \\ -1 & \text{When } k \text{ is odd} \end{cases}, \tag{D34}$$

and apply the conjugate transpose to Eq. (D33), we have

$$\begin{aligned}
\sigma_\beta^{-1} \tilde{G}_{k,A_S}^\dagger \sigma_\beta &= \frac{1}{\pi^{k/4}} \int_{-\infty < s_1, \dots, s_{k-1} \leq 0, -\infty < s_k < \infty} A_S(2\sigma s_k) \cdots A_S \left(2\sigma \sum_{p=1}^k s_p \right) \\
&\quad e^{i2\sigma\omega \sum_{p=1}^k (-1)^p \sum_{q=p}^k s_q - \omega\beta\Lambda(k)} \exp \left(-\sum_{p=1}^k \left(\sum_{q=p}^k s_q \right)^2 \right) \exp \left(\frac{k\beta^2}{4\sigma^2} - i\frac{\beta}{\sigma} (s_1 + 2s_2 + \cdots + ks_k) \right) ds_1 \cdots ds_k. \tag{D35}
\end{aligned}$$

With another change of variable $\tau_p = \sum_{q=p}^k s_q$, we obtain Eq. (D14). This concludes the proof.

3. Bounds of Term 1.1 and Term 1.2

In this section, we bound Term 1.1 and Term 1.2 separately so that the bound of Term 1 can be obtained by

$$\text{Term1} \leq \sum_{n \geq 1} \frac{(2\Gamma)^{2n}}{((2\pi)^{1/4})^{2n}} \|A_S\|^{2n} \sum_{\substack{k=0 \\ \text{even}}}^{2n} (\text{Term1.1} + \text{Term1.2}). \tag{D36}$$

We notice that Term 1.1 can be upper bounded by the inequality $|\sin(x)| \leq |x|$ as,

$$\begin{aligned} \text{Term 1.1} &= 2 \exp\left(\frac{(2n-k)\beta^2}{4\sigma^2}\right) \int_{-\infty < s_1 \leq s_2 \leq \dots \leq s_{2n-k} < \infty, -\infty < t_1 \leq t_2 \leq \dots \leq t_k < \infty} e^{-\sum_{p=1}^{2n-k} s_p^2 - \sum_{p=1}^k t_p^2} \\ &\quad \left| \int \gamma(\omega) e^{i2\sigma\omega \sum_{p=1}^{2n-k} (-1)^p s_p - i2\sigma\omega \sum_{p=1}^k (-1)^p t_p} d\omega \right| \left| \sin\left(\frac{\beta}{2\sigma} \sum_{p=1}^{2n-k} s_p\right) \right| ds_1 \dots ds_{2n-k} dt_1 \dots dt_k \\ &\leq \frac{\beta}{\sigma} \exp\left(\frac{(2n-k)\beta^2}{4\sigma^2}\right) \int_{-\infty < s_1 \leq s_2 \leq \dots \leq s_{2n-k} < \infty, -\infty < t_1 \leq t_2 \leq \dots \leq t_k < \infty} e^{-\sum_{p=1}^{2n-k} s_p^2 - \sum_{p=1}^k t_p^2} \\ &\quad \left| \int \gamma(\omega) e^{i2\sigma\omega \sum_{p=1}^{2n-k} (-1)^p s_p - i2\sigma\omega \sum_{p=1}^k (-1)^p t_p} d\omega \right| \left| \sum_{p=1}^{2n-k} s_p \right| ds_1 \dots ds_{2n-k} dt_1 \dots dt_k. \end{aligned} \quad (\text{D37})$$

Using the conditions on $\gamma(\omega)$ in Theorem D.1, we obtain the following upper bound via integration by parts,

$$\left| \int \gamma(\omega) e^{i2\sigma\omega \sum_{p=1}^{2n-k} (-1)^p s_p - \sum_{p=1}^k (-1)^p t_p} d\omega \right| \leq \frac{1}{2\sigma} \frac{1}{|\sum_{p=1}^{2n-k} (-1)^p s_p - \sum_{p=1}^k (-1)^p t_p|} \int |\gamma'(\omega)| d\omega. \quad (\text{D38})$$

The goal becomes to prove the following integral is $\mathcal{O}(\frac{1}{\sigma})$. The integral can be separated as the summation of I and II,

$$\begin{aligned} &\int_{-\infty < s_1 \leq s_2 \leq \dots \leq s_{2n-k} < \infty, -\infty < t_1 \leq t_2 \leq \dots \leq t_k < \infty} e^{-\sum_{p=1}^{2n-k} s_p^2 - \sum_{p=1}^k t_p^2} \left| \int \gamma(\omega) e^{i2\sigma\omega \sum_{p=1}^{2n-k} (-1)^p s_p - \sum_{p=1}^k (-1)^p t_p} d\omega \right| \left| \sum_{p=1}^{2n-k} s_p \right| ds_1 \dots ds_{2n-k} dt_1 \dots dt_k \\ &= \int_{\substack{-\infty < s_1 \leq s_2 \leq \dots \leq s_{2n-k} < \infty, -\infty < t_1 \leq t_2 \leq \dots \leq t_k < \infty, \\ |\sum_{p=1}^{2n-k} (-1)^p s_p - \sum_{p=1}^k (-1)^p t_p| \geq \delta}} e^{-\sum_{p=1}^{2n-k} s_p^2 - \sum_{p=1}^k t_p^2} \\ &\quad \underbrace{\left| \int \gamma(\omega) e^{i2\sigma\omega \sum_{p=1}^{2n-k} (-1)^p s_p - \sum_{p=1}^k (-1)^p t_p} d\omega \right| \left| \sum_{p=1}^{2n-k} s_p \right| ds_1 \dots ds_{2n-k} dt_1 \dots dt_k}_\text{I} \\ &+ \int_{\substack{-\infty < s_1 \leq s_2 \leq \dots \leq s_{2n-k} < \infty, -\infty < t_1 \leq t_2 \leq \dots \leq t_k < \infty, \\ |\sum_{p=1}^{2n-k} (-1)^p s_p - \sum_{p=1}^k (-1)^p t_p| < \delta}} e^{-\sum_{p=1}^{2n-k} s_p^2 - \sum_{p=1}^k t_p^2} \\ &\quad \underbrace{\left| \int \gamma(\omega) e^{i2\sigma\omega \sum_{p=1}^{2n-k} (-1)^p s_p - \sum_{p=1}^k (-1)^p t_p} d\omega \right| \left| \sum_{p=1}^{2n-k} s_p \right| ds_1 \dots ds_{2n-k} dt_1 \dots dt_k}_\text{II}. \end{aligned} \quad (\text{D39})$$

To decouple the Fourier variable from the remaining Gaussian integrals, we introduce the following distance-preserving change of variables.

Lemma D.5. *Given variables t_1, t_2, \dots, t_k , there exists an orthogonal matrix Q such that $\vec{t} = Q\vec{t}$, and*

$$t_1^2 + t_2^2 + \dots + t_k^2 = \tilde{t}_1^2 + \tilde{t}_2^2 + \dots + \tilde{t}_k^2, \quad \tilde{t}_1 = \sum_{p=1}^k (-1)^p t_p / \sqrt{k}. \quad (\text{D40})$$

This change of variable induces a change of integral area through \mathcal{T} , i.e., for a domain $D \subset \mathbb{R}^k$, its image is written $\mathcal{T}(D)$.

Proof. By Gram-Schmidt process, we can extend the vector $\left(\frac{-1}{\sqrt{k}}, \frac{1}{\sqrt{k}}, \dots, \frac{(-1)^k}{\sqrt{k}}\right)$ to the orthogonal matrix. \square

By Lemma D.5, there exists orthogonal map Q_s, Q_t for the change of variable $\vec{s} = Q_s \vec{s}, \vec{t} = Q_t \vec{t}$ such that

$$\tilde{s}_1 = \sum_{p=1}^{2n-k} (-1)^p s_p / \sqrt{2n-k}, \quad \tilde{t}_1 = \sum_{p=1}^k (-1)^p t_p / \sqrt{k}. \quad (\text{D41})$$

Then,

$$I = \int_{\tilde{s}, \tilde{t}, |\sqrt{2n-k}\tilde{s}_1 - \sqrt{k}\tilde{t}_1| \geq \delta} e^{-\sum_{p=1}^{2n-k} \tilde{s}_p^2 - \sum_{p=1}^k \tilde{t}_p^2} \left| \int \gamma(\omega) e^{i2\sigma\omega(\sqrt{2n-k}\tilde{s}_1 - \sqrt{k}\tilde{t}_1)} d\omega \right| \left| \underbrace{(1, 1, \dots, 1)}_{2n-k} Q_S^T \tilde{s} \right| d\tilde{s}_1 \dots d\tilde{s}_{2n-k} d\tilde{t}_1 \dots d\tilde{t}_k. \quad (D42)$$

By Hölder and triangle inequality,

$$\left| \underbrace{(1, 1, \dots, 1)}_{2n-k} Q_S^T \tilde{s} \right| \leq \sqrt{2n-k} \left(|\tilde{s}_1| + \left(\sum_{p=2}^{2n-k} \tilde{s}_p^2 \right)^{1/2} \right). \quad (D43)$$

Combining this with the integration by parts, we have

$$\begin{aligned} I \leq & \sqrt{2n-k} \frac{1}{2\sigma} \int |\gamma'(\omega)| d\omega \int_{|\sqrt{2n-k}\tilde{s}_1 - \sqrt{k}\tilde{t}_1| \in (\delta, \infty)} e^{-(\tilde{s}_1^2 + \tilde{t}_1^2)} \frac{|\tilde{s}_1|}{|\sqrt{2n-k}\tilde{s}_1 - \sqrt{k}\tilde{t}_1|} d\tilde{s}_1 d\tilde{t}_1 \\ & \int_{\mathcal{T}(-\infty < s_2 \leq \dots \leq s_{2n-k} < \infty, -\infty < t_2 \leq \dots \leq t_k < \infty)} e^{-\sum_{p=2}^{2n-k} \tilde{s}_p^2 - \sum_{p=2}^k \tilde{t}_p^2} d\tilde{s}_2 \dots d\tilde{s}_{2n-k} d\tilde{t}_2 \dots d\tilde{t}_k \\ & + \sqrt{2n-k} \frac{1}{2\sigma} \int |\gamma'(\omega)| d\omega \int_{|\sqrt{2n-k}\tilde{s}_1 - \sqrt{k}\tilde{t}_1| \in (\delta, \infty)} e^{-(\tilde{s}_1^2 + \tilde{t}_1^2)} \frac{1}{|\sqrt{2n-k}\tilde{s}_1 - \sqrt{k}\tilde{t}_1|} d\tilde{s}_1 d\tilde{t}_1 \\ & \int_{\mathcal{T}(-\infty < s_2 \leq \dots \leq s_{2n-k} < \infty, -\infty < t_2 \leq \dots \leq t_k < \infty)} e^{-\sum_{p=2}^{2n-k} \tilde{s}_p^2 - \sum_{p=2}^k \tilde{t}_p^2} \left(\sum_{p=2}^{2n-k} \tilde{s}_p^2 \right)^{1/2} d\tilde{s}_2 \dots d\tilde{s}_{2n-k} d\tilde{t}_2 \dots d\tilde{t}_k. \end{aligned} \quad (D44)$$

Next, we perform the additional change of variable

$$\begin{cases} x = \sqrt{2n-k}\tilde{s}_1 - \sqrt{k}\tilde{t}_1 \\ y = \sqrt{k}\tilde{s}_1 + \sqrt{2n-k}\tilde{t}_1 \end{cases}, \quad (D45)$$

which gives

$$\begin{aligned} I \leq & \sqrt{2n-k} \frac{1}{2\sigma} \|\gamma'\|_{L^1} \frac{1}{2n} \int_{|x| \in (\delta, \infty)} e^{-\frac{x^2+y^2}{2n}} \frac{|\sqrt{2n-k}x + \sqrt{k}y|}{2n|x|} dx dy \\ & \int_{\mathcal{T}(-\infty < s_2 \leq \dots \leq s_{2n-k} < \infty, -\infty < t_2 \leq \dots \leq t_k < \infty)} e^{-\sum_{p=2}^{2n-k} \tilde{s}_p^2 - \sum_{p=2}^k \tilde{t}_p^2} ds_2 \dots ds_{2n-k} dt_2 \dots dt_k \\ & + \sqrt{2n-k} \frac{1}{2\sigma} \|\gamma'\|_{L^1} \frac{1}{2n} \int_{|x| \in (\delta, \infty)} e^{-\frac{x^2+y^2}{2n}} \frac{1}{|x|} dx dy \\ & \int_{\mathcal{T}(-\infty < s_2 \leq \dots \leq s_{2n-k} < \infty, -\infty < t_2 \leq \dots \leq t_k < \infty)} e^{-\sum_{p=2}^{2n-k} \tilde{s}_p^2 - \sum_{p=2}^k \tilde{t}_p^2} \left(\sum_{p=2}^{2n-k} \tilde{s}_p^2 \right)^{1/2} ds_2 \dots ds_{2n-k} dt_2 \dots dt_k. \end{aligned} \quad (D46)$$

By choosing $\delta = \mathcal{O}(1/\sigma)$, we have

$$\begin{aligned} & \int_{|x| \in (\delta, \infty)} e^{-\frac{x^2+y^2}{2n}} \frac{|\sqrt{2n-k}x + \sqrt{k}y|}{2n|x|} dx dy \leq \frac{\sqrt{2n-k}}{2n} \int_{|x| \in (\delta, \infty)} e^{-\frac{x^2+y^2}{2n}} dx dy + \frac{\sqrt{k}}{2n} \int_{|x| \in (\delta, \infty)} e^{-\frac{x^2+y^2}{2n}} \frac{|y|}{|x|} dx dy \\ & = \sqrt{2n-k}(\sqrt{\pi})^2 + \sqrt{k}\mathcal{O}\left(\log(\sqrt{2n}/\delta)\right) = \mathcal{O}\left(\sqrt{k}\log(\sqrt{2n}\sigma)\right), \end{aligned} \quad (D47)$$

and

$$\int_{|x| \in (\delta, \infty)} e^{-\frac{x^2+y^2}{2n}} \frac{1}{|x|} dx dy = \sqrt{2n}\mathcal{O}\left(\log(\sqrt{2n}/\delta)\right) = \sqrt{2n}\mathcal{O}\left(\log(\sqrt{2n}\sigma)\right). \quad (D48)$$

The remaining Gaussian integral can be upper bounded by the standard Gaussian bound. Using the change of variable

$x = \sum_{p=2}^{2n-k} \tilde{s}_p^2$ and the Gautschi's inequality, we obtain

$$\begin{aligned} & \int_{\mathcal{T}(-\infty < s_2 \leq \dots \leq s_{2n-k} < \infty, -\infty < t_2 \leq \dots \leq t_k < \infty)} e^{-\sum_{p=2}^{2n-k} \tilde{s}_p^2 - \sum_{p=2}^k \tilde{t}_p^2} \left(\sum_{p=2}^{2n-k} \tilde{s}_p^2 \right)^{1/2} ds_2 \dots ds_{2n-k} dt_2 \dots dt_k \\ & \leq (\sqrt{\pi})^{k-1} \int_0^\infty e^{-x} x^{\frac{2n-k-2}{2}} \frac{2\pi^{\frac{2n-k-1}{2}}}{\Gamma(\frac{2n-k-1}{2})} dx = 2 \frac{\Gamma(\frac{2n-k}{2})}{\Gamma(\frac{2n-k-1}{2})} \pi^{n-1} \leq 2 \sqrt{\frac{2n-k}{2}} \pi^{n-1}. \end{aligned} \quad (\text{D49})$$

and

$$\int_{\mathcal{T}(-\infty < s_2 \leq \dots \leq s_{2n-k} < \infty, -\infty < t_2 \leq \dots \leq t_k < \infty)} e^{-\sum_{p=2}^{2n-k} \tilde{s}_p^2 - \sum_{p=2}^k \tilde{t}_p^2} ds_2 \dots ds_{2n-k} dt_2 \dots dt_k \leq (\sqrt{\pi})^{2n}. \quad (\text{D50})$$

Consequently, combine those result together, we find

$$\begin{aligned} \text{I} & \leq \|\gamma'\|_{L^1} \frac{1}{\sigma} \frac{\sqrt{k(2n-k)}}{n} \pi^n \mathcal{O}(\log(\sqrt{2n}\sigma)) + \|\gamma'\|_{L^1} \frac{1}{\sigma} \frac{\sqrt{2n}(2n-k)}{n} \pi^n \mathcal{O}(\log(\sqrt{2n}\sigma)) \\ & \leq \|\gamma'\|_{L^1} \frac{(2\pi)^n}{\sigma} \mathcal{O}(\log(\sqrt{2n}\sigma)) \end{aligned} \quad (\text{D51})$$

We now turn to II. Using

$$\begin{aligned} & \int_{|x|<\delta} e^{-\frac{x^2+y^2}{2n}} \left| \frac{\sqrt{2n-k}}{2n} x + \frac{\sqrt{k}}{2n} y \right| dx dy \leq \frac{\sqrt{2n-k}}{2n} \int_{|x|<\delta} e^{-\frac{x^2+y^2}{2n}} |x| dx dy + \frac{\sqrt{k}}{2n} \int_{|x|<\delta} e^{-\frac{x^2+y^2}{2n}} |y| dx dy \\ & \leq \sqrt{(2n-k)/(2n)} \mathcal{O}(\delta^2) + \sqrt{k} \mathcal{O}(\delta). \end{aligned}$$

we have,

$$\begin{aligned} \text{II} & = \int_{-\infty < s_1 \leq s_2 \leq \dots \leq s_{2n-k} < \infty, -\infty < t_1 \leq t_2 \leq \dots \leq t_k < \infty, |\sum_{p=1}^{2n-k} (-1)^p s_p - \sum_{p=1}^k (-1)^p t_p| < \delta} e^{-\sum_{p=1}^{2n-k} s_p^2 - \sum_{p=1}^k t_p^2} \\ & \quad \left| \int \gamma(\omega) e^{i2\sigma\omega \sum_{p=1}^{2n-k} (-1)^p s_p - i2\sigma\omega \sum_{p=1}^k (-1)^p t_p} d\omega \right| \left| \sum_{p=1}^{2n-k} s_p \right| ds_1 \dots ds_{2n-k} dt_1 \dots dt_k \\ & \leq \int_{-\infty < s_1 \leq s_2 \leq \dots \leq s_{2n-k} < \infty, -\infty < t_1 \leq t_2 \leq \dots \leq t_k < \infty, |\sum_{p=1}^{2n-k} (-1)^p s_p - \sum_{p=1}^k (-1)^p t_p| < \delta} e^{-\sum_{p=1}^{2n-k} s_p^2 - \sum_{p=1}^k t_p^2} \left| \sum_{p=1}^{2n-k} s_p \right| ds_1 \dots ds_{2n-k} dt_1 \dots dt_k \\ & \leq \frac{1}{2n} \int_{|x|<\delta} e^{-\frac{x^2+y^2}{2n}} \left| \frac{\sqrt{2n-k}}{2n} x + \frac{\sqrt{k}}{2n} y \right| dx dy \int_{\mathcal{T}(-\infty < s_2 \leq \dots \leq s_{2n-k} < \infty, -\infty < t_2 \leq \dots \leq t_k < \infty)} e^{-\sum_{p=2}^{2n-k} \tilde{s}_p^2 - \sum_{p=2}^k \tilde{t}_p^2} d\tilde{s}_2 \dots d\tilde{s}_{2n-k} d\tilde{t}_2 \dots d\tilde{t}_k \\ & \quad + \frac{1}{2n} \int_{|x|<\delta} e^{-\frac{x^2+y^2}{2n}} dx dy \int_{\mathcal{T}(-\infty < s_2 \leq \dots \leq s_{2n-k} < \infty, -\infty < t_2 \leq \dots \leq t_k < \infty)} e^{-\sum_{p=2}^{2n-k} \tilde{s}_p^2 - \sum_{p=2}^k \tilde{t}_p^2} \sqrt{\sum_{p=2}^{2n-k} \tilde{s}_p^2} d\tilde{s}_2 \dots d\tilde{s}_{2n-k} d\tilde{t}_2 \dots d\tilde{t}_k \\ & \leq \left(\frac{\sqrt{(2n-k)/2n}}{2n} \mathcal{O}\left(\frac{1}{\sigma^2}\right) + \frac{\sqrt{k}}{n} \mathcal{O}\left(\frac{1}{\sigma}\right) \right) (\sqrt{\pi})^{2n-2} + \mathcal{O}\left(\frac{1}{\sigma}\right) (\sqrt{\pi})^k \\ & = \mathcal{O}\left(\pi^n \left(\frac{1}{n\sigma^2} + \frac{1}{\sqrt{n}\sigma} \right)\right) = \mathcal{O}\left(\frac{1}{\sqrt{n}\sigma} \pi^n\right) = \mathcal{O}\left(\frac{1}{n\sigma} (2\pi)^n\right). \end{aligned} \quad (\text{D52})$$

Putting everything together, we obtain

$$\text{Term 1.1} \leq \frac{\beta}{\sigma} \exp\left(\frac{(2n-k)\beta^2}{4\sigma^2}\right) (\text{I} + \text{II}) = \frac{\beta(2\pi)^n}{\sigma^2} \exp\left(\frac{(2n-k)\beta^2}{4\sigma^2}\right) \mathcal{O}\left(\|\gamma'\|_{L^1} \log(\sqrt{2n}\sigma) + \frac{1}{n}\right). \quad (\text{D53})$$

A similar calculation yields an upper bound for Term 1.2. We decompose the integration domain into a neighborhood of $\sum_{p=1}^{2n-k} (-1)^p s_p - \sum_{p=1}^k (-1)^p t_p = 0$ and its complement, i.e.

$\int_{-\infty < s_1 \leq s_2 \leq \dots \leq s_{2n-k} < \infty, -\infty < t_1 \leq t_2 \leq \dots \leq t_k < \infty} e^{-\sum_{p=1}^{2n-k} s_p^2 - \sum_{p=1}^k t_p^2} \left| \int \gamma(\omega) e^{i2\sigma\omega \sum_{p=1}^{2n-k} (-1)^p s_p - i2\sigma\omega \sum_{p=1}^k (-1)^p t_p} d\omega \right| ds_1 \dots ds_{2n-k} dt_1 \dots dt_k =$
 III + VI. When $\sum_{p=1}^{2n-k} (-1)^p s_p - \sum_{p=1}^k (-1)^p t_p > \delta$, III can be bounded using Eq. (D38) and performing the change of variables in Eqs. (D41) and (D45), which yields

$$\begin{aligned} \text{III} &\leq \frac{\|\gamma'\|}{2\sigma} \int_{-\infty < s_1 \leq s_2 \leq \dots \leq s_{2n-k} < \infty, -\infty < t_1 \leq t_2 \leq \dots \leq t_k < \infty} \frac{e^{-\sum_{p=1}^{2n-k} s_p^2 - \sum_{p=1}^k t_p^2}}{|\sum_{p=1}^{2n-k} (-1)^p s_p - \sum_{p=1}^k (-1)^p t_p|} ds_1 \dots ds_{2n-k} dt_1 \dots dt_k \\ &\leq \frac{\|\gamma'\|}{2n\sigma} \int_{|x| > \delta} e^{-\frac{x^2+y^2}{2n}} \frac{1}{|x|} dx dy \int_{\mathbb{R}^{2n-2}} e^{-\sum_{p=2}^{2n-k} \tilde{s}_p^2 - \sum_{p=2}^k \tilde{t}_p^2} d\tilde{s}_2 \dots d\tilde{s}_{2n-k} d\tilde{t}_2 \dots d\tilde{t}_k = \mathcal{O}\left(\frac{\|\gamma'\|}{2n\sigma} \frac{(2\pi)^n}{\sqrt{n}} \log(\sqrt{2n}\sigma)\right), \end{aligned} \quad (\text{D54})$$

where the last inequality is from Eqs. (D48) and (D50). When $\sum_{p=1}^{2n-k} (-1)^p s_p - \sum_{p=1}^k (-1)^p t_p < \delta$, with the same change of variables, we have

$$\begin{aligned} \text{VI} &\leq \int_{-\infty < s_1 \leq s_2 \leq \dots \leq s_{2n-k} < \infty, -\infty < t_1 \leq t_2 \leq \dots \leq t_k < \infty, |\sum_{p=1}^{2n-k} (-1)^p s_p - \sum_{p=1}^k (-1)^p t_p| < \delta} e^{-\sum_{p=1}^{2n-k} s_p^2 - \sum_{p=1}^k t_p^2} ds_1 \dots ds_{2n-k} dt_1 \dots dt_k \\ &\leq \int_{|x| < \delta} e^{-\frac{x^2+y^2}{2n}} dx \int_{\mathbb{R}^{2n-2}} e^{-\sum_{p=2}^{2n-k} \tilde{s}_p^2 - \sum_{p=2}^k \tilde{t}_p^2} d\tilde{s}_2 \dots d\tilde{s}_{2n-k} d\tilde{t}_2 \dots d\tilde{t}_k = \mathcal{O}\left(\frac{(2\pi)^n}{\sigma\sqrt{2n}}\right). \end{aligned} \quad (\text{D55})$$

Combining them together, we conclude that

$$\begin{aligned} \text{Term 1.2} &= \left| \exp\left(\frac{(2n-k)\beta^2}{4\sigma^2}\right) - 1 \right| \int_{-\infty < s_1 \leq s_2 \leq \dots \leq s_{2n-k} < \infty, -\infty < t_1 \leq t_2 \leq \dots \leq t_k < \infty} e^{-\sum_{p=1}^{2n-k} s_p^2 - \sum_{p=1}^k t_p^2} \\ &\quad \left| \int \gamma(\omega) e^{i2\sigma\omega \sum_{p=1}^{2n-k} (-1)^p s_p - i2\sigma\omega \sum_{p=1}^k (-1)^p t_p} d\omega \right| ds_1 \dots ds_{2n-k} dt_1 \dots dt_k \\ &\leq \frac{(2\pi)^n}{\sigma\sqrt{n}} \left| \exp\left(\frac{(2n-k)\beta^2}{4\sigma^2}\right) - 1 \right| \mathcal{O}\left(\log(\sqrt{2n}\sigma)\|\gamma'\|_{L^1}\right). \end{aligned} \quad (\text{D56})$$

Appendix E: Ground state preparation beyond Lindblad limit

For ground state preparation, we let the state of the environment be $\rho_E = |0\rangle\langle 0|$, we have the following result:

Theorem E.1. (Ground state) Assume H has a spectral gap Δ and let $|\psi_0\rangle$ be the ground state of H . Then for any $\epsilon > 0$, if

$$\sigma = \Omega\left(\frac{1}{\Delta} \log^{3/2}(\|H\|/\epsilon)\right), \quad T = \tilde{\Omega}(\sigma), \quad \Gamma = \mathcal{O}(1) (\Leftrightarrow \alpha = \mathcal{O}(\sigma^{-1/2})), \quad (\text{E1})$$

then

$$\|\Phi_\Gamma(|\psi_0\rangle\langle\psi_0|) - |\psi_0\rangle\langle\psi_0|\|_1 < \alpha^2\epsilon \quad (\text{E2})$$

To prove Theorem E.1, we consider the zero temperature setting $\beta = \infty$. In which case, the evolution operator admits the following expression as $\beta \rightarrow \infty$,

$$\begin{aligned} \Phi_\Gamma \rho_n &= \int g(\omega) \text{Tr}_E[U^\Gamma(T)(\rho_n \otimes \rho_E)U^{\Gamma\dagger}(T)](\omega) d\omega \\ &= U_S(2T)\rho_n U_S(2T)^\dagger \\ &\quad + \mathbb{E}_{A_S} \left(\sum_{n \geq 1} \Gamma^{2n} (-1)^n \sum_{k=0}^{2n} (-1)^k \int_{-\infty}^0 (g(\omega) + g(-\omega)) U_S(T) G_{2n-k, A_S}^\dagger(\omega) U_S(T) \rho_n U_S^\dagger(T) G_{k, A_S}(\omega) U_S^\dagger(T) d\omega \right). \end{aligned} \quad (\text{E3})$$

We define the N finite summation as

$$\begin{aligned} \Phi_\Gamma^N \rho_n &= U_S(2T)\rho_n U_S(2T)^\dagger \\ &\quad + \mathbb{E}_{A_S} \left(\sum_{n=1}^N \Gamma^{2n} (-1)^n \sum_{k=0}^{2n} (-1)^k \int_{-\infty}^0 (g(\omega) + g(-\omega)) U_S(T) G_{2n-k, A_S}^\dagger(\omega) U_S(T) \rho_n U_S^\dagger(T) G_{k, A_S}(\omega) U_S^\dagger(T) d\omega \right). \end{aligned} \quad (\text{E4})$$

Then, the tail part can be bounded as:

$$\|\Phi_\Gamma \rho_n - \Phi_\Gamma^N \rho_n\|_1 \leq \sum_{n>N} \Gamma^{2n} \sum_{k=0}^{2n} \|A_S\|^{2n} \sum_{k=0}^{2n} \frac{1}{(2n-k)!k!} \left(\int_{-\infty}^{\infty} f(t) dt \right)^{2n} = \sum_{n>N} \frac{(\mathcal{O}(\Gamma\|A_S\|))^{2n}}{(2n)!} \quad (\text{E5})$$

In the following part of the proof, we assume A_S is a hermitian operator for simplicity. The calculation for the non-hermitian case is almost the same. We assume that there is a spectral gap $\Delta = \lambda_1 - \lambda_0 > 0$ of the system Hamiltonian H . This property can be utilized to show the decay property of the finite summation term by analyzing the Heisenberg picture system operator in the frequency space. The system Hamiltonian can be decomposed as

$$H = \sum_{\lambda_i \in \text{spec}(H)} \lambda_i |\psi_i\rangle\langle\psi_i|,$$

where the ground state $|\psi_0\rangle$ corresponds to the ground energy λ_0 . In the Heisenberg picture, any system operator A_S has the frequency space expansion,

$$A_S(t) = \sum_{i,j} e^{i(\lambda_i - \lambda_j)t} |\psi_i\rangle\langle\psi_i| A_S |\psi_j\rangle\langle\psi_j| = \sum_{\nu} e^{i\nu t} \sum_{\lambda_i - \lambda_j = \nu} |\psi_i\rangle\langle\psi_i| A_S |\psi_j\rangle\langle\psi_j| = \sum_{\nu \in B(H)} e^{i\nu t} A_S(\nu), \quad (\text{E6})$$

where $B(H) = \text{spec}(H) - \text{spec}(H)$ is the set of Bohr frequencies and

$$A_S(\nu) = \sum_{\lambda_i - \lambda_j = \nu} |\psi_i\rangle\langle\psi_i| A_S |\psi_j\rangle\langle\psi_j|. \quad (\text{E7})$$

Consequently,

$$A_S(t_1) A_S(t_2) \cdots A_S(t_n) = \sum_{\nu_1, \dots, \nu_n \in B(H)} e^{i \sum_{k=1}^n \nu_k t_k} A_S(\nu_1) A_S(\nu_2) \cdots A_S(\nu_n). \quad (\text{E8})$$

Using the projection operator in Eq. (E7), the product of system operators on the frequency space follow

$$\begin{aligned} & A_S(\nu_1) A_S(\nu_2) \cdots A_S(\nu_n) \\ &= \sum_{E_k - E_{k+1} = \nu_k, k=1,2,\dots,n} |\psi_{E_1}\rangle\langle\psi_{E_1}| A_S |\psi_{E_2}\rangle\langle\psi_{E_2}| A_S \cdots |\psi_{E_n}\rangle\langle\psi_{E_n}| A_S |\psi_{E_{n+1}}\rangle\langle\psi_{E_{n+1}}| \end{aligned} \quad (\text{E9})$$

with $E_k \in \text{spec}(H)$. When substituting ρ_n into Eq. (E3) with the ground state $|\psi_0\rangle\langle\psi_0|$, it suffices to simplify the form of $\tilde{G}_{2n-k, A_S}^\dagger(\omega) |\psi_0\rangle$ and $\langle\psi_0| \tilde{G}_{k, A_S}(\omega)$ separately.

For $1 \leq n \leq N$, we have

$$\begin{aligned} \tilde{G}_{n, A_S}^\dagger(\omega) |\psi_0\rangle &= \int_{-\infty < s_1 \leq \dots \leq s_n < \infty} A_S(s_n) \cdots A_S(s_1) e^{i\omega \sum_{k=1}^n (-1)^k s_k} f(s_1) \cdots f(s_n) ds_1 \cdots ds_n |\psi_0\rangle \\ &= \int_{-\infty < s_n \leq \dots \leq s_1 < \infty} A_S(s_1) \cdots A_S(s_n) e^{i\omega \sum_{k=1}^n (-1)^{k+n+1} s_k} f(s_1) \cdots f(s_n) ds_1 \cdots ds_n |\psi_0\rangle \\ &= \sum_{\nu_1, \nu_2, \dots, \nu_n \in B(H)} \underbrace{\int_{-\infty}^{\infty} \cdots \int_{-\infty}^{s_{n-1}} f(s_1) \cdots f(s_n) \exp \left(i \sum_{k=1}^n (\nu_k + (-1)^{k+n+1} \omega) s_k \right) ds_n \cdots ds_1 A_S(\nu_1) \cdots A_S(\nu_n) |\psi_0\rangle}_{\text{I}_n(|\psi_0\rangle)} \\ &= \underbrace{\sum_{\sum_i \nu_i < \Delta} \int_{-\infty}^{\infty} \cdots \int_{-\infty}^{s_{n-1}} f(s_1) \cdots f(s_n) \exp \left(i \sum_{k=1}^n (\nu_k + (-1)^{k+n+1} \omega) s_k \right) ds_n \cdots ds_1 A_S(\nu_1) \cdots A_S(\nu_n) |\psi_0\rangle}_{\text{I}_n(|\psi_0\rangle)} \\ &+ \underbrace{\sum_{\sum_i \nu_i \geq \Delta} \int_{-\infty}^{\infty} \cdots \int_{-\infty}^{s_{n-1}} f(s_1) \cdots f(s_n) \exp \left(i \sum_{k=1}^n (\nu_k + (-1)^{k+n+1} \omega) s_k \right) ds_n \cdots ds_1 A_S(\nu_1) \cdots A_S(\nu_n) |\psi_0\rangle}_{\text{II}_n(|\psi_0\rangle)} \end{aligned} \quad (\text{E10})$$

For the first term, it can be rewritten using the projection operator in Eq. (E9) as

$$\begin{aligned}
I_n(|\psi_0\rangle) &= \sum_{\sum_i \nu_i < \Delta} \int_{-\infty}^{\infty} \cdots \int_{-\infty}^{s_{n-1}} f(s_1) \cdots f(s_n) \exp \left(i \sum_{k=1}^n (\nu_k + (-1)^{k+n+1} \omega) s_k \right) ds_n \cdots ds_1 \\
&\quad \sum_{E_i - E_{i+1} = \nu_i, i=1,2,\dots,n} |\psi_{E_1}\rangle \langle \psi_{E_1}| A_S |\psi_{E_2}\rangle \langle \psi_{E_2}| A_S \cdots |\psi_{E_n}\rangle \langle \psi_{E_n}| A_S |\psi_{E_{n+1}}\rangle \langle \psi_{E_{n+1}}| |\psi_0\rangle \\
&= \sum_{\sum_i \nu_i < \Delta} \int_{-\infty}^{\infty} \cdots \int_{-\infty}^{s_{n-1}} f(s_1) \cdots f(s_n) \exp \left(i \sum_{k=1}^n (\nu_k + (-1)^{k+n+1} \omega) s_k \right) ds_n \cdots ds_1 \\
&\quad \sum_{E_i - E_{i+1} = \nu_i, i=1,2,\dots,n, E_1 - E_0 = \sum_i \nu_i < \Delta} |\psi_{E_1}\rangle \langle \psi_{E_1}| A_S |\psi_{E_2}\rangle \langle \psi_{E_2}| A_S \cdots |\psi_{E_n}\rangle \langle \psi_{E_n}| A_S |\psi_0\rangle.
\end{aligned} \tag{E11}$$

Since the Hamiltonian is gapped with $\Delta > 0$, every non-ground eigenvalue lies at least Δ above E_0 . Therefore, if the accumulated energy input satisfies $E_1 - E_0 = \sum_{i=1}^n \nu_i < \Delta$, we must have $E_1 = E_0$ and

$$\begin{aligned}
I_n(|\psi_0\rangle) &= \sum_{\sum_i \nu_i = 0} \int_{-\infty}^{\infty} \cdots \int_{-\infty}^{s_{n-1}} f(s_1) \cdots f(s_n) \exp \left(i \sum_{k=1}^n (-1)^{k+n+1} \omega s_k \right) ds_n \cdots ds_1 \\
&\quad \left(\sum_{E_i - E_{i+1} = \nu_i, i=1,2,\dots,n} \langle \psi_0 | A_S |\psi_{E_2}\rangle \langle \psi_{E_2}| A_S \cdots |\psi_{E_n}\rangle \langle \psi_{E_n}| A_S |\psi_0\rangle \right) |\psi_0\rangle \\
&= \int_{-\infty}^{\infty} \cdots \int_{-\infty}^{s_{n-1}} f(s_1) \cdots f(s_n) \exp \left(i \sum_{k=1}^n (-1)^{k+n+1} \omega s_k \right) ds_n \cdots ds_1 \langle \psi_0 | A_S^n |\psi_0\rangle |\psi_0\rangle = d_n |\psi_0\rangle,
\end{aligned} \tag{E12}$$

where

$$d_n := \int_{-\infty}^{\infty} \cdots \int_{-\infty}^{s_{n-1}} f(s_1) \cdots f(s_n) \exp \left(i \sum_{k=1}^n (-1)^{k+n+1} \omega s_k \right) ds_n \cdots ds_1 \langle \psi_0 | A_S^n |\psi_0\rangle.$$

It reveals that the first term is always proportional to $|\psi_0\rangle$. From another side, the second term can be bounded as

$$\|\Pi_n(|\psi_0\rangle)\| \leq \|A_S\|^n \sum_{\sum_i \nu_i \geq \Delta} \left| \int_{-\infty}^{\infty} \cdots \int_{-\infty}^{s_{n-1}} f(s_1) \cdots f(s_n) \exp \left(i \sum_{k=1}^n (\nu_k + (-1)^{k+n+1} \omega) s_k \right) ds_n \cdots ds_1 \right| \tag{E13}$$

It is sufficient to calculate the multivariable Fourier transform of f .

Lemma E.2 (Multivariable Fourier transformation of f).

$$\left| \int_{-\infty}^{\infty} \cdots \int_{-\infty}^{s_{n-1}} f(s_1) \cdots \exp \left(i \sum_{k=1}^n \alpha_k s_k \right) ds_n \cdots ds_1 \right| \leq \frac{n^{n/2}}{n!} \exp \left(-\frac{\sigma^2}{n} \left(\sum_{k=1}^n \alpha_k \right)^2 \right) \tag{E14}$$

Proof. We begin with change of variable $t_n = s_n$, $t_{n-1} = s_{n-1} - s_n$, $t_{n-2} = s_{n-2} - s_{n-1}$, \dots , $t_1 = s_1 - s_2$ to partially decouple the multivariable Fourier transformation,

$$\begin{aligned}
&\int_{-\infty}^{\infty} \cdots \int_{-\infty}^{s_{n-1}} f(s_1) \cdots \exp \left(i \sum_{k=1}^n \alpha_k s_k \right) ds_n \cdots ds_1 \\
&= \int_0^{\infty} \cdots \int_0^{\infty} \int_{-\infty}^{\infty} f \left(\sum_{k=1}^n t_k \right) f \left(\sum_{k=2}^n t_k \right) \cdots f(t_n) \exp \left(i \sum_{k=1}^n \left(\sum_{j=1}^k \alpha_j \right) t_k \right) dt_n \cdots dt_1.
\end{aligned} \tag{E15}$$

Substituting the expression of $f(t)$ back to the above expression, we obtain

$$\frac{1}{(2\pi)^{n/4} \sigma^n} \int_0^{\infty} \cdots \int_0^{\infty} \int_{-\infty}^{\infty} \exp \left(-\frac{1}{4\sigma^2} \sum_{k=1}^n \left(\sum_{p=k}^n t_p \right)^2 \right) \exp \left(i \sum_{p=1}^n \left(\sum_{k=1}^p \alpha_k \right) t_p \right) dt_n \cdots dt_1 \tag{E16}$$

Notice that

$$\sum_{k=1}^n \left(\sum_{p=k}^n t_p \right)^2 = n \left(t_n + \frac{1}{n} \sum_{k=1}^{n-1} \sum_{p=k}^{n-1} t_p \right)^2 - \frac{1}{n} \left(\sum_{k=1}^{n-1} \sum_{p=k}^{n-1} t_p \right)^2 + \sum_{k=1}^{n-1} \left(\sum_{p=k}^{n-1} t_p \right)^2, \quad (\text{E17})$$

Eq. (E15) can be further simplified by calculating the inner integral with respect to t_n ,

$$\begin{aligned} & \int_0^\infty \cdots \int_0^\infty \int_{-\infty}^\infty \exp\left(-\frac{n}{4\sigma^2}(t_n + \frac{1}{n} \sum_{k=1}^{n-1} \sum_{p=k}^{n-1} t_p)^2 + i \left(\sum_{k=1}^n \alpha_k\right) t_n\right) dt_n \\ & \exp\left(\frac{1}{4\sigma^2 n} \left(\sum_{k=1}^{n-1} \sum_{p=k}^{n-1} t_p\right)^2 - \frac{1}{4\sigma^2} \sum_{k=1}^{n-1} \left(\sum_{p=k}^{n-1} t_p\right)^2 + i \sum_{p=1}^{n-1} \left(\sum_{k=1}^p \alpha_k\right) t_p\right) dt_{n-1} \cdots dt_1 \\ & = \frac{2\sigma\sqrt{\pi}}{\sqrt{n}} \exp\left(-\frac{\sigma^2}{n} \left(\sum_{k=1}^n \alpha_k\right)^2\right) \int_0^\infty \cdots \int_0^\infty dt_{n-1} \cdots dt_1 \\ & \exp\left(\frac{1}{4\sigma^2 n} \left(\sum_{k=1}^{n-1} \sum_{p=k}^{n-1} t_p\right)^2 - \frac{1}{4\sigma^2} \sum_{k=1}^{n-1} \left(\sum_{p=k}^{n-1} t_p\right)^2 + i \sum_{p=1}^{n-1} \left(\sum_{k=1}^p \alpha_k\right) t_p - \frac{i}{n} \sum_{k=1}^n \alpha_k \sum_{k=1}^{n-1} \sum_{p=k}^{n-1} t_p\right). \end{aligned} \quad (\text{E18})$$

Thus, it can be upper bounded by the half line integral of decoupled Gaussian distribution,

$$\begin{aligned} & \left| \int_0^\infty \cdots \int_0^\infty \int_{-\infty}^\infty \exp\left(-\frac{n}{4\sigma^2}(t_n + \frac{1}{n} \sum_{k=1}^{n-1} \sum_{p=k}^{n-1} t_p)^2 + i \sum_{k=1}^n \alpha_k t_n\right) dt_n \right. \\ & \left. \exp\left(\frac{1}{4\sigma^2 n} \left(\sum_{k=1}^{n-1} \sum_{p=k}^{n-1} t_p\right)^2 - \frac{1}{4\sigma^2} \sum_{k=1}^{n-1} \left(\sum_{p=k}^{n-1} t_p\right)^2 + i \sum_{p=1}^{n-1} \left(\sum_{k=1}^p \alpha_k\right) t_p\right) dt_{n-1} \cdots dt_1 \right| \\ & \leq \frac{2\sigma\sqrt{\pi}}{\sqrt{n}} \exp\left(-\frac{\sigma^2}{n} \left(\sum_{k=1}^n \alpha_k\right)^2\right) \int_0^\infty \cdots \int_0^\infty \exp\left(\frac{1}{4\sigma^2 n} \left(\sum_{k=1}^{n-1} \sum_{p=k}^{n-1} t_p\right)^2 - \frac{1}{4\sigma^2} \sum_{k=1}^{n-1} \left(\sum_{p=k}^{n-1} t_p\right)^2\right) dt_{n-1} \cdots dt_1 \\ & \leq \frac{2\sigma\sqrt{\pi}}{\sqrt{n}} \exp\left(-\frac{\sigma^2}{n} \left(\sum_{k=1}^n \alpha_k\right)^2\right) \int_0^\infty \cdots \int_0^\infty \exp\left(-\frac{1}{4\sigma^2 n} \sum_{k=1}^{n-1} \left(\sum_{p=k}^{n-1} t_p\right)^2\right) dt_{n-1} \cdots dt_1 \end{aligned} \quad (\text{E19})$$

Notice that with another change of variable, $s_k = \sum_{p=k}^{n-1} t_p$, the nested integral can be calculated explicitly as

$$\begin{aligned} & \int_0^\infty \cdots \int_0^\infty \exp\left(-\frac{1}{4\sigma^2 n} \sum_{k=1}^{n-1} \left(\sum_{p=k}^{n-1} t_p\right)^2\right) dt_{n-1} \cdots dt_1 = \int_{-\infty < s_1 \leq s_2 \leq \cdots s_{n-1} < \infty} \exp\left(-\frac{1}{4\sigma^2 n} \sum_{k=1}^{n-1} s_k^2\right) ds_{n-1} \cdots ds_1 \\ & = \frac{1}{(n-1)!} \left(\int_{-\infty}^\infty \exp\left(-\frac{s^2}{4\sigma^2 n}\right) ds \right)^{n-1} = \frac{(2\sigma\sqrt{n\pi})^{n-1}}{(n-1)!} \end{aligned} \quad (\text{E20})$$

Combined with the above inequalities, we conclude the proof. \square

Replacing the Fourier coefficients in Lemma E.2 with

$$\sum_{k=1}^n \alpha_k = \sum_{k=1}^n \nu_k + (-1)^{k+n+1} \omega = \begin{cases} \sum_{k=1}^n \nu_k & n \text{ is even} \\ \sum_{k=1}^n \nu_k - \omega & n \text{ is odd} \end{cases} \geq \Delta$$

as $\omega < 0$, we have

$$\begin{aligned} \|\Pi_n(|\psi_0\rangle)\| & \leq \|A_S\|^n |B(H)|^n 2\pi^{n/4} \frac{n^{\frac{n}{2}-1}}{(n-1)! 2^{n/4}} \frac{1}{\exp(-\frac{\sigma^2}{n} (\sum_{k=1}^n \nu_k + (-1)^k \omega)^2)} \\ & \leq \|A_S\|^n |B(H)|^n 2\pi^{n/4} \frac{n^{\frac{n}{2}-1}}{(n-1)! 2^{n/4}} \exp\left(-\frac{\Delta^2 \sigma^2}{n}\right) \\ & = \frac{(\mathcal{O}(\|A_S\| |B(H)| n^{1/2}))^n}{n!} \exp\left(-\frac{\Delta^2 \sigma^2}{n}\right) \end{aligned} \quad (\text{E21})$$

For the finite dimension case, the Hamiltonian H can be approximated by H_η such that the eigenvalue are equal spaced with η and with the same ground state. One typical construction of H_η is

$$H_\eta = \sum_i g_\eta(\lambda_i) |\psi_i\rangle\langle\psi_i|, g_\eta(x) = \eta \left\lfloor \frac{x}{\eta} + \frac{1}{2} \right\rfloor. \quad (\text{E22})$$

It induces $\|H - H_\eta\| \leq \eta$. Assume the above analysis are done with H_η , then $|B(H)| \leq \|H\|/\eta$, and

$$\begin{aligned} \|\Pi_n(|\psi_0\rangle)\| &\leq \|A_S\|^n \frac{\|H\|^n}{\eta^n} 2\pi^{n/4} \frac{n^{\frac{n}{2}-1}}{(n-1)!} \frac{1}{2^{n/4}} \exp\left(-\frac{\Delta^2\sigma^2}{n}\right) \\ &= \frac{(\mathcal{O}(\|A_S\|\|H\|\eta^{-1}n^{1/2}))^n}{n!} \exp\left(-\frac{\Delta^2\sigma^2}{n}\right) \end{aligned} \quad (\text{E23})$$

Additionally, by Duhamel's principle, $\|U_{S,H}(t) - U_{S,H_\eta}(t)\| \leq |t|\eta$, we have

$$\|U_{S,H}^\dagger(t)AU_{S,H}(t) - U_{S,H_\eta}^\dagger(t)AU_{S,H_\eta}(t)\| \leq 2\eta|t|\|A\|. \quad (\text{E24})$$

Thus, by multiplying them together,

$$\begin{aligned} &\|A_{S,H}(t_{k+1})A_{S,H}(t_{k+2}) \cdots A_{S,H}(t_{2n})|\psi_0\rangle\langle\psi_0|A_{S,H}(t_1) \cdots A_{S,H}(t_k) \\ &- A_{S,H_\eta}(t_{k+1})A_{S,H_\eta}(t_{k+2}) \cdots A_{S,H_\eta}(t_{2n})|\psi_0\rangle\langle\psi_0|A_{S,H_\eta}(t_1) \cdots A_{S,H_\eta}(t_k)\| \leq 2\eta\|A_S\|^{2n} \left(\sum_{i=1}^{2n} |t_i| \right) \end{aligned} \quad (\text{E25})$$

Define $G_{n,[\cdot],A_S}$ as the G operator with Hamiltonian $[\cdot]$ and A_S . Also, let the operator $\tilde{\Phi}_{\Gamma,H_\eta}$ of the same form as in Eq. (D4), with only the Hamiltonian in the operator $G_{n,[\cdot],A_S}$ replaced with H_η ,

$$\tilde{\Phi}_{\Gamma,H_\eta}(\rho) := U_{S,H}(T)\mathbb{E}_{A_S} \left(\sum_n \Gamma^{2n} (-1)^n \sum_{k=0}^{2n} (-1)^k \int \gamma(\omega) \tilde{G}_{2n-k,H_\eta,A_S}^\dagger(\omega) U_{S,H}(T) \rho U_{S,H}^\dagger(T) \tilde{G}_{k,H_\eta,A_S}(\omega) d\omega \right) U_{S,H}^\dagger(T).$$

This inequality helps bound the difference between $\tilde{\Phi}_{\Gamma,H}$ and $\tilde{\Phi}_{\Gamma,H_\eta}$:

$$\begin{aligned} &\|\tilde{\Phi}_{\Gamma,H}^N|\psi_0\rangle\langle\psi_0| - \tilde{\Phi}_{\Gamma,H_\eta}^N|\psi_0\rangle\langle\psi_0|\|_1 \\ &\leq \mathbb{E}_{A_S} \left(\sum_{n=1}^N \Gamma^{2n} \sum_{k=0}^{2n} \int_{-\infty}^0 (g(\omega) + g(-\omega)) \|U_{S,H}(T) \tilde{G}_{2n-k,H,A_S}^\dagger(\omega) U_{S,H}(T) |\psi_0\rangle\langle\psi_0| U_{S,H}^\dagger(T) \tilde{G}_{k,H,A_S}(\omega) U_{S,H}^\dagger(T) \right. \\ &\quad \left. - U_{S,H}(T) \tilde{G}_{2n-k,H_\eta,A_S}^\dagger(\omega) U_{S,H}(T) |\psi_0\rangle\langle\psi_0| U_{S,H}^\dagger(T) \tilde{G}_{k,H_\eta,A_S}(\omega) U_{S,H}^\dagger(T)\|_1 d\omega \right) \\ &\leq \mathbb{E}_{A_S} \left(\sum_{n=1}^N \Gamma^{2n} \sum_{k=0}^{2n} \int_{-\infty}^0 (g(\omega) + g(-\omega)) \|\tilde{G}_{2n-k,H,A_S}^\dagger(\omega) |\psi_0\rangle\langle\psi_0| \tilde{G}_{k,H,A_S}(\omega) - \tilde{G}_{2n-k,H_\eta,A_S}^\dagger(\omega) |\psi_0\rangle\langle\psi_0| \tilde{G}_{k,H_\eta,A_S}(\omega)\|_1 d\omega \right) \\ &\leq \sum_{n=1}^N \Gamma^{2n} \sum_{k=0}^{2n} 2\eta\|A_S\|^{2n} \int_{-\infty < t_{2n} \leq \cdots \leq t_{k+1} < \infty, -\infty < t_1 \leq \cdots \leq t_k < \infty} \left(\sum_{i=1}^{2n} |t_i| \right) f(t_1) \cdots f(t_{2n}) dt_1 \cdots dt_{2n} \\ &= \sum_{n=1}^N \Gamma^{2n} \sum_{k=0}^{2n} 2\eta\|A_S\|^{2n} \frac{2n}{k!(2n-k)!} \left(\int_{-\infty}^{\infty} |t| f(t) dt \right) \left(\int_{-\infty}^{\infty} f(t) dt \right)^{2n-1} \\ &\leq 2\eta \sum_{n=1}^N \frac{(\Gamma\|A_S\|)^{2n}}{(2n-1)!} \sum_{k=0}^{2n} \binom{2n}{k} \left(\frac{4\sigma}{(2\pi)^{1/4}} \right) \left(2^{3/4} \pi^{1/4} \right)^{2n-1} \\ &= \mathcal{O}(\eta\alpha^2\sigma^2\|A_S\|^2 \cosh(\mathcal{O}(\alpha\sigma^{1/2}\|A_S\|))). \end{aligned} \quad (\text{E26})$$

Here, we use $\Gamma = \alpha\sigma^{1/2}$ in the last inequality.

Notice $\alpha = \mathcal{O}(\sigma^{-1/2})$. We choose

$$\eta = \Theta(\sigma^{-2}\epsilon), \quad (\text{E27})$$

such that

$$\|\tilde{\Phi}_{\Gamma,H}^N |\psi_0\rangle\langle\psi_0| - \tilde{\Phi}_{\Gamma,H_\eta}^N |\psi_0\rangle\langle\psi_0| \|_1 = \mathcal{O} \left(\eta \alpha^2 (\sigma^2 + T\sigma) \|A_S\|^2 \cosh(\mathcal{O}(\alpha\sigma^{1/2} \|A_S\|)) \right) \leq \frac{\alpha^2 \epsilon}{3}.$$

Now, we first show $\tilde{\Phi}_{\Gamma,H_\eta}^N |\psi_0\rangle\langle\psi_0| \approx c |\psi_0\rangle\langle\psi_0|$. Given $N > 0$, we define

$$d_N = 1 + \sum_{n=1}^N \Gamma^{2n} (-1)^n \sum_{k=0}^{2n} (-1)^k \int_{-\infty}^0 (g(\omega) + g(-\omega)) d_{2n-k}(\omega) d_k^*(\omega) d\omega \in \mathbb{R}. \quad (\text{E28})$$

We note that $d_0(\omega) = 1$ and

$$|d_{2n-k}| \leq \|A_S\|^{2n-k} \int_{-\infty < s_{2n-k} \leq \dots \leq s_1 < \infty} f(s_1) \dots f(s_{2n-k}) ds_{2n-k} \dots ds_1 = \frac{(\mathcal{O}(\|A_S\|))^{2n-k}}{(2n-k)!} \quad (\text{E29})$$

when $2n - k \geq 1$.

Combining this and Eq. (E23), we have

$$\begin{aligned} \left\| \tilde{\Phi}_{\Gamma,H_\eta}^N |\psi_0\rangle\langle\psi_0| - d_N |\psi_0\rangle\langle\psi_0| \right\|_1 &\leq 2 \left\| \sum_{n=1}^N \Gamma^{2n} (-1)^n \sum_{k=1}^{2n-1} (-1)^k \int_{-\infty}^0 (g(\omega) + g(-\omega)) d_{2n-k} |\psi_0\rangle \Pi_k^* (|\psi_0\rangle) d\omega \right\| \\ &+ \left\| \sum_{n=1}^N \Gamma^{2n} (-1)^n \sum_{k=1}^{2n-1} (-1)^k \int_{-\infty}^0 (g(\omega) + g(-\omega)) \Pi_{2n-k} (|\psi_0\rangle) \Pi_k^* (|\psi_0\rangle) d\omega \right\| \\ &+ 2 \left\| \sum_{n=1}^N \Gamma^{2n} (-1)^n \int_{-\infty}^0 (g(\omega) + g(-\omega)) \Pi_{2n} (|\psi_0\rangle) d\omega \right\| \\ &= \sum_{n=1}^N (\mathcal{O}(\Gamma \|A_S\|))^{2n} \sum_{k=1}^{2n} \frac{\|H\|^k k^{k/2}}{\eta^k k! (2n-k)!} \exp\left(-\frac{\sigma^2 \Delta^2}{k}\right) \\ &+ \sum_{n=1}^N (\mathcal{O}(\Gamma \|A_S\| \|H\| \eta^{-1}))^{2n} \sum_{k=1}^{2n-1} \frac{(2n-k)^{(2n-k)/2} k^{k/2}}{(2n-k)! (k)!} \exp(-\sigma^2 \Delta^2 \frac{2n}{k(2n-k)}) \\ &\leq \sum_{n=1}^N (\mathcal{O}(\|H\| \eta^{-1}))^{2n} \sum_{k=1}^{2n} \frac{(2n-k)^{(2n-k)/2} k^{k/2}}{(2n-k)! (k)!} \exp\left(-\frac{\sigma^2 \Delta^2}{2n}\right) \end{aligned} \quad (\text{E30})$$

Here, the first and third terms in the initial inequality combine to produce the first term in the equality. In the last inequality, we use $\Gamma = \mathcal{O}(1)$ ($\alpha = \mathcal{O}(\sigma^{-1/2})$) and $\|A_S\| \leq 1$.

Noticing that $\sum_{k=1}^{2n} \frac{(2n-k)^{(2n-k)/2} k^{k/2}}{(2n-k)! (k)!} \leq \frac{(\Theta(1))^n}{\sqrt{n!}}$. We obtain

$$\begin{aligned} &\sum_{n=1}^N (\mathcal{O}(\|H\| \eta^{-1}))^{2n} \sum_{k=1}^{2n} \frac{(2n-k)^{(2n-k)/2} k^{k/2}}{(2n-k)! (k)!} \exp\left(-\frac{\sigma^2 \Delta^2}{2n}\right) \\ &= \sum_{n=1}^N \frac{(\mathcal{O}(\|H\|^2 \eta^{-2}))^n}{\sqrt{n!}} \exp\left(-\frac{\sigma^2 \Delta^2}{2n}\right) \\ &\leq (\max\{\mathcal{O}(\|H\|^2 \eta^{-2}), 1\})^N \sqrt{N} \exp\left(-\frac{\sigma^2 \Delta^2}{2N}\right) = (\mathcal{O}(\|H\|^2 \sigma^4 \epsilon^{-2}))^N \sqrt{N} \exp\left(-\frac{\sigma^2 \Delta^2}{2N}\right) \end{aligned} \quad (\text{E31})$$

Plugging this back into (E30), we obtain

$$\left\| \tilde{\Phi}_{\Gamma,H_\eta}^N |\psi_0\rangle\langle\psi_0| - d_N |\psi_0\rangle\langle\psi_0| \right\|_1 = (\mathcal{O}(\|H\|^2 \sigma^4 \epsilon^{-2}))^N \sqrt{N} \exp\left(-\frac{\sigma^2 \Delta^2}{2N}\right),$$

Combine the above bounds with Theorem D.2, we have

$$\begin{aligned} \|\Phi_{\Gamma,H} |\psi_0\rangle\langle\psi_0| - |\psi_0\rangle\langle\psi_0| \|_1 &\leq \|\Phi_{\Gamma,H} |\psi_0\rangle\langle\psi_0| - \tilde{\Phi}_{\Gamma,H}^N |\psi_0\rangle\langle\psi_0| \|_1 + \|\tilde{\Phi}_{\Gamma,H}^N |\psi_0\rangle\langle\psi_0| - \tilde{\Phi}_{\Gamma,H}^N |\psi_0\rangle\langle\psi_0| \|_1 \\ &+ \|\tilde{\Phi}_{\Gamma,H}^N |\psi_0\rangle\langle\psi_0| - \tilde{\Phi}_{\Gamma,H_\eta}^N |\psi_0\rangle\langle\psi_0| \|_1 + \|\tilde{\Phi}_{\Gamma,H_\eta}^N |\psi_0\rangle\langle\psi_0| - |\psi_0\rangle\langle\psi_0| \|_1 \\ &\leq \sum_{n>N}^{\infty} \frac{(\mathcal{O}(1))^{2n}}{2n!} + \mathcal{O}\left(\alpha^2 \sigma^2 \frac{1}{T} \exp\left(-\frac{T^2}{4\sigma^2}\right)\right) + \frac{\alpha^2 \epsilon}{3} + (\mathcal{O}(\|H\|^2 \sigma^4 \epsilon^{-2}))^N \sqrt{N} \exp\left(-\frac{\sigma^2 \Delta^2}{2N}\right) \end{aligned} \quad (\text{E32})$$

Set $N = \Theta(\log(\alpha^{-1}\epsilon^{-1}))$, we have $\sum_{n>N}^{\infty} \frac{(\mathcal{O}(1))^{2n}}{2n!} < \frac{\alpha^2\epsilon}{3}$. To make the last term smaller than $\alpha^2\epsilon/6$, it suffices to show

$$\exp\left(\frac{\sigma^2\Delta^2}{2N}\right) \geq (\alpha^2\epsilon)^{-1} \left(\mathcal{O}(\|H\|^2\sigma^4\epsilon^{-2})\right)^N \sqrt{N}.$$

Recall $\alpha = \Theta(\sigma^{-1/2})$. This can be satisfied by choosing $\sigma = \Omega\left(\Delta^{-1}\log^{3/2}(\|H\|/\epsilon)\right)$. We conclude the proof.

Appendix F: Mixing time analysis for thermal state preparation

In this section, we analyze the mixing time of the quantum channel Φ_{Γ} defined in (1) and establish the rigorous end-to-end complexity guarantee for thermal state preparation. The structure of this section is as follows:

- In Appendix F 1, we review the result in [22] and approximate leading order term in (C4) using KMS-Lindbladian dynamics plus higher-order correction terms. The result also includes a choice of the function $g(\omega)$ in (1) to ensure the approximation holds.
- In Appendix F 2, we present a novel perturbation theory in Theorem F.2 for Φ_{Γ} and show that the spectral gap of Φ_{Γ} can be lower bounded by that of the approximated KMS-Lindbladian dynamics even beyond the Lindblad limit.
- In Appendix F 3, we combine the results in the previous two subsections to establish the mixing time bound for Φ_{Γ} and present the end-to-end complexity guarantee for thermal state preparation.
- In Appendix F 4, we provide the proof of Theorem F.2.

In this section, the main technique part is analyzing the rescaled mixing time $t_{\text{mix}} = \alpha^2\tau_{\text{mix}}$. Thus, we will mainly use the notation $\alpha := \Gamma/\sqrt{\sigma}$ instead of Γ for simplicity. We will also use Φ_{Γ} and Φ_{α} interchangeably when there is no confusion.

1. Approximate Φ_{Γ} using KMS-Lindbladian dynamics

Following Theorem C.2, we define

$$\mathcal{M}_1[\rho] = -\mathbb{E}_{A_S} \left(\sum_{k=0}^2 (-1)^k \sigma \int \gamma(\omega) G_{2-k, A_S}^{\dagger}(\omega) \rho G_{k, A_S}(\omega) d\omega \right), \quad (\text{F1})$$

$$\mathcal{M}_2[\rho] = \frac{1}{\alpha^2} \mathbb{E}_{A_S} \left(\sum_{n=2}^{\infty} \Gamma^{2n} (-1)^n \sum_{k=0}^{2n} (-1)^k \int \gamma(\omega) G_{2n-k, A_S}^{\dagger}(\omega) \rho G_{k, A_S}(\omega) d\omega \right), \quad (\text{F2})$$

Here \mathcal{M}_1 corresponds to the Lindbladian derived in [22], as shown in Theorem F.1, and \mathcal{M}_2 collects all higher-order correction terms beyond Lindblad dynamics, starting from $\mathcal{O}(\alpha^4)$ term in α expansion, i.e.

$$\Phi_{\Gamma}\rho = \rho + \alpha^2 \mathcal{M}_1[\rho] + \alpha^2 \mathcal{M}_2[\rho]. \quad (\text{F3})$$

Given a jump operator V , we define the associated dissipative operator as

$$\mathcal{D}_V(\rho) = V\rho V^{\dagger} - \frac{1}{2}\{V^{\dagger}V, \rho\}. \quad (\text{F4})$$

According to [22, Theorem 27] and [46, Appendix B (B2)], we can show that \mathcal{M}_1 can be approximated by a Lindbladian that satisfies KMS detailed balance condition up to small error when $T = \Omega(\sigma)$ and $\sigma = \Omega(\beta)$.

Theorem F.1. *For any $\sigma > \beta$, we set*

$$g(\omega) = \frac{1}{Z} \exp\left(-\frac{(\beta\omega + 1)^2}{2(2 - \frac{\beta^2}{4\sigma^2})}\right), \quad Z = \sqrt{2\pi\left(2 - \frac{\beta^2}{4\sigma^2}\right)}. \quad (\text{F5})$$

Then, there exists a Lindbladian $\mathcal{L}_{\sigma,\text{KMS}}$ that satisfies KMS detailed balance condition (defined in Appendix C) and a Hermitian operator $H_{\sigma,\text{Lamb}}$ such that

$$\|\mathcal{M}_1 - (-i[H_{\sigma,\text{Lamb}}, \cdot] + \mathcal{L}_{\sigma,\text{KMS}})\|_{1 \leftrightarrow 1} = \mathcal{O}\left(\sigma \exp(-T^2/(4\sigma^2)) + \frac{\beta}{\sigma}\right),$$

and

$$\left\|\sigma_{\beta}^{-1/4} H_{\sigma,\text{Lamb}} \sigma_{\beta}^{1/4} - \sigma_{\beta}^{1/4} H_{\sigma,\text{Lamb}} \sigma_{\beta}^{-1/4}\right\| = \mathcal{O}\left(\frac{\beta}{\sigma}\right).$$

Here, $\mathcal{L}_{\sigma,\text{KMS}}$ takes the form of

$$\mathcal{L}_{\sigma,\text{KMS}}[\rho] = \mathbb{E}_{A_S} \left(-i[B_{A_S}, \rho] + \int_{-\infty}^{\infty} \gamma(\omega) \mathcal{D}_{V_{A_S, f_{\sigma}, \infty}(\omega)}(\rho) d\omega \right), \quad (\text{F6})$$

with $\gamma(\omega) = g(\omega)$, $V_{A_S, f_{\sigma}, \infty}(\omega) = \int_{-\infty}^{\infty} f_{\sigma}(t) A_S(t) \exp(-i\omega t) dt$, and

$$B_{A_S} = -\frac{1}{Z} \int_{-\infty}^{\infty} h_1(t_1) e^{-iHt_1} \left(\int_{-\infty}^{\infty} h_2(t_2) A_S(t_2) A_S(-t_2) dt_2 \right) e^{iHt_1} dt_1,$$

where $h_1(t) = \frac{1}{2\sigma\pi\beta} \exp\left(\frac{\beta^2}{32\sigma^2}\right) \left(\frac{1}{\cosh\frac{1}{2\pi t/\beta}} * \sin(-\beta t/(4\sigma^2)) \exp(-t^2/(2\sigma^2))\right)$ and

$$h_2(t) = 2\sqrt{\frac{2}{\beta^2} - \frac{1}{4\sigma^2}} \exp\left(\left(-\frac{4t^2}{\beta} - 2it\right)\frac{1}{\beta}\right).$$

In the weak coupling limit ($\Gamma \ll 1$), the channel Φ_{Γ} is well-approximated by the Lindbladian dynamics generated by $-i[H_{\sigma,\text{Lamb}}, \cdot] + \mathcal{L}_{\sigma,\text{KMS}}$. This generator admits the thermal state σ_{β} as its unique fixed point [22], with a mixing time determined by the spectral gap of $\mathcal{L}_{\sigma,\text{KMS}}$. Consequently, the fixed point of Φ_{Γ} remains close to σ_{β} [19, 20, 22, 51], and its mixing time is comparable to that of $\mathcal{L}_{\sigma,\text{KMS}}$ [22, 46]. Now, we extend the analysis beyond the Lindblad limit, focusing on the regime where Γ is not necessarily small.

2. Perturbation result for the spectral gap

Define the rescaled mixing time $t_{\text{mix},\Phi}(\epsilon)$ as in Eq. (C3). According to Theorem D.1, to achieve ϵ -accuracy in trace distance, the total Hamiltonian simulation time is

$$T_{\text{total}} := \tau_{\text{mix},\Phi}(\epsilon/4) \times 2T = \tilde{\mathcal{O}}\left(t_{\text{mix},\Phi}(\epsilon/4) \frac{\sigma}{\alpha^2}\right) = \tilde{\mathcal{O}}\left(\frac{\beta^2 t_{\text{mix},\Phi}^3(\epsilon/4)}{(\alpha^2\sigma)\epsilon^2}\right),$$

where we use $\sigma = \tilde{\Theta}(\beta t_{\text{mix},\Phi}(\epsilon/4)/\epsilon)$ from Theorem D.1 in the last equality. Therefore, to characterize the end-to-end complexity of the system-bath interaction algorithm, it suffices to upper bound the rescaled mixing time $t_{\text{mix},\Phi}(\epsilon)$ and lower bound the product $\alpha^2\sigma$.

Now, we are ready to state our main perturbation result, which gives an upper bound on the rescaled mixing time $t_{\text{mix},\Phi}(\epsilon)$ beyond the Lindblad limit

Theorem F.2. *Given $0 \leq \beta < \infty$. We choose $g(\omega)$ as in Theorem F.1 Eq. (F5). Let $\mathcal{L}_{\sigma,\text{KMS}}$ be the Lindbladian defined in Eq. (F6) and λ_{gap} be its spectral gap in the KMS inner product (defined in Appendix C). If $\alpha^2\sigma = \mathcal{O}(\lambda_{\text{gap}})$, $\sigma = \tilde{\Omega}(\beta\lambda_{\text{gap}}^{-1})$, and $T = \Omega(\sigma)$, then for any $\epsilon > 0$, we have*

$$t_{\text{mix},\Phi_{\Gamma}}(\epsilon) = \tilde{\mathcal{O}}\left(\frac{1}{\lambda_{\text{gap}}} \log\left(\frac{\|\sigma_{\beta}^{-1/2}\|}{\epsilon}\right)\right).$$

A detailed proof is provided in Appendix F4. A potential concern regarding this theorem is the dependence of λ_{gap} on σ : if the gap decreases as σ increases, the condition $\sigma = \tilde{\Omega}(\beta\lambda_{\text{gap}}^{-1})$ might fail. Fortunately, [22] demonstrated that the spectral gap of \mathcal{L}_{KMS} remains non-vanishing as $\sigma \rightarrow +\infty$ for simple physical models. [46] subsequently generalized

this to a much broader class of models, proving that with the $g(\omega)$ defined in Theorem F.1 Eq. (F5), the spectral gap is monotonically non-decreasing with respect to σ . We extend these results by combining this monotonicity with Theorem F.2 to demonstrate that the system-bath interaction algorithm achieves fast mixing times even beyond the Lindblad limit. Crucially, our analysis framework is highly general; it can be integrated with **all existing** spectral gap estimates for KMS generators to derive upper bounds on the mixing time beyond the Lindblad limit.

Methods: The proof of Theorem F.2 relies heavily on a perturbation analysis of the spectral gap of $\Phi_{\text{part},\alpha}$. To establish the contraction of Φ_Γ , we adopt the strategy of [22] by utilizing the weighted Hilbert-Schmidt norm, $\|\sigma_\beta^{-1/4} \cdot \sigma_\beta^{-1/4}\|_2$. Following the argument of [22], we first observe that the weighted Hilbert-Schmidt norm is invariant under the action of \mathcal{U}_S , i.e., $\|\sigma_\beta^{-1/4} \mathcal{U}_S(\rho) \sigma_\beta^{-1/4}\|_2 = \|\sigma_\beta^{-1/4} \rho \sigma_\beta^{-1/4}\|_2$. Consequently, to determine the contraction of $\Phi_\Gamma = \mathcal{U}_S \circ \Phi_{\text{part},\alpha} \circ \mathcal{U}_S$, it suffices to analyze $\Phi_{\text{part},\alpha}$.

In the case when α is not necessarily small, $\Phi_{\text{part},\alpha}$ can not be described by the Lindblad dynamics. This prohibits us from directly applying the spectral gap analysis for Lindbladians. Instead, we see $\Phi_{\text{part},\alpha}$ as a discrete perturbed channel of the Lindbladian dynamics generated by $-i[H_{\sigma,\text{Lamb}}, \cdot] + \mathcal{L}_{\sigma,\text{KMS}}$. Leveraging the analysis in Theorem D.1, \mathcal{M}_2 preserves the thermal state. Thus, it suffices to study its effect on the contraction rate of the channel. One technical challenge is that, the leading order term in \mathcal{M}_2 corresponds to the fourth term in the Taylor expansion of $\Phi_{\text{part},\alpha}$, which is positive and tends to shrink the spectral gap. However, thanks to the choice of filter function f_σ and inherent detailed balance condition that it satisfies, we can adopt similar idea as in the proof of Theorem D.1 to show that \mathcal{M}_2 has a small operator norm in the weighted Hilbert-Schmidt inner product, which scales as $\mathcal{O}(\alpha^2\sigma)$. This implies that, as long as $\alpha^2\sigma$ is small compared to the inverse spectral gap of $\mathcal{L}_{\sigma,\text{KMS}}$, the gap perturbation caused by \mathcal{M}_2 can be controlled and the contraction rate of $\Phi_{\text{part},\alpha}$ is still comparable with that of $\mathcal{L}_{\sigma,\text{KMS}}$.

3. Total Runtime Bounds Beyond the Lindblad Limit

Combining Theorem F.2 with the existing literature of spectral gap estimation for KMS generators [29, 32–35, 47], we can derive explicit total runtime bounds for the system-bath interaction algorithm beyond the Lindblad limit for various physical models [52]. We summarize the models and present our results below:

- High temperature local spin Hamiltonian [29, 32]:

Let $H = \sum_i h_i$ be a local Hamiltonian defined on a D -dimensional lattice, where each local term h_i is supported on a ball of constant radius. Furthermore, each qubit j is acted upon by only a constant number of terms h_i . Assume the system coupling operators are chosen as $\mathcal{A} = \{\pm X_j, \pm Y_j, \pm Z_j\}_{j=1}^n$. Then, there exists a constant β_c that only depends on the locality of H such that for any $0 < \beta < \beta_c$ and $\sigma > \beta$, we have $\lambda_{\text{gap}}(\mathcal{L}_{\sigma,\text{KMS}}) = \Omega(1/n)$ [53].

- Weak interaction fermionic system at all temperatures [47]:

Let a local fermionic Hamiltonian H defined on a D -dimensional lattice of fermionic systems, $\Lambda = [0, L]^D$, given by

$$H = H_0 + H_1 = \sum_{ij} M_{i,j} c_i^\dagger c_j + \varepsilon \sum_j h_j, \quad \|h_j\| \leq 1, \quad (\text{F7})$$

where $(M_{i,j})$ is a Hermitian matrix, and c_j^\dagger and c_j are the creation and annihilation operators at site j . The terms $\{h_j\}$ are local fermionic perturbations and are parity preserving, meaning that each h_j contains an even number of creation and annihilation operators. We further assume that H_0 is $(1, l)$ -geometrically local and $\sum_j h_j$ are (r_0, l) -geometrically local. Specifically, each term in H_0 is a product of fermionic operators acting on a set of sites whose Manhattan diameter is at most 1, and each h_j is a product of fermionic operators acting on a set of sites whose Manhattan diameter is at most r_0 . In addition, each site i appears in at most l non-trivial $c_i^\dagger c_j$ and h_j terms.

Assume the system coupling operators are chosen as $\mathcal{A} = \{\pm c_j^\dagger, c_j\}_{j=1}^n$. For any fixed $\beta > 0$, there exists a constant $\varepsilon_c = \Omega(1)$ that only depends on r_0, l, D, β such that for any $0 \leq \varepsilon < \varepsilon_c$ and $\sigma > \beta$, we have $\lambda_{\text{gap}}(\mathcal{L}_{\sigma,\text{KMS}}) = \Omega(1/n)$.

- Weak interaction spin system at all temperatures [33, 34, 47]: Let a local Hamiltonian H over a D -dimensional lattice of spin systems $\Lambda = [0, L]^D$ with the following form (the system size is $N = (L+1)^D$):

$$H = H_0 + H_1 = - \sum_i Z_i + \varepsilon \sum_j h_j, \quad \|h_j\| \leq 1. \quad (\text{F8})$$

Here, $H_0 = -\sum_i Z_i$ is referred to as the non-interacting term because its indices do not overlap. The choice of Z_i as the non-interacting term is made for convenience, and can be substituted with other simple, gapped local terms that also have non-overlapping indices. We assume the interacting term H_1 is an (r_0, l) -geometrically local Hamiltonian. A specific example of the Hamiltonian in Eq. (F8) is the D -dimensional TFIM model, which is a $(2, 2D + 1)$ -local Hamiltonian.

Assume the system coupling operators are chosen as $\mathcal{A} = \{\pm X_j, \pm Y_j, \pm Z_j\}_{j=1}^n$. For any fixed $\beta > 0$, there exists a constant $\varepsilon_c = \Omega(1)$ that only depends on r_0, l, D, β such that for any $0 \leq \varepsilon < \varepsilon_c$ and $\sigma > \beta$, we have $\lambda_{\text{gap}}(\mathcal{L}_{\sigma, \text{KMS}}) = \Omega(1/n)$.

- 1D local Hamiltonian at all temperatures [35]: Let a 1D local Hamiltonian $H = \sum_{j=1}^n h_j$, where $\{h_j\}$ satisfies the same assumption as (F8) but is defined on a 1D lattice. Assume the system coupling operators are chosen as $\mathcal{A} = \{\pm X_j, \pm Y_j, \pm Z_j\}_{j=1}^n$. Then, for any $0 \leq \beta < \infty$ and $\sigma > \beta$, we have $\lambda_{\text{gap}}(\mathcal{L}_{\sigma, \text{KMS}}) = \Omega(1/n)$.

Using the above spectral gap estimations and Theorem F.2, it is straightforward to derive the following total runtime bounds for the system-bath interaction algorithm beyond the Lindblad limit:

Corollary F.3 (Total runtime bound beyond Lindblad limit). *For all the above models with proper choice of β , by choosing $\alpha = \Theta(\sqrt{\epsilon/n^3})$, $\sigma = \tilde{\Theta}(n^2/\epsilon)$, and $T = \tilde{\Theta}(\sigma)$, we have $t_{\text{mix}, \Phi}(\epsilon) = \tilde{\mathcal{O}}(n^2)$. Therefore, the system-bath interaction algorithm can prepare an ϵ -approximation of the thermal state σ_β with total Hamiltonian simulation time*

$$T_{\text{total}} = \tilde{\mathcal{O}}\left(\frac{n^7}{\epsilon^2}\right).$$

The above theorem is a direct generalization of the end-to-end complexity results in [46] beyond the Lindblad limit. Because α is not required to be small, the above result saves a factor of n^3/ϵ^2 in total runtime compared to the previous best result in [46, Theorem 7]. On the other hand, we believe that the dependence on n in the total runtime is far from optimal and can be further improved in the case of different models. There are several directions of the improvement:

- Relaxing the requirement of $\alpha^2\sigma = \mathcal{O}(\lambda_{\text{gap}})$ in Theorem F.2. Currently, Theorem F.2 requires $\alpha^2\sigma = \mathcal{O}(1/n)$. In our perturbation framework, this strict condition is necessary to control the gap perturbation caused by the higher-order term \mathcal{M}_2 . Although \mathcal{M}_2 preserves the thermal state, its dominant term tends to shrink the spectral gap. Since the norm of \mathcal{M}_2 scales as $\mathcal{O}(\alpha^2\sigma)$, $\alpha^2\sigma$ must be sufficiently small relative to the inverse gap to prevent the gap from closing. However, our perturbation analysis does not currently exploit the fact that the terms constituting \mathcal{M}_2 are quasi-local when A_S is local and H is local Hamiltonian. When σ is not large, these terms produce only constant perturbations to the local gaps. Existing spectral gap analyses often rely on deriving a global gap from local gaps [35, 54]; this approach appears compatible with the quasi-local structure of \mathcal{M}_2 . If such a derivation can be extended to this context, it would suffice to bound the local gap perturbation. In that case, the effect of \mathcal{M}_2 would be controlled by $\alpha^2\sigma/n$, meaning the relaxed condition $\alpha^2\sigma = \mathcal{O}(1)$ should suffice to guarantee a non-vanishing global gap.
- Relaxing the dependence of $\log(\|\sigma_\beta^{-1/2}\|/\epsilon)$. In Corollary F.3, the factor of n^3 arises from the dependence on the initial condition, a known limitation of mixing time analysis based solely on the spectral gap. For certain systems where the Davies generator can be efficiently approximated, it might be possible to improve this dependence to $\log(n)$ using techniques like Modified Logarithmic Sobolev Inequalities (MLSI) [26, 28]. The main technical challenge is to extend the entropy decay analysis from continuous Lindbladian dynamics to the discrete channel Φ_Γ , which prohibits us from directly taking derivative of the entropy functional. Another possible way to improve the dependence on the initial condition is to use the oscillator norm technique developed in [21, 32, 47]. This technique can directly bound the convergence in observables without going through the spectral gap, thus avoiding the dependence on the initial condition. However, even in the Lindblad limit regime, the forward unitary map \mathcal{U}_S and nonvanishing coherent part $-i[H_{\text{Lamb}}, \rho]$ prohibits us from directly applying this technique. We leave this as an interesting future direction to investigate.
- Relaxing the interaction strength requirement to strong coupling regime. In our analysis, we require $\alpha^2\sigma = (1)$. Although this goes beyond the Lindblad limit, the interaction strength is still relatively weak since $\alpha/\sqrt{\sigma} \ll 1$. Surprisingly, our numerical results suggest that even in the strong coupling regime where $\alpha/\sqrt{\sigma} = \Omega(1)$, the fixed point of Φ_Γ remains close to the thermal state, and the mixing time still decreases with α^{-2} factor. It would be an interesting future direction to theoretically understand the performance of the system-bath interaction algorithm in this strong coupling regime. This can potentially further reduce the total runtime.

4. Proof of Theorem F.2

Recall (F2), we define

$$\mathcal{M}_{2,\infty} = \frac{1}{\alpha^2} \mathbb{E}_{A_S} \left(\sum_{n \geq 2} \Gamma^{2n} (-1)^n \sum_{k=0}^{2n} (-1)^k \int \gamma(\omega) G_{2n-k, A_S, \infty}^\dagger(\omega) \rho G_{k, A_S, \infty}(\omega) d\omega \right)$$

with

$$G_{k, A_S, \infty}(\omega) = \int_{-\infty < t_1 \leq \dots \leq t_k < \infty} A_S(t_1) A_S^\dagger(t_2) \dots e^{-i\omega \sum_{p=1}^k (-1)^p t_p} f_\sigma(t_1) \dots f_\sigma(t_k) dt_1 \dots dt_k$$

We first provide an upper bound for the norm of $\mathcal{M}_{2,\infty}$:

Lemma F.4. *Assuming $\Gamma^2 = \alpha^2 \sigma = \mathcal{O}(1)$, we have*

$$\|\mathcal{M}_{2,\infty}\|_{2 \leftrightarrow 2} = \mathcal{O}(\alpha^2 \sigma), \quad (\text{F9})$$

$$\|\sigma_\beta^{-1/4} \mathcal{M}_{2,\infty} [\sigma_\beta^{1/4} \cdot \sigma_\beta^{1/4}] \sigma_\beta^{-1/4}\|_{2 \leftrightarrow 2} = \mathcal{O}(\alpha^2 \sigma), \quad (\text{F10})$$

Proof of Lemma F.4. We first prove (F9). We fix n, k in the summation of (F2) and take an arbitrary matrix ρ (not necessary density operator). Following the same calculation in (D16), we have

$$\begin{aligned} & \int \gamma(\omega) G_{2n-k, A_S}^\dagger(\omega) \rho G_{k, A_S}(\omega) d\omega \\ &= \int_{-\infty < s_1 \leq s_2 \leq \dots \leq s_{2n-k} < \infty, -\infty < t_1 \leq t_2 \leq \dots \leq t_k < \infty} A_S(2\sigma s_{2n-k}) \dots A_S(2\sigma s_1) \rho A_S(2\sigma t_1) \dots A_S(2\sigma t_k) e^{-\sum_{p=1}^{2n-k} s_p^2 - \sum_{p=1}^k t_p^2} \\ & \quad \cdot \int \gamma(\omega) e^{i2\sigma\omega \sum_{p=1}^{2n-k} (-1)^p s_p - i2\sigma\omega \sum_{p=1}^k (-1)^p t_p} d\omega ds_1 \dots ds_{2n-k} dt_1 \dots dt_k \end{aligned}$$

Because $\|BAC\|_2 \leq \|B\| \|C\| \|A\|_2$, we have

$$\begin{aligned} & \left\| \int \gamma(\omega) G_{2n-k, A_S}^\dagger(\omega) \rho G_{k, A_S}(\omega) d\omega \right\|_2 \\ & \leq \frac{1}{\pi^{n/2}} \|A_S\|^{2n} \|\rho\|_2 \int_{-\infty < s_1 \leq s_2 \leq \dots \leq s_{2n-k} < \infty, -\infty < t_1 \leq t_2 \leq \dots \leq t_k < \infty} e^{-\sum_{p=1}^{2n-k} s_p^2 - \sum_{p=1}^k t_p^2} \\ & \quad \cdot \left| \int \gamma(\omega) e^{i2\sigma\omega \sum_{p=1}^{2n-k} (-1)^p s_p - i2\sigma\omega \sum_{p=1}^k (-1)^p t_p} d\omega \right| ds_1 \dots ds_{2n-k} dt_1 \dots dt_k \\ & \leq \frac{(\Theta(1))^n}{\sigma \sqrt{n}} \mathcal{O}(\log(\sqrt{2n}\sigma) \|\gamma'\|_{L^1}) \end{aligned}$$

where we use (D56) in the last inequality. Plugging this back into (F2) and summing over $n \geq 2, k$ gives

$$\begin{aligned} \|\mathcal{M}_{2,\infty}\|_{2 \leftrightarrow 2} &= \frac{1}{\alpha^2} \mathcal{O} \left(\sum_{n \geq 2} \frac{(\Theta(\alpha^2 \sigma))^n \sqrt{n}}{\sigma} \mathcal{O}(\log(\sqrt{2n}\sigma) \|\gamma'\|_{L^1}) \right) \\ &= \alpha^2 \sigma \underbrace{\mathcal{O} \left(\sum_{n \geq 2} (\Theta(\alpha^2 \sigma))^{n-2} \sqrt{n} \mathcal{O}(\log(\sqrt{2n}\sigma) \|\gamma'\|_{L^1}) \right)}_{=\mathcal{O}(1) \text{ when } \alpha^2 \sigma = \mathcal{O}(1)} \end{aligned}$$

This concludes the proof of (F9).

To prove (F10), we use Lemma D.4 to get the formula of $\sigma_\beta^{-1/4} G \sigma_\beta^{1/4}$. The rest of the proof is similar to the above calculation. \square

Next, to prove Theorem F.2, we first provide a framework for studying the mixing time of the CPTP maps that take the form of

$$\Phi = \mathcal{U}_S(T) \circ (I + \mathcal{M}\alpha^2) [\cdot] \circ \mathcal{U}_S(T),$$

where $I + \mathcal{M}\alpha^2$ is quantum channel. This framework is inspired by [12, 13, 55]. To start, we first introduce the detailed balance condition:

Definition F.5 (Detailed balance condition with unitary drift [13, 55]). *For the superoperator \mathcal{M} and full-rank state σ_β , take a similarity transformation and decompose into the Hermitian and the anti-Hermitian parts*

$$\begin{aligned}\mathcal{K}(\sigma_\beta, \mathcal{M}) &= \sigma_\beta^{-1/4} \mathcal{M} \left[\sigma_\beta^{1/4} \cdot \sigma_\beta^{1/4} \right] \sigma_\beta^{-1/4} = \mathcal{H}(\sigma_\beta, \mathcal{M}) + \mathcal{A}(\sigma_\beta, \mathcal{M}) \\ \mathcal{K}(\sigma_\beta, \mathcal{M})^\dagger &= \sigma_\beta^{1/4} \mathcal{M}^\dagger \left[\sigma_\beta^{-1/4} \cdot \sigma_\beta^{-1/4} \right] \sigma_\beta^{1/4} = \mathcal{H}(\sigma_\beta, \mathcal{M}) - \mathcal{A}(\sigma_\beta, \mathcal{M})\end{aligned}$$

We say the superoperator \mathcal{M} satisfies the detailed balance with unitary drift if there exists a Hermitian operator H_C such that

$$\mathcal{A}(\sigma_\beta, \mathcal{M}) = -i\sigma_\beta^{1/4} [H_C, \sigma_\beta^{-1/4}(\cdot) \sigma_\beta^{-1/4}] \sigma_\beta^{1/4}.$$

We note that the above detailed balance condition allows a coherent term that commutes with σ_β in \mathcal{M} . It is straightforward to check that if \mathcal{M} satisfies the detailed balance with unitary drift and is traceless when applying density operator, then $\mathcal{H}(\sigma_\beta, \mathcal{M})(\sqrt{\sigma_\beta}) = 0$ and $\mathcal{M}(\sigma_\beta) = 0$.

Define

$$\mathcal{M}_\infty = \mathcal{L}_{\sigma, \text{KMS}} - i[H_{\sigma, \text{Lamb}}, \cdot] + \mathcal{M}_{2, \infty}, \quad \Phi_{\text{part}, \Gamma, \infty}(\rho) = \rho + \mathcal{M}_\infty(\rho)\alpha^2.$$

Comparing with $\Phi_{\text{part}, \Gamma}$, $\Phi_{\text{part}, \Gamma, \infty}(\rho)$ takes $T = \infty$ and modify the Lindbladian part to the KMS Lindbladian. According to Lemma D.2 and Theorem F.1, we have

$$\|\Phi_{\text{part}, \Gamma, \infty}(\rho) - \Phi_{\text{part}, \Gamma}(\rho)\|_{1 \rightarrow 1} = \mathcal{O} \left(\frac{\alpha^2 \beta}{\sigma} + \frac{\Gamma^2 \sigma}{T} \exp(-T^2/(4\sigma^2)) \right).$$

Define $\Phi_{\Gamma, \infty} = \mathcal{U}_S(T) \circ \Phi_{\text{part}, \Gamma, \infty} \circ \mathcal{U}_S(T)$, we have

$$\|\Phi_{\Gamma, \infty}(\rho) - \Phi_{\Gamma}(\rho)\|_{1 \rightarrow 1} = \mathcal{O} \left(\frac{\alpha^2 \beta}{\sigma} + \frac{\Gamma^2 \sigma}{T} \exp(-T^2/(4\sigma^2)) \right).$$

Given $\epsilon > 0$, let $t_{\text{mix}, \Phi_{\Gamma, \infty}}(\epsilon)$ be the rescaled mixing time of $\Phi_{\Gamma, \infty}$ defined in Definition C.1, according to [22, Theorem 8],

$$\frac{t_{\text{mix}, \Phi_{\Gamma, \infty}}(\epsilon/2)}{\alpha^2} \|\Phi_{\Gamma, \infty}(\rho) - \Phi_{\Gamma}(\rho)\|_{1 \rightarrow 1} \leq \epsilon/2 \Rightarrow t_{\text{mix}, \Phi_{\Gamma}}(2\epsilon) \leq t_{\text{mix}, \Phi_{\Gamma, \infty}}(\epsilon/2). \quad (\text{F11})$$

Thus, to give an upper bound for $t_{\text{mix}, \Phi_{\Gamma}}(\epsilon)$, it suffices to give an upper bound for $t_{\text{mix}, \Phi_{\Gamma, \infty}}(\epsilon)$. Specifically,

$$\sigma = \Omega \left(\frac{\beta t_{\text{mix}, \Phi_{\Gamma, \infty}}(\epsilon)}{\epsilon} \right), \quad T = \Omega \left(\sigma \sqrt{\log \left(\frac{\sigma t_{\text{mix}, \Phi_{\Gamma, \infty}}(\epsilon)}{\epsilon} \right)} \right) \Rightarrow t_{\text{mix}, \Phi_{\Gamma}}(4\epsilon) \leq t_{\text{mix}, \Phi_{\Gamma, \infty}}(\epsilon).$$

Here, the form of σ looks similar to that in Theorem D.1, thus, no extra ϵ -dependence is introduced in the final choice of σ by this approximation step.

Now, we focus on upper bounding $t_{\text{mix}, \Phi_{\Gamma, \infty}}(\epsilon)$. First,

$$\mathcal{K}(\sigma_\beta, \mathcal{M}_\infty) = \mathcal{K}(\sigma_\beta, \mathcal{L}_{\sigma, \text{KMS}}) + \mathcal{K}(\sigma_\beta, -i[H_{\sigma, \text{Lamb}}, \cdot]) + \mathcal{K}(\sigma_\beta, \mathcal{M}_{2, \infty}),$$

we decompose each superoperator into Hermitian and anti-Hermitian parts, $\mathcal{K} = \mathcal{H} + \mathcal{A}$, and analyze the properties of each Hermitian superoperator $\mathcal{H}_1, \mathcal{H}_2, \mathcal{H}_3$.

- According to Theorem F.1,

$$\mathcal{K}(\sigma_\beta, \mathcal{L}_{\sigma, \text{KMS}}) = \mathcal{K}^\dagger(\sigma_\beta, \mathcal{L}_{\sigma, \text{KMS}}) = \mathcal{H}(\sigma_\beta, \mathcal{L}_{\sigma, \text{KMS}}) := \mathcal{H}_1.$$

- The Hermitian part of $\mathcal{K}(\sigma_\beta, -i[H_{\sigma, \text{Lamb}}, \cdot])$ follows

$$\left\| \underbrace{\mathcal{H}(\sigma_\beta, -i[H_{\sigma, \text{Lamb}}, \cdot])}_{:=\mathcal{H}_2} \right\|_{2 \leftrightarrow 2} = \left\| -\frac{i}{2} \left\{ \sigma_\beta^{-1/4} H_{\sigma, \text{Lamb}} \sigma_\beta^{1/4} - \sigma_\beta^{1/4} H_{\sigma, \text{Lamb}} \sigma_\beta^{-1/4}, \rho \right\} \right\|_{2 \leftrightarrow 2} = \mathcal{O}(\beta/\sigma).$$

- Furthermore, according to Lemma F.4 Eq. (F10), we have

$$\left\| \underbrace{\mathcal{H}(\sigma_\beta, \mathcal{M}_2)}_{:=\mathcal{H}_3} \right\|_{2 \leftrightarrow 2} \leq \|\mathcal{K}(\sigma_\beta, \mathcal{M}_2)\|_{2 \leftrightarrow 2} = \mathcal{O}(\alpha^2 \sigma).$$

Because \mathcal{H}_1 is Hermitian with respect to Hilbert–Schmidt inner product and $\mathcal{H}_1(\sqrt{\sigma_\beta}) = 0$, we can define the spectral gap of \mathcal{H}_1 as follows:

$$\lambda_{\text{gap}}(\mathcal{H}_1) := \inf_{\text{Tr}(X\sqrt{\sigma_\beta})=0, X \neq 0} \frac{-\langle X, \mathcal{H}_1(X) \rangle_2}{\langle X, X \rangle_2}.$$

It is straightforward to check that this gap matches with the spectral gap of \mathcal{L}_{KMS} in the KMS inner product:

$$\begin{aligned} \text{Gap}(\mathcal{L}_{\sigma, \text{KMS}}) &= \inf_{\text{Tr}(A\sigma_\beta)=0, A \neq 0} \frac{-\langle A, \mathcal{L}_{\text{KMS}}^\dagger(A) \rangle_{1/2, \sigma_\beta}}{\langle A, A \rangle_{1/2, \sigma_\beta}} \\ &= \inf_{\text{Tr}(A\sigma_\beta)=0, A \neq 0} \frac{-\langle \sigma^{1/4} A \sigma_\beta^{1/4}, \mathcal{K}^\dagger(\sigma_\beta, \mathcal{L}_{\text{KMS}})(\sigma_\beta^{1/4} A \sigma_\beta^{1/4}) \rangle}{\langle \sigma_\beta^{1/4} A \sigma_\beta^{1/4}, \sigma_\beta^{1/4} A \sigma_\beta^{1/4} \rangle} \\ &= \inf_{\text{Tr}(\sigma_\beta^{1/4} A \sigma_\beta^{1/4} \sqrt{\sigma_\beta})=0, A \neq 0} \frac{-\langle \sigma_\beta^{1/4} A \sigma_\beta^{1/4}, \mathcal{H}_1(\sigma_\beta^{1/4} A \sigma_\beta^{-1/4}) \rangle}{\langle \sigma_\beta^{1/4} A \sigma_\beta^{1/4}, \sigma_\beta^{1/4} A \sigma_\beta^{1/4} \rangle} = \lambda_{\text{gap}}(\mathcal{H}_1), \end{aligned}$$

where $\langle A, B \rangle_{1/2, \sigma_\beta} = \text{Tr}(\sigma_\beta^{1/2} A^\dagger \sigma_\beta^{1/2} B)$ and $\langle A, B \rangle = \text{Tr}(A^\dagger B)$ is the Hilbert–Schemitz inner product. In the third equality, we use that, if $\text{Tr}(A\sigma_\beta) = 0$, then $\sigma_\beta^{-1/4} A \sigma_\beta^{-1/4}$ is orthogonal to $\sqrt{\sigma_\beta}$ under Hilbert Schemitz inner product. The spectral gap of \mathcal{H}_1 is same as the spectral gap of \mathcal{L}_{KMS} , which has been well studied in the framework in [29, 32–35, 47].

Now, we are ready to prove Theorem F.2.

Proof of Theorem F.2. Given any density operator ρ_1, ρ_2 , we define $\mathcal{E} = \rho_1 - \rho_2$. We consider the change of $\|\sigma_\beta^{-1/4} \mathcal{E} \sigma_\beta^{-1/4}\|_2$ after applying $\Phi_{\Gamma, \infty}$. First, because \mathcal{U}_S commutes with $\sigma_\beta^{-1/4}(\cdot) \sigma_\beta^{-1/4}$, we have

$$\|\sigma_\beta^{-1/4} \mathcal{U}_S(\mathcal{E}) \sigma_\beta^{-1/4}\|_2 = \|\mathcal{U}_S(\sigma_\beta^{-1/4} \mathcal{E} \sigma_\beta^{-1/4})\|_2 = \|\sigma_\beta^{-1/4} \mathcal{E} \sigma_\beta^{-1/4}\|_2.$$

Thus, by the definition in Definition F.5,

$$\|\sigma_\beta^{-1/4} \Phi_{\Gamma, \infty}(\mathcal{E}) \sigma_\beta^{-1/4}\|_2 = \|\sigma_\beta^{-1/4} (I + \mathcal{M}_\infty \alpha^2) (\mathcal{U}_S(\mathcal{E})) \sigma_\beta^{-1/4}\|_2 = \|(I + \mathcal{K}(\sigma_\beta, \mathcal{M}_\infty) \alpha^2) [\sigma_\beta^{-1/4} \mathcal{U}_S(\mathcal{E}) \sigma_\beta^{-1/4}] \|_2. \quad (\text{F12})$$

Let $\tilde{\mathcal{E}} = \mathcal{U}_S(\mathcal{E})$. Then

$$\|(I + \mathcal{K}(\sigma_\beta, \mathcal{M}_\infty) \alpha^2) [\sigma_\beta^{-1/4} \tilde{\mathcal{E}} \sigma_\beta^{-1/4}] \|_2^2 = \langle \sigma_\beta^{-1/4} \tilde{\mathcal{E}} \sigma_\beta^{-1/4}, (I + 2(\mathcal{H}_1 + \mathcal{H}_2 + \mathcal{H}_3) \alpha^2 + \mathcal{K}^\dagger \mathcal{K} \alpha^4) \sigma_\beta^{-1/4} \tilde{\mathcal{E}} \sigma_\beta^{-1/4} \rangle_2.$$

Because $\tilde{\mathcal{E}}$ is traceless, we have $\sigma_\beta^{-1/4} \tilde{\mathcal{E}} \sigma_\beta^{-1/4}$ is orthogonal to $\sqrt{\sigma_\beta}$ under Hilbert Schemitz inner product. This implies that

$$\langle \sigma_\beta^{-1/4} \tilde{\mathcal{E}} \sigma_\beta^{-1/4}, (I + 2\mathcal{H}_1 \alpha^2) \sigma_\beta^{-1/4} \tilde{\mathcal{E}} \sigma_\beta^{-1/4} \rangle_2 \leq (1 - 2\lambda_{\text{gap}}(\mathcal{H}_1) \alpha^2) \|\sigma_\beta^{-1/4} \tilde{\mathcal{E}} \sigma_\beta^{-1/4}\|_2^2.$$

For the other terms, we have

$$\begin{aligned}
& \left\langle \sigma_\beta^{-1/4} \tilde{\mathcal{E}} \sigma_\beta^{-1/4}, (2(\mathcal{H}_2 + \mathcal{H}_3)\alpha^2 + \mathcal{K}^\dagger \mathcal{K} \alpha^4) \sigma_\beta^{-1/4} \tilde{\mathcal{E}} \sigma_\beta^{-1/4} \right\rangle_2 \\
& \leq (2\|\mathcal{H}_2\|_{2 \rightarrow 2} \alpha^2 + 2\|\mathcal{H}_3\|_{2 \rightarrow 2} \alpha^2 + \|\mathcal{K}\|_{2 \rightarrow 2} \alpha^4) \left\| \sigma_\beta^{-1/4} \tilde{\mathcal{E}} \sigma_\beta^{-1/4} \right\|_2^2 \\
& = \mathcal{O} \left(\left(\frac{\beta}{\sigma} + \alpha^2 \sigma \right) \alpha^2 \left\| \sigma_\beta^{-1/4} \tilde{\mathcal{E}} \sigma_\beta^{-1/4} \right\|_2^2 \right).
\end{aligned}$$

Putting the above two bounds together, we have

$$\left\| (I + \mathcal{K}(\sigma_\beta, \mathcal{M}_\infty) \alpha^2) \left[\sigma_\beta^{-1/4} \tilde{\mathcal{E}} \sigma_\beta^{-1/4} \right] \right\|_2^2 = \left(1 - 2\lambda_{\text{gap}}(\mathcal{H}_1) \alpha^2 + \mathcal{O} \left(\left(\frac{\beta}{\sigma} + \alpha^2 \sigma \right) \alpha^2 \right) \right) \left\| \sigma_\beta^{-1/4} \tilde{\mathcal{E}} \sigma_\beta^{-1/4} \right\|_2^2.$$

Plugging this back into (F12), we have

$$\begin{aligned}
& \left\| \sigma_\beta^{-1/4} \Phi_{\Gamma, \infty}(\mathcal{E}) \sigma_\beta^{-1/4} \right\|_2 = \left(1 - \lambda_{\text{gap}}(\mathcal{H}_1) \alpha^2 + \mathcal{O} \left(\left(\frac{\beta}{\sigma} + \alpha^2 \sigma \right) \alpha^2 \right) \right) \left\| \sigma_\beta^{-1/4} \tilde{\mathcal{E}} \sigma_\beta^{-1/4} \right\|_2 \\
& = \left(1 - \lambda_{\text{gap}}(\mathcal{H}_1) \alpha^2 + \mathcal{O} \left(\left(\frac{\beta}{\sigma} + \alpha^2 \sigma \right) \alpha^2 \right) \right) \left\| \sigma_\beta^{-1/4} \mathcal{E} \sigma_\beta^{-1/4} \right\|_2 \\
& \leq \left(1 - \frac{\lambda_{\text{gap}}(\mathcal{H}_1)}{2} \alpha^2 \right) \left\| \sigma_\beta^{-1/4} \mathcal{E} \sigma_\beta^{-1/4} \right\|_2,
\end{aligned}$$

where we use the condition of $\sigma = \Omega(\beta/\lambda_{\text{gap}}(\mathcal{H}_1))$ and $\alpha^2 \sigma = \mathcal{O}(\lambda_{\text{gap}}(\mathcal{H}_1))$ in the last inequality.

This implies that after k iterations of $\Phi_{\Gamma, \infty}$,

$$\left\| \sigma_\beta^{-1/4} \Phi_{\Gamma, \infty}^k(\mathcal{E}) \sigma_\beta^{-1/4} \right\|_2 \leq \left(1 - \frac{\lambda_{\text{gap}}(\mathcal{H}_1)}{2} \alpha^2 \right)^k \left\| \sigma_\beta^{-1/4} \mathcal{E} \sigma_\beta^{-1/4} \right\|_2.$$

Finally, using $\|BAB\|_1 \leq \|B\|_4^2 \|A\|_2$, we have

$$\|\mathcal{E}\|_1 \leq \left\| \rho_\beta^{1/4} \right\|_4^2 \left\| \sigma_\beta^{-1/4} \mathcal{E} \sigma_\beta^{-1/4} \right\|_2 = \left\| \sigma_\beta^{-1/4} \mathcal{E} \sigma_\beta^{-1/4} \right\|_2 \leq \left\| \sigma_\beta^{-1/4} \right\|^2 \|\mathcal{E}\|_2 \leq \left\| \sigma_\beta^{-1/2} \right\| \|\mathcal{E}\|_1.$$

This implies

$$\|\Phi^k(\mathcal{E})\|_1 \leq \left(1 - \frac{\lambda_{\text{gap}}(\mathcal{H}_1)}{2} \alpha^2 \right)^k \left\| \sigma_\beta^{-1/4} \mathcal{E} \sigma_\beta^{-1/4} \right\|_2 \leq \left(1 - \frac{\lambda_{\text{gap}}(\mathcal{H}_1)}{2} \alpha^2 \right)^k \left\| \sigma_\beta^{-1/2} \right\| \|\mathcal{E}\|_1.$$

This implies that to ensure $\|\Phi^k(\mathcal{E})\|_1 \leq \epsilon$, it suffices to choose

$$k = \mathcal{O} \left(\frac{1}{\alpha^2 \lambda_{\text{gap}}(\mathcal{H}_1)} \log \left(\frac{\left\| \sigma_\beta^{-1/2} \right\|}{\epsilon} \right) \right).$$

Thus, the rescaled mixing time of $\Phi_{\Gamma, \infty}$ is

$$t_{\text{mix}, \Phi_{\Gamma, \infty}}(\epsilon) = \alpha^2 k = \mathcal{O} \left(\frac{1}{\lambda_{\text{gap}}(\mathcal{H}_1)} \log \left(\frac{\left\| \sigma_\beta^{-1/2} \right\|}{\epsilon} \right) \right).$$

Putting this back to the earlier approximation step in (F11), we have

$$t_{\text{mix}, \Phi_\Gamma}(4\epsilon) = \mathcal{O} \left(\frac{1}{\lambda_{\text{gap}}(\mathcal{H}_1)} \log \left(\frac{\left\| \sigma_\beta^{-1/2} \right\|}{\epsilon} \right) \right)$$

with

$$\sigma = \Omega \left(\frac{\beta}{\lambda_{\text{gap}}(\mathcal{H}_1)} \right), \quad T = \Omega \left(\sigma \sqrt{\log \left(\frac{\sigma}{\epsilon} \cdot \frac{1}{\lambda_{\text{gap}}(\mathcal{H}_1)} \right)} \right), \quad \alpha^2 \sigma = \mathcal{O}(\lambda_{\text{gap}}(\mathcal{H}_1)).$$

This concludes the proof. \square

Appendix G: Numerical implementation

We consider the transverse field Ising model (TFIM), the Hubbard model, and 1D axial next-nearest-neighbor Ising (ANNNI) model to verify our analysis results and explore the performance of the algorithm in even stronger coupling parameter. We investigate both thermal state and ground state preparation for the first two models and only ground state for the last model, varying the coupling parameter α to examine its impact on convergence behavior and accuracy.

1. Thermal state preparation

a. *Transverse field Ising model (TFIM)* Recall the transverse field Ising model (TFIM) in (3):

$$H = -J \sum_{i=1}^{L-1} Z_i Z_{i+1} - g \sum_{i=1}^L X_i,$$

where we set $J = 1, g = 1.2$. We now provide more detailed numerical results for thermal state preparation with different choices of parameters.

- The thermal state setting with $L = 4$ in the regime $\Gamma = \Theta(1)$: The additional numerical results are presented in Fig. 3. As shown in Fig. 3a, the state converges to the thermal state with very high accuracy, and the convergence rate improves as α increases. Moreover, Fig. 3b illustrates that the steady state of the channel approaches the target thermal state as σ increases, while remaining nearly constant with respect to variations in α . By computing the spectral gap after constructing the discrete quantum channel Φ_Γ explicitly, Fig. 3c shows the spectral gap remains independent of σ and scales as α^2 , which is similar to the result we showed for Hubbard model Fig. 2b.
- Thermal State preparation with $L = 4$ in the strong coupling regime $\Gamma = \Theta(\sigma)$: We extend our numerical experiments to the strong coupling regime. For thermal state preparation, we keep σ, T , and ω the same as before and vary α as $\alpha/\sqrt{2} = 1, 0.5, 0.25, 0.1, 0.05, 0.01$, as shown in Fig. 4a and Fig. 4b. We observe that when $\alpha/\sqrt{\sigma} \leq 1/2$, the fixed point remains close to the target state, and the spectral gap continues to scale as α^2 in this regime. These observations suggest that accurate thermal state preparation remains feasible even under strong system–bath interactions, with a correspondingly faster convergence rate. Furthermore, the apparent coupling threshold at $\alpha/\sqrt{\sigma} \approx 0.5$ seems to be independent of system size, as we observe similar behavior in both 4-qubit and 8-qubit systems. This phenomenon lies beyond our current theoretical guarantees and suggests that the robustness of system–bath interaction models may be even greater than what our analysis presently establishes.

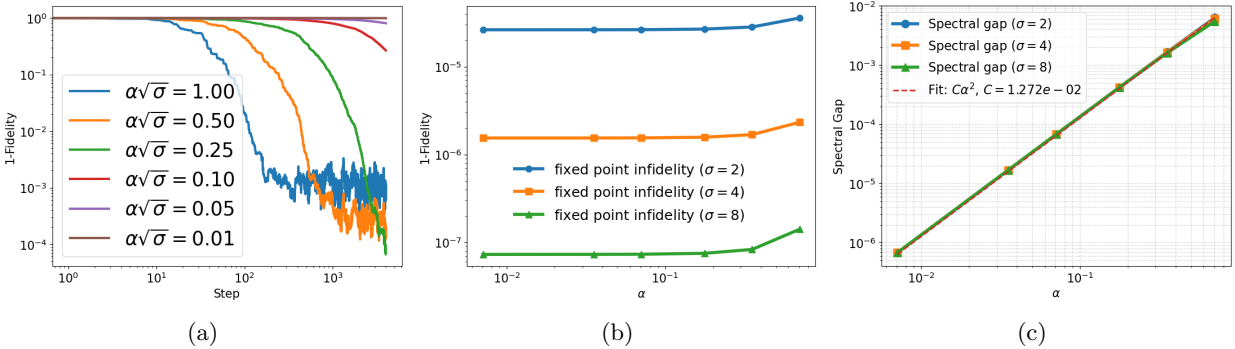


Figure 3: Thermal state preparation for TFIM with $L = 4$ sites in the regime $\Gamma = \Theta(1)$. In (a)–(c), we use $\sigma = 2, 4, 8$, choose the coupling parameter α such that $\alpha\sqrt{\sigma} = 1.0, 0.5, 0.25, 0.10, 0.05, 0.01$ and set the interaction time $T = 5\sigma$; the frequency ω is sampled uniformly from the interval $[0, 5]$. (a) The evolution of infidelity, i.e., $1 - F$, versus the iteration steps. (b) The fix point infidelity between the target thermal state and the stationary state of Φ_Γ , shown versus different σ . (c) The spectral gap of Φ_Γ .

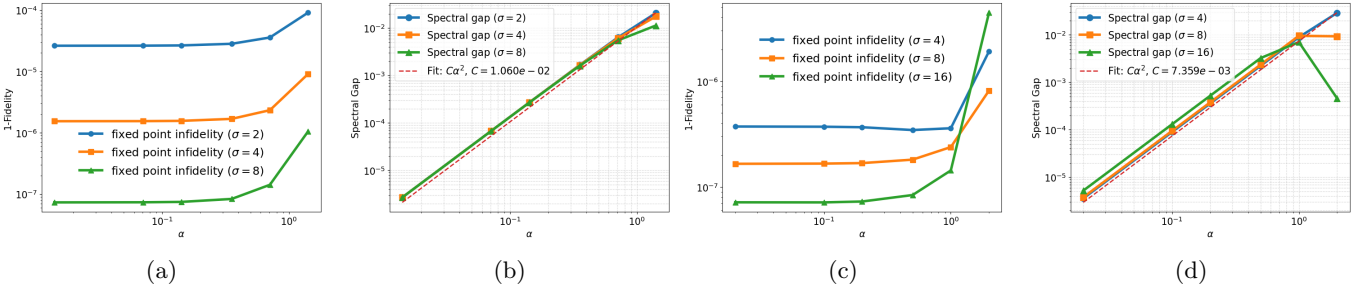


Figure 4: Thermal and ground state preparation for TFIM with 4 sites in the regime $\Gamma = \Theta(\sigma)$ ($\alpha/\sqrt{\sigma} = \Omega(1)$). (a) Infidelity between target thermal state ($\beta = 1$) and the stationary state of Φ_Γ for varying σ and $\alpha/\sqrt{2} = 1, 0.5, 0.25, 0.1, 0.05, 0.01$. (b) Spectral gap of Φ_Γ with different α, σ , and $\beta = 1$ and the same values of $\alpha/\sqrt{2}$. (c) Infidelity between target ground state ($\beta = \infty$) and the stationary state of Φ_Γ for varying σ and $\alpha = 2, 1, 0.5, 0.2, 0.1, 0.02$. (d) Spectral gap of Φ_Γ with different $\alpha, \sigma, \beta = \infty$, and the same values of α .

b. 1-D Hubbard model Consider the 1-D Hubbard model defined on $L = 2, 4$ spinful sites with open boundary conditions in (4)

$$H = -t \sum_{j=1}^{L-1} \sum_{\sigma \in \{\uparrow, \downarrow\}} c_{j,\sigma}^\dagger c_{j+1,\sigma} + U \sum_{j=1}^L (n_{j,\uparrow} - \frac{1}{2})(n_{j,\downarrow} - \frac{1}{2})$$

where the number operator $n_{j,\sigma} = c_{j,\sigma}^\dagger c_{j,\sigma}$ and the dimension is 2^{2L} . Here we choose $t = 1, U = -4$. Similar to the TFIM case, we consider the thermal state case with the same choice of parameters α, σ . We observe very similar results in Fig. 5 and Fig. 7. Furthermore, the numerical experiments can be extended to the regime where $\Gamma = \Theta(\sigma)$ ($\alpha/\sqrt{\sigma} = \mathcal{O}(1)$), as shown in Fig. 8. Similar to the TFIM example, when $\alpha/\sqrt{\sigma} \leq 1/2$, the fixed point closely matches the target state, and the spectral gap increases as α^2 .

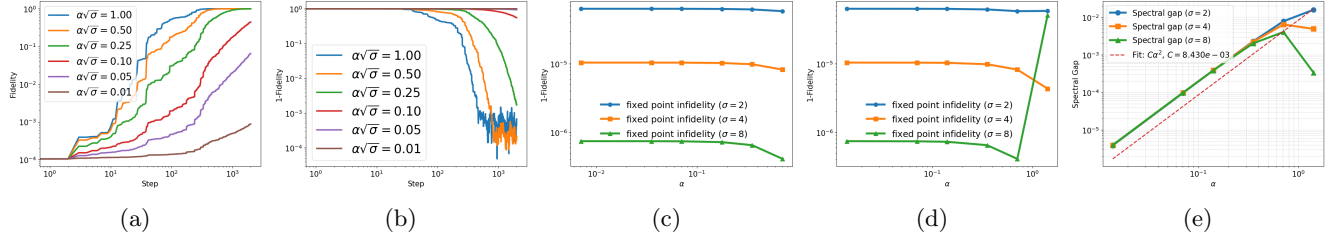


Figure 5: Thermal state preparation of Hubbard with $L = 2$ sites. (a)–(c) In the regime $\Gamma = \Theta(1)$. (a) The evolution of fidelity. We set $\sigma = 2$ and $\alpha\sqrt{\sigma}$. (b) The evolution of infidelity. (c) Infidelity between target thermal state and the stationary state of Φ_Γ with different σ . Fidelity increases with σ . (d)–(e) Strong coupling regime $\Gamma = \Theta(\sigma)$. (d) Infidelity between target thermal state and the stationary state of Φ_Γ with different σ and $\beta = 1$. Here $\alpha/\sqrt{2} = 1, 0.5, 0.25, 0.1, 0.05, 0.01$. (e) Spectral gap.

2. Ground state preparation

We also consider the ground state preparation of TFIM, Hubbard and ANNNI model. For those large scale numerical experiments, including TFIM-8, Hubbard-4, we simulate the state vector instead of density operator to reduce the computational cost. Thus, we report the evolution of energy along a single trajectory. Unless stated otherwise, the remaining parameters are chosen as in the previous experiments. Similar to the thermal state case, even in the strong-coupling regime ($\alpha/\sqrt{\sigma} \approx 0.5$), the algorithm still converges to the ground state with high accuracy, and the convergence speed increases as α grows.

a. TFIM We study the ground state preparation for the TFIM model with $L = 4, 8$ sites. In the regime $\Gamma = \Omega(1)$ with $L = 4$ (Fig. 6), we set $\alpha = 0.5, 0.25, 0.125, 0.05, 0.025, 0.005, \sigma = 4, 8, 16, T = 5\sigma$, and also sample ω uniformly from $[0, 5]$. Similar to the thermal state case, figures in Fig. 6a and Fig. 6b justifies the convergence behavior of the

fidelity and energy in the algorithm. In the strong coupling regime $\Gamma = \Omega(\sigma)$ with size $L = 4$ (Fig. 4c, Fig. 4d) and $L = 8$ (Fig. 9c), we can still observe the convergence of the energy. Moreover, once the coupling parameter α is below a moderate large constant, the fidelity and spectral gap are essentially insensitive to the change of σ .

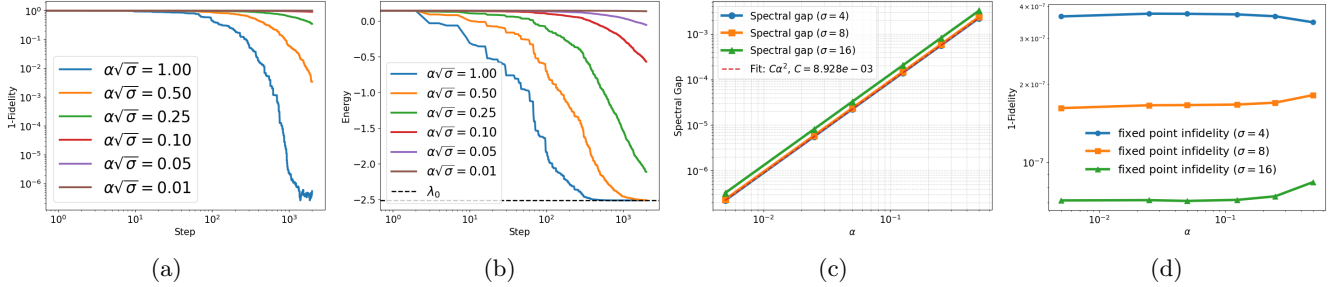


Figure 6: Ground/Thermal state preparation of TFIM with $L = 4$ sites in the regime $\Gamma = \Omega(1)$. (a) The evolution of infidelity. Here, we set $\sigma = 4$ and $\alpha\sqrt{\sigma}$. (b) The evolution of energy. Here λ_0 is the ground state energy and we set $\sigma = 2$ and $\alpha\sqrt{\sigma} = 1.00, 0.50, 0.25, 0.10, 0.05, 0.01$. Figures (c)-(d) thermal state use $\alpha = 0.5, 0.25, 0.125, 0.05, 0.025, 0.005$. (c) The spectral gap. (d) The evolution of infidelity.

b. Hubbard model We consider the ground state preparation for the Hubbard model with $L = 2, 4$ sites. In the regime $\Gamma = \Theta(1)$ with sites $L = 2$ (Fig. 7), the energy trajectories relax toward the ground state energy across a wide range of α and converges faster as α increases. The spectral gap scales approximately quadratically in α while only mild depend on σ . The infidelity exhibit rapid decay over iterations. Specifically, the fixed point infidelity remains small and is approximately unchanged over different choice of σ . In the stronger coupling case with $L = 2$ (Figs. 8a and 8b) and $L = 4$ (Fig. 9d), the fixed point infidelity and spectral gap curves indicate that: up to moderately large coupling, the preparation performance is essentially insensitive to σ , with noticeable deviation only as α becomes large enough to slow mixing and reduce the achievable final accuracy.

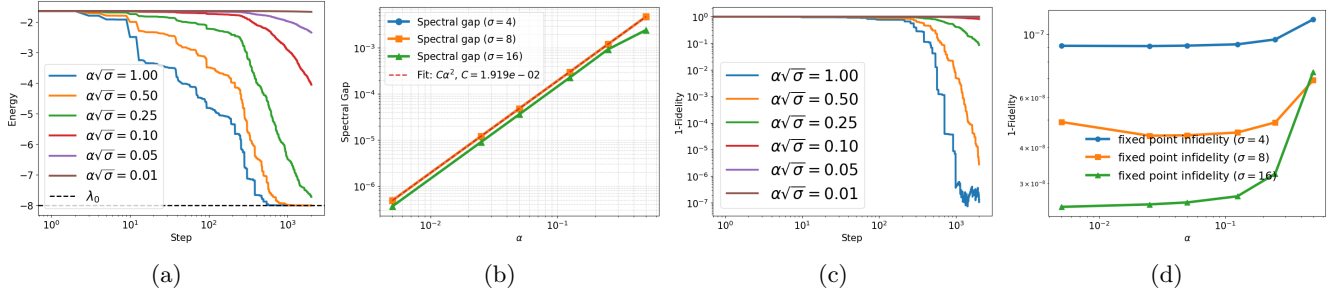


Figure 7: Ground state preparation of the Hubbard model with $L = 2$ sites in the regime $\Gamma = \Theta(1)$. We set $\alpha = 0.5, 0.25, 0.125, 0.05, 0.025, 0.005$, $\sigma = 4, 8, 16$, $T = 5\sigma$, and also sample ω uniformly from $[0, 5]$. (a) The evolution of energy, λ_0 is the ground state energy. (b) Spectral gap of Φ_Γ . (c) The evolution of infidelity. Here, we set $\sigma = 4$ and $\alpha\sqrt{\sigma}$. (d) Infidelity between target thermal state and the stationary state of Φ_Γ with different σ . Fidelity increases with σ .

c. ANNNI model Consider the 1-D axial next-nearest-neighbor Ising (ANNNI) model with $L = 4$ sites defined as

$$H_{\text{ANNNI}} = \frac{J_1}{4} \sum_i Z_i Z_{i+1} + \frac{J_2}{4} \sum_i Z_i Z_{i+2} - \frac{G}{2} \sum_i X_i, \quad (\text{G1})$$

with $J_1 = 2$, $J_2 = 0.6$, $G = 0.2$, and $\rho_0 = |0\rangle\langle 0|$. In our test, we set $\alpha = 2, 1, 0.5, 0.2, 0.1, 0.02$, $\sigma = 4, 8, 16$, and $T = 5\sigma$. The resulting spectral gaps are shown in Fig. 8c. Similar to the TFIM and Hubbard models, our algorithm converges to the correct ground state whenever $\alpha/\sqrt{\sigma} \leq \frac{1}{2}$, and the convergence rate increases proportionally to α^2 .

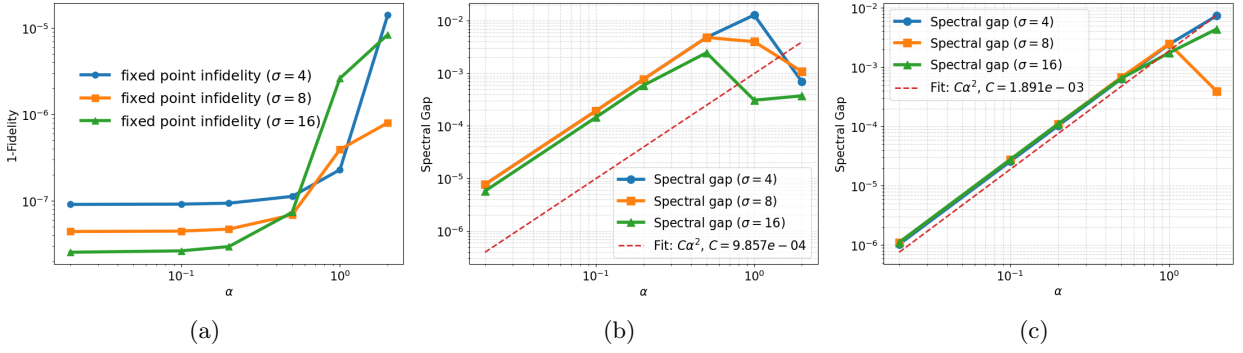


Figure 8: Ground state preparation in the regime $\Gamma = \Theta(\sigma)$ ($\alpha/\sqrt{\sigma} = \Omega(1)$). (a)-(b) Hubbard model with $L = 2$ sites. The parameters are $\alpha = 2, 1, 0.5, 0.2, 0.1, 0.02$, $\sigma = 4, 8, 16$. (a) Infidelity between target ground state and the stationary state of Φ_Γ . (b) Spectral gap of Φ_Γ . (c) Ground state preparation for ANNNI model with $L = 4$ sites in the regime $\Gamma = \Theta(\sigma)$ ($\alpha/\sqrt{\sigma} = \Theta(1)$). Spectral gap with different σ .

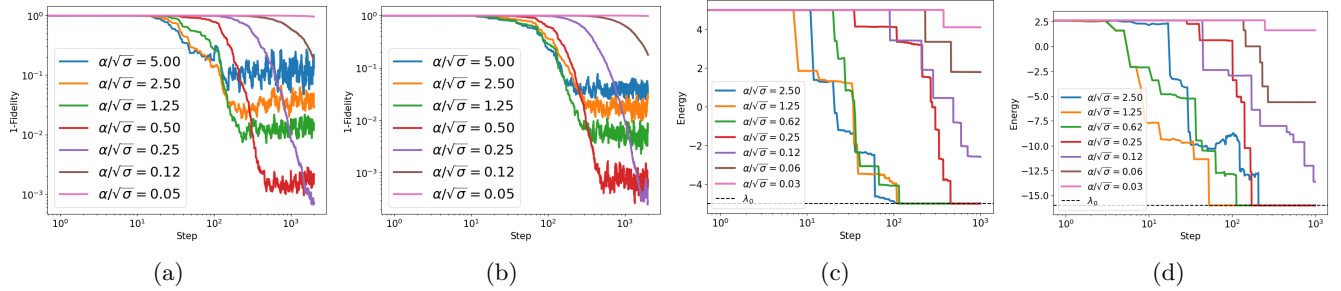


Figure 9: State preparation for larger systems in the strong coupling regime $\Gamma = \Theta(\sigma)$. λ_0 denotes the ground state energy. (a) Infidelity of the thermal state preparation for TFIM with $L = 8$ sites. (b) Infidelity of the thermal state preparation for the Hubbard model with $L = 4$ sites. (c) Evolution of energy of ground state preparation for TFIM with $L = 8$ sites. (d) Evolution of energy of ground state preparation for the Hubbard model with $L = 4$ sites.